DANMARKS OG GRØNLANDS GEOLOGISKE UNDERSØGELSE **RAPPORT 2022/7**

Screening of seabed geological conditions for the offshore wind farm (OWF) area Nordsøen 1, Område E

Desk study for the Danish Energy Agency

Niels Nørgaard-Pedersen, Thomas G. Vangkilde-Pedersen & Steen Lomholt

GEOLOGICAL SURVEY OF DENMARK AND GREENLAND
DANISH MINISTRY OF CLIMATE, ENERGY AND UTILITIES

G E U S

DANMARKS OG GRØNLANDS GEOLOGISKE UNDERSØGELSE **RAPPORT 2022/7**

Screening of seabed geological conditions for the offshore wind farm (OWF) area Nordsøen 1, Område E

Desk study for the Danish Energy Agency

Niels Nørgaard-Pedersen, Thomas G. Vangkilde-Pedersen & Steen Lomholt

GEOLOGICAL SURVEY OF DENMARK AND GREENLAND
DANISH MINISTRY OF CLIMATE, ENERGY AND UTILITIES

G E U S

Content

Appendices

A. Maps
A1: Screening area map
A2: Bathymetry map
A3: Seismic profiles and sediment core site map
A4: Seafloor sediment map
A5: Buried valley map
A6: Holocene unit (isopach map)
A7: Base Holocene unit (m below sea level)
A8: Weichsel Meltwater Unit (isopach map)
A9: Eemian unit (isopach map)
A10: Top Saale unit (m below sea floor)
A11: Top Saale unit (m below sea level)

B. Selected long seismic sections (with unit interpretation)

C. Table with all available sediment cores (with link to description)

1. Dansk resumé

Der er udført en detaljeret screening af de overfladenære geologiske forhold i Nordsøen 1 område E med henblik på at belyse egnetheden for fundering af vindmøller i området. Området er karakteriseret ved en relativt god datatæthed med hensyn til dækning af nyere seismiske linjer og boringer af god kvalitet. Havbunden er relativt flad med dybder på 18-32 m og overfladesedimentet er overvejende sandet. Generelt vurderes store dele af området til at være egnet til vindmølle fundering. De overfladenære geologiske enheder ned til ca. 50 m under havbund består af moræneleraflejringer overlejret af smeltevandsaflejringer bestående af vekslende lag af sand og ler, samt af marine lerede og sandede aflejringer. De ældre marine aflejringer, som hovedsageligt findes i den østlige del af området, består af blødt ler med en tykkelse på op til 10-20 m. Denne enhed kan muligvis udgøre en udfordring i forhold til vindmøllefundering. Den samme enhed blev identificeret i Horns Rev 3 og Thor OWF-områderne, og det anbefales at benytte erfaringer fra disse projekter til evaluering af potentielle udfordringer og funderingsløsninger. Risikoen for at der forefindes arkæologiske fund i området vurderes til at være lav. Ud over enkelte kendte vrag af nyere dato, er der en meget begrænset mulighed for, at der kan gøres fund fra den ældre stenalder.

2. Summary

Screening of surface-near geological conditions in Nordsøen 1 area E has established a detailed view of the composition and structure of major Quaternary geological units and the general geological development. The area is characterised by a quite dense network of shallow seismic data and sediment cores, sufficiently for an evaluation of the variability of soil conditions and general suitability for OWF location.

Area E is relatively shallow (18-32 m) and flat and the upper c. 50 m or more of the sub bottom is characterised by Quaternary glacial and interglacial deposits composed of interbedded sandy and clayey units. Below the Quaternary units, Miocene deposits also of sandy to clayey composition are found. The central to eastern part of the area is characterised by major quaternary buried valleys or channels eroding 300-400 m into the Miocene sequence.

Mapping of the Quaternary unit's base/top and thickness has revealed that Saalian (penultimate glacial) or older glacial deposits are found very close to the seabed in the central to southern part of the screening area. The glacial sediments can be expected to be of heterogeneous composition and over-consolidated, due to prior ice-loading and subaerial exposure. The sediments consist of clayey or sandy tills with variable stone content, deformed meltwater sediment layers (sand, gravel and clay) and locally glaciotectonically disturbed slabs of Miocene sediments (sands and clays). A similar setting with high-lying Saalian deformed to undeformed glacial units was observed by earlier investigations of the Horns Rev 2 OWF area and parts of the Horns Rev 3 and Thor OWF areas.

Meltwater sediments from both the late Saalian glacial period and the Weichselian (last) glacial period occur as channel elements and as major sheets, which have partly levelled the older glacial landscape. The unconsolidated glaciofluvial and -lacustrine meltwater sediments are varying between sandy and soft silty-clayey subunits. Soft Eemian (last interglacial) marine clayey sediments are confined to the eastern part of the area where the unit reaches a thickness of about 5-10 m. This clay unit is also known from the eastern part of Thor and Horns Rev 3 OWF.

The uppermost marine Holocene unit is mostly composed of fine-medium grained sand but soft silty and clayey or even gyttja like sediments, possibly early Holocene, appear in filled-in depressions in the central to southeastern part of the area. Peat layers have only been observed in a limited number of sediment cores, and typically only few decimetres in thickness.

Based on the mapping results of the screening of area E and settings of nearby OWF's, it is concluded that area E in general is suitable for foundation of wind turbines. However, the area exhibits different character with respect to the level of the glacial surface, the occurrence of several hundred meter deep buried valleys and composition and thickness of surficial sediment units composed mostly of sandy or clayey deposits. The occurrence of soft marine clays with up to 10-20 m in total thickness in the eastern part of the area, as well as minor areas in the western part, is a point of attention, as these areas may be less suitable for wind

turbine foundation. The same clay unit was identified by Thor and Horns Rev 3 OWF integrated geological model studies and geotechnical parameters from these projects may thus serve as a guide for potential challenges and foundation solutions. Apart from known positions of newer historical shipwrecks, the probability of making archaeological finds in the screening area is expected to be low.

3. Introduction

The Danish Energy Agency (DEA) has asked GEUS to perform a geological desktop screening study of the offshore wind farm (OWF) area Nordsøen 1, Område E to be used as background for evaluation of the suitability for wind farm sites in the area.

The area extents from c. 20 km west of Nissum and Ringkøbing Fjords along the west coast of Jutland and c. 20 km further west in the north and c. 60 km further west in the south. It covers an area of 3.174 km^2 including the 286 km^2 Thor OWF site (Figure 3-1).

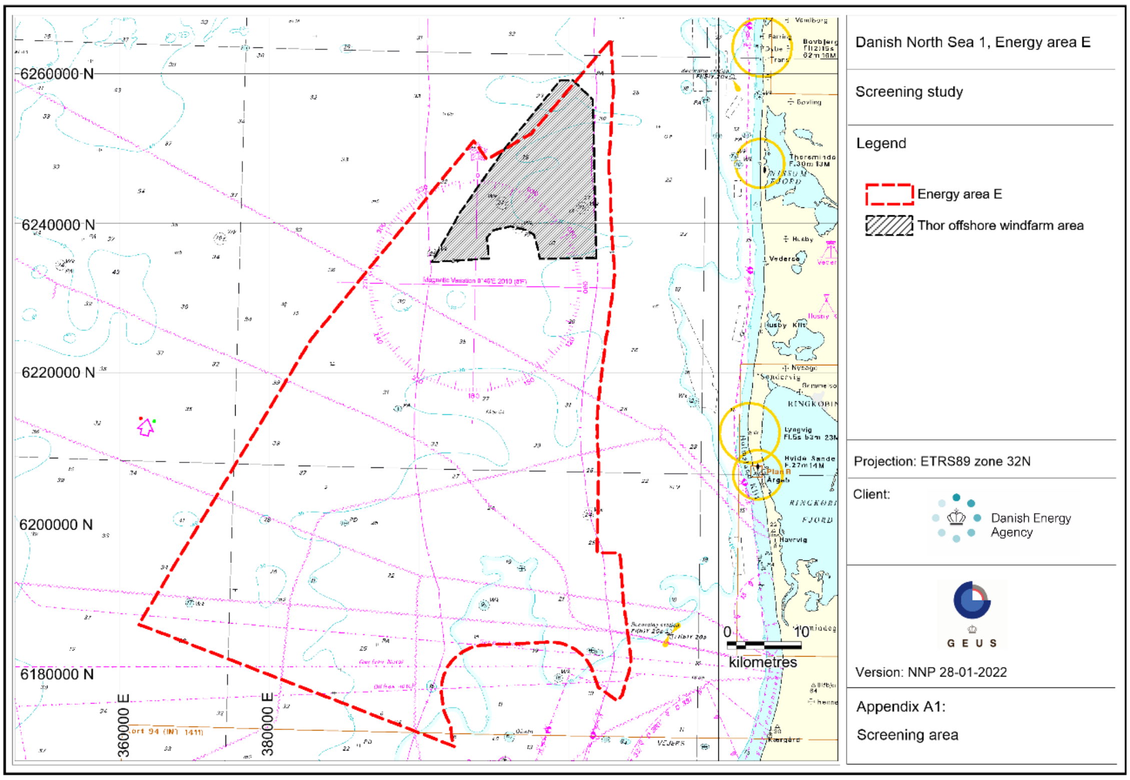

Figure 3-1. Screening area Nordsøen 1, område E.

The screening study is based on existing data and include a short description of the regional geological development of the Danish North Sea area and the establishment of a conceptual geological model for the understanding of the local geological conditions and possible implications for the geotechnical conditions and archaeological interests.

The work is based on a combination of published work, GEUS archive seismic and sediment core data and includes mapping of important geological units. The mapping results are presented as seismic profile examples and maps of thickness and depth below sea level and sea floor of the identified main stratigraphic units. The results may form a framework for selection of potential study areas for future wind farm areas.

4. Available data

A combination of published work, GEUS archive seismic data and sediment core data have been used as a basis for this desktop screening study. The published work includes technical reports from the Danish Energy Agency, the Danish Environmental Protection Agency (EPA), Energinet, GEUS and others as well as various scientific papers and reports. The written material have been used together with primary data from the GEUS Marta database, which is the main supply of shallow seismic data and vibrocore data (Figure 4-1). In addition, data not yet included in the Marta database from the raw material mapping of the EPA in the past few years have been used.

4.1 Background reports

A number of existing reports and publications has been used as background material for the screening of the geological conditions in the study area and description of the general geology of the region.

Especially ongoing work for the EPA on raw material mapping and Thor and Horns Rev Offshore Wind Farm technical reports from Energinet has been useful as well as previous reports from the EPA and the Danish Coastal Authority.

4.2 GEUS shallow seismic archive and sediment core archive

The Marine raw material database (Marta) of GEUS is developed in cooperation with the EPA and holds seismic data from raw material investigations in Danish waters, subject to reporting obligations. The Marta database also link to information about boreholes, grabs and other sediment samples in GEUS' borehole database (Jupiter) and to relevant reports from primarily raw material studies since 1980, but also from other studies.

The seismic data include both older analogue data and newer data in digital format. Some of the seismic data are still confidential, but an increasing part of the seismic lines can be downloaded directly from the web portal of the Marta database in SEG-Y file format.

The MARTA database further contains information on mapped raw material resource areas. This information is based on the results of processing and interpretation by GEUS of all reported raw material surveys and include the locations of the resource areas as well as the quality of the raw material deposits: resource type, geological formation type and resource certainty parameters (proven, probable, or speculative).

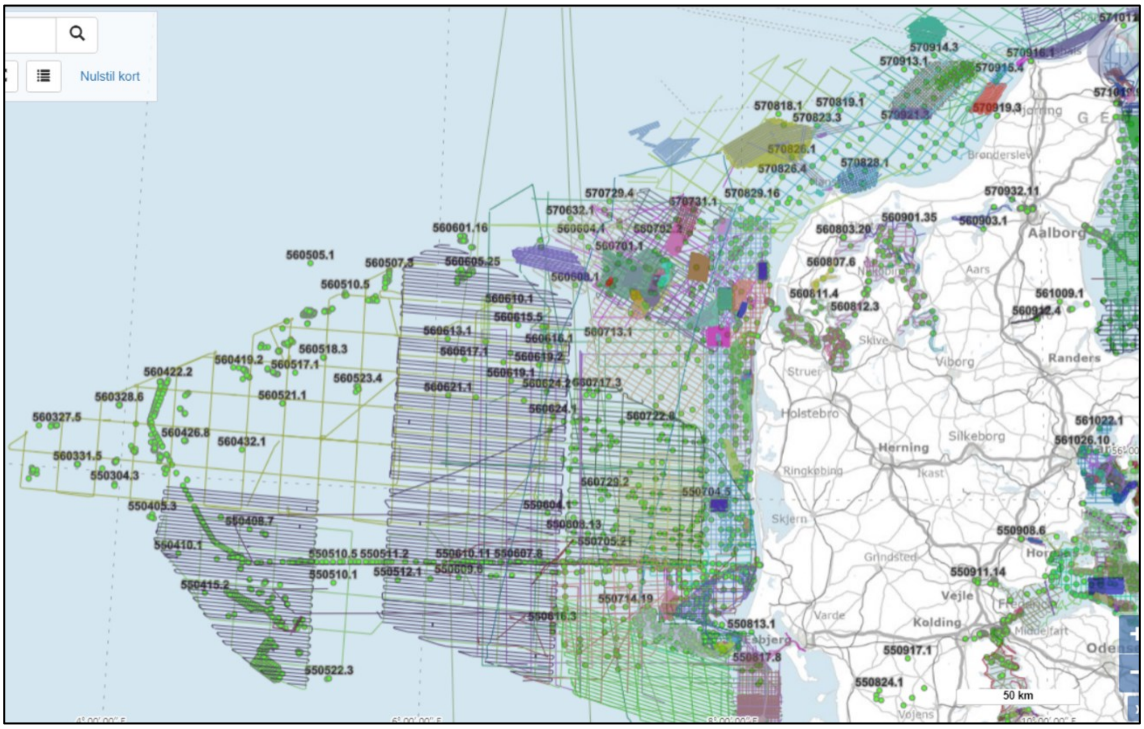

Figure 4-1. Shallow seismic lines and sediment core sites in the Danish North Sea area (from GEUS' Marta database).

4.3 Ongoing work on raw materials mapping

GEUS is currently reporting recent raw material mapping activities in the Danish North Sea area for the EPA including new shallow seismic data and sediment core data acquired in the study area in 2019 and 2020, respectively. The results of these investigations are not published yet, but the data and interpretations has been part of the basis for this screening study.

5. Geological setting

The North Sea is a shallow epicontinental sea on the European continental shelf, located between the British Isles and the mainland of northwestern Europe (Norway, Denmark, Germany and the Netherlands). It is connected to the Atlantic Ocean through the English Channel in the south and the Norwegian Sea in the North.

Today the water depth of the Danish North Sea is steadily increasing from 10-30 m in the eastern parts along the Danish west coast, and up to 80 m to the west in the Central Graben. In Skagerrak the water depth increases towards Norske Rende in northwest with the greatest depths in Danish waters being 500 m, while Dogger Banke is a large shallow area in the central part of the North Sea with 25 to 35 m water depth, see Figure 5-1.

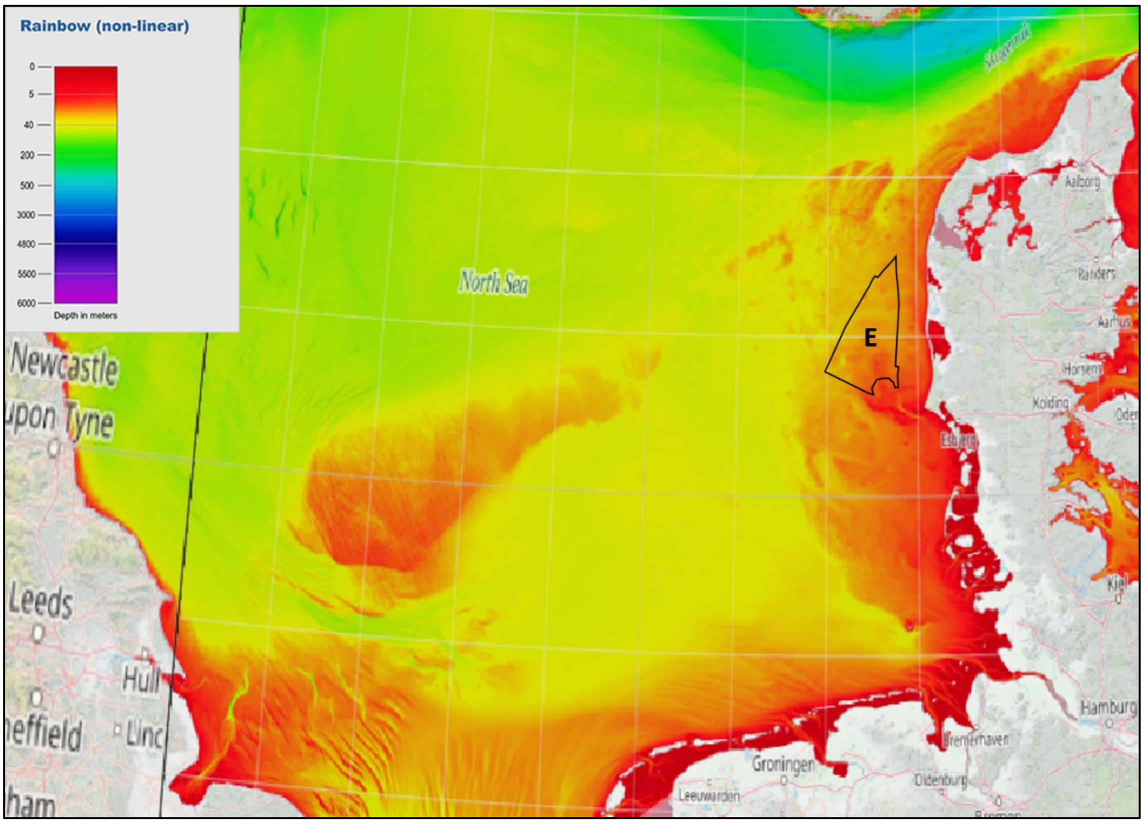

Figure 5-1 Bathymetrical map of the North Sea (From EMODnet). The black polygon shows the area E in the Danish North Sea.

5.1 Regional geological framework

About 150 million years ago during the Jurassic and Cretaceous periods, the rifting that formed the northern part of the Atlantic Ocean, caused tectonic uplift of the British Isles. Since then, a shallow sea has almost continuously existed between the highs of the Fennoscandian Shield and the British Isles, growing and shrinking with the rise and fall of eustatic sea level during geological time.

The deep tectonic structures in the North Sea area are dominated by the Ringkøbing-Fyn basement high and graben structures formed by rifting associated with the Alpine orogeny to the south.

The screening area is situated over the southern rim of the Danish Basin on the Ringkøbing-Fyn basement high and with the Horn Graben to the west (Figure 5-2). The area appears to be very calm in terms of seismicity from earthquakes, especially compared to the area just north of the screening area (Figure 5-3).

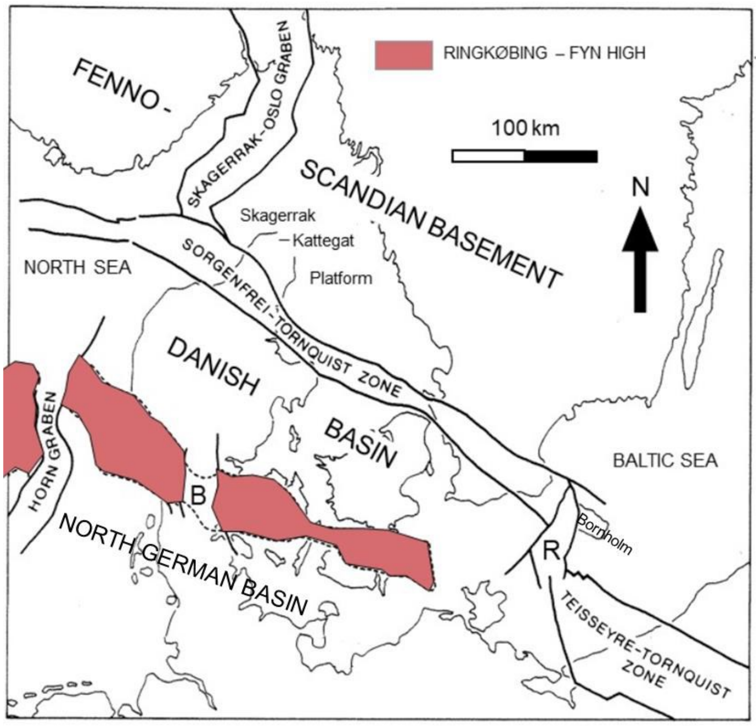

Figure 5-2 Structural elements of the Danish subsurface showing the Ringkøbing–Fyn High (red color) and the Horn Graben (from Gravesen et al., 2021).

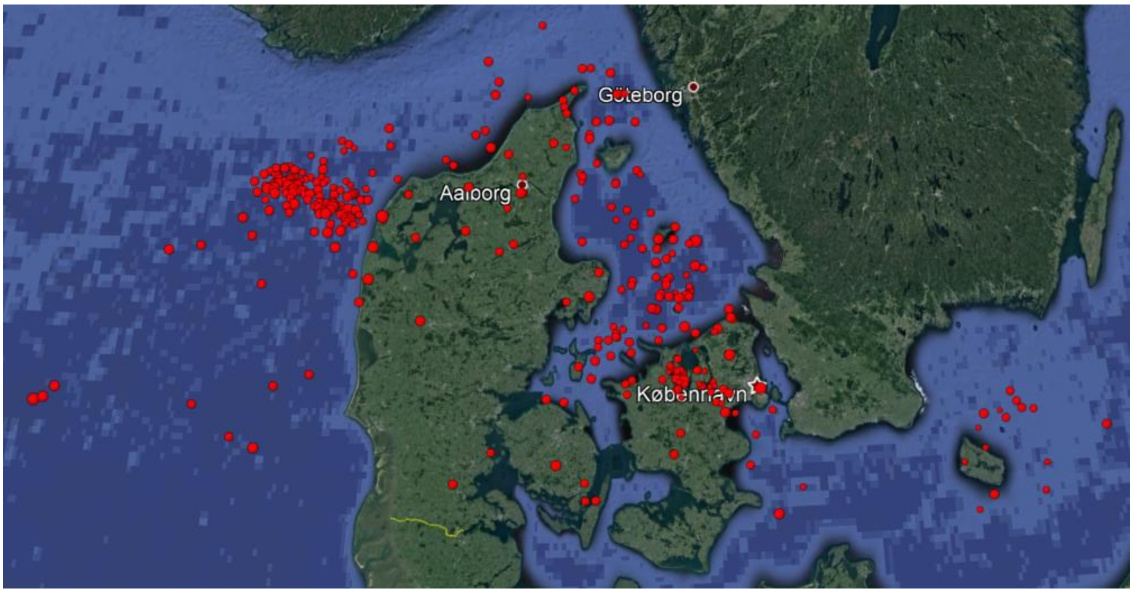

Figure 5-3 Seismicity in Denmark for the period 1930-2018 from GEUS earthquake database. Red dots show earthquake epicenters all determined using data from a minimum of three seismic stations. In addition to earthquakes the map may show data related to explosions which have not been removed (GEUS, 2018).

5.2 Pre-Quaternary deposits

The oldest deposits in the screening area are probably sandstones and claystones of Lower Permian age to the north and sandstones, claystones and shales of Triassic age to the south. The Permian and Triassic deposits are followed by Upper Jurassic and Lower Cretaceous claystones and sandstones and marl and claystones, respectively.

No, or only thin, Zechstein salt deposits are expected in the screening area and no salt structures, while further north, in the central parts of the Danish Basin, salt deposits are common and may show large variations in thickness due to salt movements into salt diapirs and salt pillows (Peryt et al., 2010), see Figure 5-4.

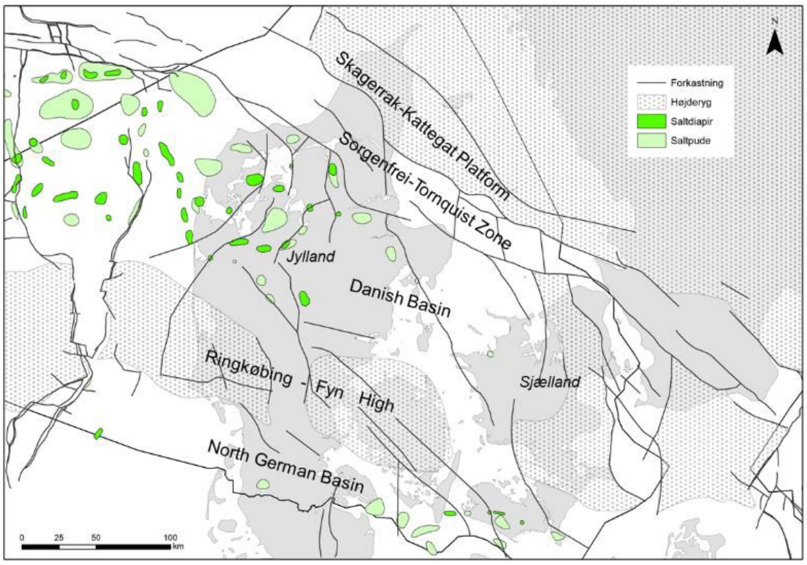

Figure 5-4 Map showing Zechstein salt pillows and diapirs in the Danish Basin (from Gravesen et al., 2021).

In Upper Cretaceous, the North Sea was covered by a relatively deep and warm sea, and an enormous production of calcareous organisms resulted in the deposition of a widespread and thick chalk sequence, also known from onshore exposures. By the end of the Cretaceous period, the sedimentary regime again changed to clastic deposits and during the Tertiary and Quaternary, primarily clay, silt and sand was deposited in marine and deltaic environments (Huuse et al., 2001; Rasmussen et al., 2005).

During Paleogene and first part of Neogene, sediment transport from the Scandinavian area into the North Sea basin from northeast and east was dominating. Onshore, west of the screening area, three phases of shoreline progradation into the basin in the Miocene gave rise to deposition of the sand-rich Billund, Bastrup and Odderup Formations, intercalated with the clayey and silty marine Vejle Fjord, Klintinghoved and Arnum Formations (Rasmussen et al., 2010).

Later in Neogene, about 5 mill. years ago, the source of sediment transport into the North Sea changed to more southern areas. These include the Eridanos deltasystem sourced from the Baltic Sea area and the later paleo-Elbe system (Overeem et al., 2001; Ottesen et al., 2018).

5.3 Quaternary deposits

The Quaternary deposits in the North Sea are mostly of glacial origin in pro- or subglacial depositional environments intercalated with marine fine-grained sediments from the warmer interglacial periods with raised sea level.

The base of the Quaternary forms a marked erosional surface and lies relatively shallow in the eastern part of the North Sea. Here, the thickness of the Quaternary deposits is typically only some tens of metres but increasing to the west and up to more than 1.000 m in the Central Graben (Nielsen et al., 2008), see Figure 5-5.

The North Sea was covered by the Scandinavian Ice Sheet several times during the Quaternary with the oldest traces of glaciations from c. 2,6 million years ago (Menapian, Elsterian, Saalian and Weichselian ice ages), see Figure 5-6. During the glaciations clay tills and sandy tills with stones and boulders were deposited as well as large volumes of sand in meltwater rivers and clay and silt in ice dammed lakes.

Between the ice ages, interglacial periods occurred (Cromerian, Holsteinian and Eemian) with a mild climate and deposition of marine sediments in the North Sea. Eemian marine fine sand, silt and clay appears in many areas and deposits from the older interglacials have also been found.

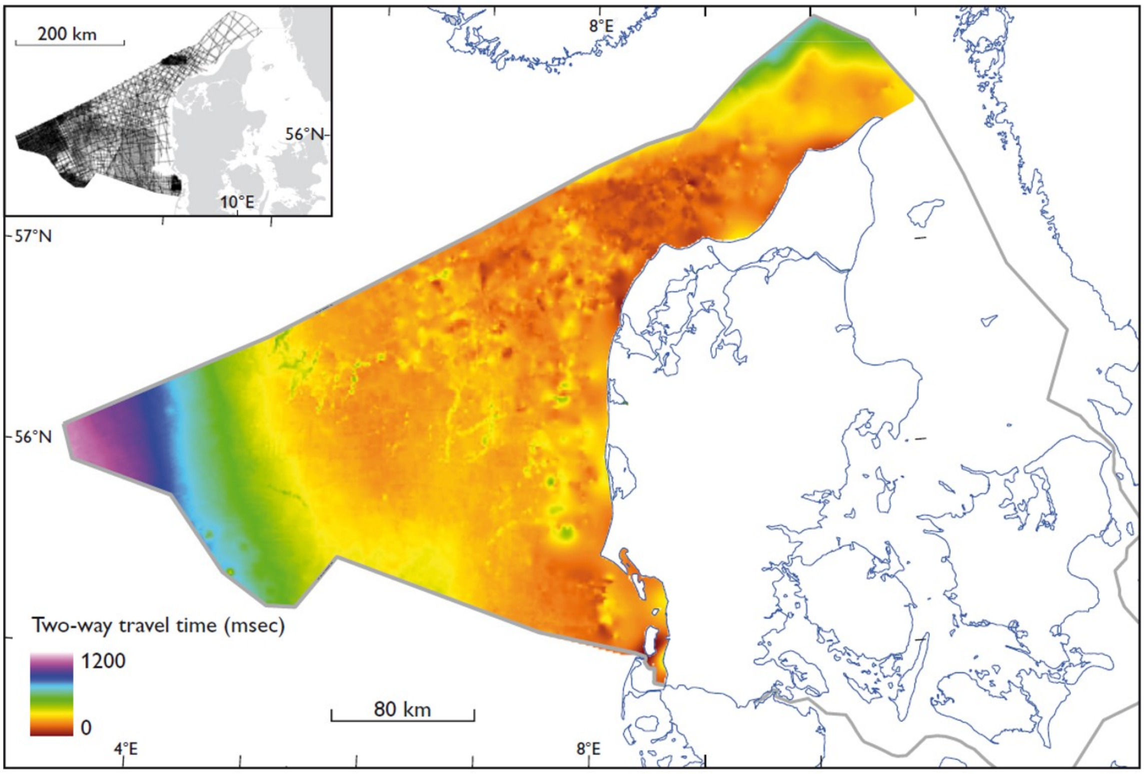

Figure 5-5. The depth to the base Quaternary surface in the Danish North Sea shown in seismic two-way travel time in milliseconds below sea surface (from Nielsen et al., 2008).

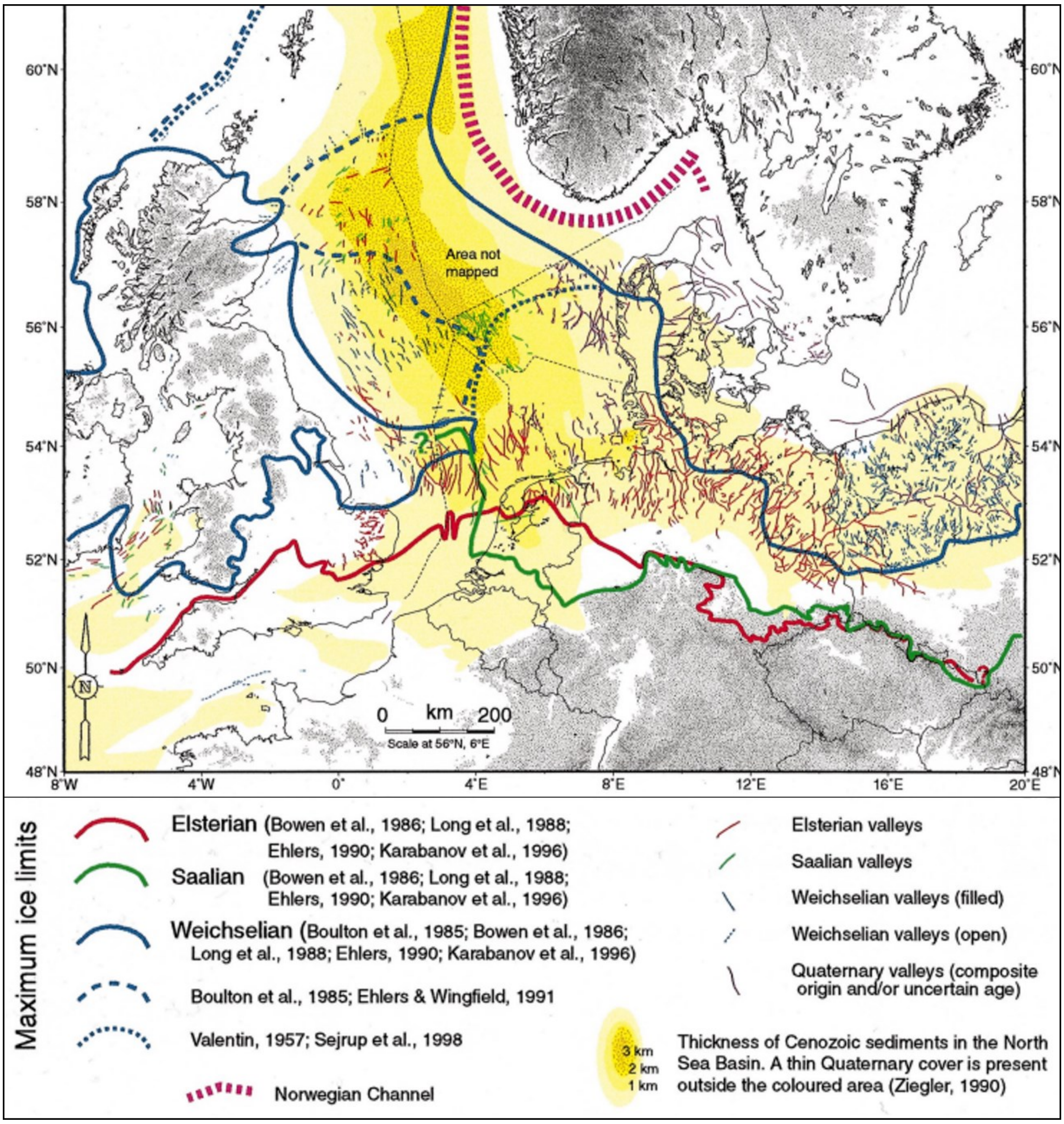

Figure 5-6. Estimated maximum ice sheet limits and mapped buried valley systems of the last three major glacial periods in the North Sea (from Huuse & Lykke-Andersen, 2000).

Drainage of meltwater from the ice sheet formed large and widespread tunnel valleys and channel systems in the North Sea area, often eroded deeply into the underlying pre-Quaternary formations (Huuse et al., 2001; Prins et al., 2020), and later filled with sediments and now appearing as so-called buried valleys or paleo-channels, see Figure 5-7.

The sediment infill of the buried valleys is generally heterogeneous and can vary from till to well sorted sand and gravel and lacustrine-marine clay deposits (O Cofaigh, 1996), while the deposits in the fluvial channels can also vary, but often contain well sorted, coarse-grained clastics (Gibling, 2006) and in places peat formations rich in organic material (Coughlan et al., 2018; Hepp et al., 2017).

Another phenomenon related to the glaciations is glaciotectonic deformations in terms of folding and thrust faults as seen e.g. in Fanø Bugt, northwest of Horns Rev, and in Jammerbugten and formed by glacier ice moving westwards.

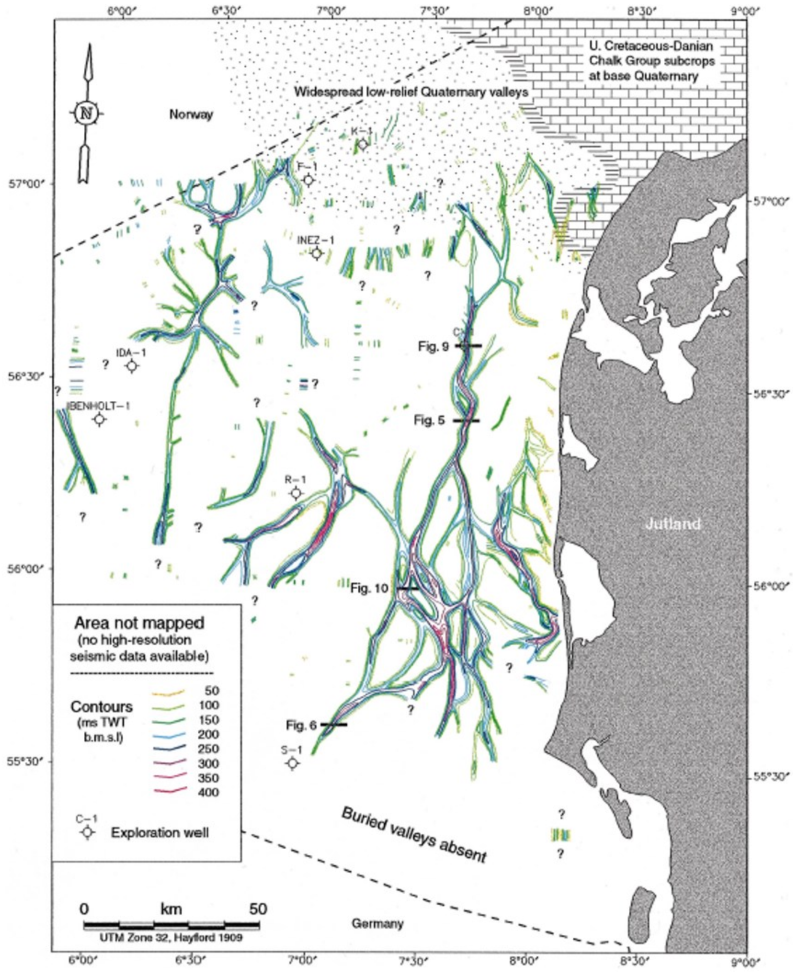

Figure 5-7. Mapped buried valleys in the eastern Danish North Sea (from Huuse & Lykke-Andersen, 2000a). See Figure 6-8 for close-up and location of screening area.

During the latest glaciation (Weichselian), the relative sea level was generally low, and sandy fluvial deposits and clayey lake sediments are dominating, but glaciomarine deposits show that marine conditions occurred in the deeper part of the Danish North Sea around 30.000-50.000 years BP (Knudsen, 1985; Larsen et al., 2009).

In late glacial time, the sea covered Skagerrak and the northern parts of the Danish North Sea, where the thickness of the ice sheet was at its maximum during the last glaciation and pressing down the crust. Local lakes with deposition of clay and gyttja existed in the more shallow parts of the North Sea and peat deposits have been found throughout the North Sea from this period.

From about 10.000 years BP the sea further transgressed into the North Sea, and during the next thousands of years, the current extent of the North Sea was formed. In the same period, the English Channel was inundated and the pattern of sea currents we know today was established and is now dominating the Norths Sea together with tide and wave energy.
Deposition of sand is taking place along coastal sandbars and shallow banks with high energy level and the northbound Jutland Coastal Current is important for the transport of

sediment along the Westcoast of Denmark (Anthony & Leth, 2002), while fine-grained material primarily is deposited in the deeper central parts of the North Sea (Bockelmann et al., 2018).

5.4 Late Quaternary stratigraphic model

Larsen & Andersen (2005) has established a stratigraphic model for the southern part of the Danish eastern North Sea, including the Horns Rev area, and providing a good understanding of the late Quaternary geological development also in the current screening area situated north of Horns Rev (Figure 5-8).

The pre-Quaternary is most probably composed of undeformed strata of Miocene age (Huuse & Lykke-Andersen, 2000b; Andersen, 2004). Above the pre-Quaternary surface is a lower glacial unit of Saalian and/or older age, and the top of this unit is correlated with the Saalian hill island landscape onshore western Jutland and to the surface of the Vovov hill island off Blåvands Huk.

In the Fanø Bugt area and northwest of Horns Rev, this lower glacial unit is disturbed by glaciotectonic deformation and forms thrust complexes also comprising sediments of Miocene age and/or with soft Miocene clay acting as décollement layer. It is likely that the same ice advance that caused the deformation, subsequently eroded the top of the thrust sheets and deposited a unit of meltwater sediments and a heterogenous glacigenic unit in connection with retreat and re-advance.

The Saalian (or older) lower glacial unit forms a bank about 30 km offshore Blåvand Huk (Vovov hill island) and between the bank and the shore, the surface of the Saalian glacial landscape forms a wide depression c. 50 m below sea level, see Figure 5-8. This basin has controlled deposition in the area since the late Saalian and is filled with sediments of late Saalian, Eemian, Weichselian and Holocene age.

In the central parts of the basin, a 10-20 m thick layer of late Saalian meltwater sediments are deposited followed by up to 13 m of Eemian marine deposits of silty clay and sandy silt corresponding to a sea level high-stand, where the sea covered almost the entire area, except the Saalian glacial deposits at the Vovov hill island. In the lower part of the succession freshwater deposits has been observed.

During the Weichselian, the sea level dropped again, and the area became land with rivers and lakes. The Weichselian ice sheet did not reach the southern part of the Danish North Sea, but it is generally assumed that the large alluvial outwash plains west of the ice margin in central Jutland extended into the North Sea area through valleys in the old Saalian landscape (Houmark-Nielsen, 2003). Thus, Weichselian meltwater sediments covering the Eemian deposits in the area are probably remnants of distal alluvial cones mostly fed from north and east.

In Holocene, the sea transgressed the area again, re-establishing the sedimentary basin. Early Holocene freshwater sediments with plant remains are occasionally noted in small depressions, but are followed by marine Holocene sand and clay layers formed by erosion and subsequent redeposition, as the area was inundated. The youngest unit in the area is a widespread 1-2 m thin mobile and dynamic surface layer of sand.

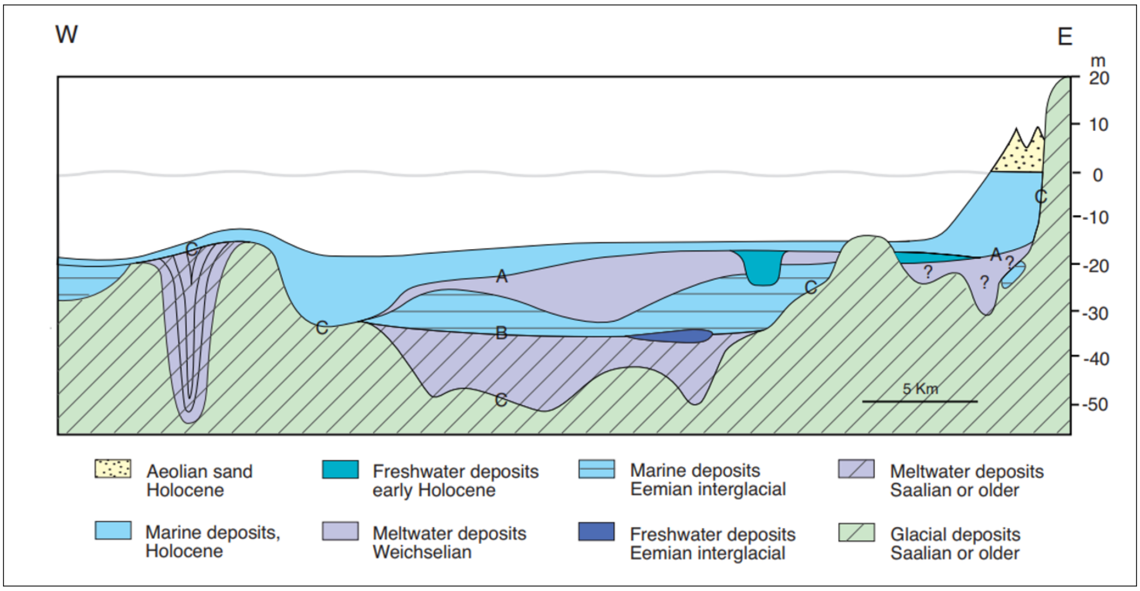

Figure 5-8. Schematic W-E profile across the wide basin in the Saalian landscape north of Horns Rev (approx. 55° 45' N). C marks the surface of the lower glacial unit of Saalian (or older) age and correlated with the Saalian hill island landscape onshore western Jutland and the Vovov hill island off Blåvands Huk. B marks the surface of a late Saalian meltwater unit. A marks the base of Holocene deposits (from Larsen & Andersen, 2005).

6. Data and geological conditions of screening area

The shallow geology of the screening area is characterized by late Quaternary glacial and interglacial deposits overlain by a variable cover of Holocene marine deposits.

Pre-Quaternary strata, most likely of Miocene age, comprise the basement to the Quaternary deposits generally located >50 m below the seabed. Glacial deposits are presumably of Saalian or older glacial origin. A complex system of buried valleys of different magnitude characterises the glacial unit and superimposed non-marine sand units are possibly of late Saalian origin. Eemian (last interglacial) marine deposits probably covered much of the glacial landscape, but later erosion has removed larger parts of the unit. Proof of an Eemian age is based on scientific studies using micropaleontological evidence and absolute dating (Konradi et al., 2005; Cohen et al., 2021). Superimposed Weichselian meltwater sand and silt/clay deposits represents large sandur plains and lake systems, which characterised the area during the late Weichselian period, when several Scandinavian ice sheet front systems reached the central part of Jutland.

Following the final ice sheet retreat and general climate amelioration, a tundra landscape in the late glacial period was substituted by a forest covered swamp and hill landscape with local fluvial streams. From about 9.000-7.000 years BP the area was progressively transgressed by the North Sea. During the first thousand years, the relatively shallow sea in the area may have been characterized by an isthmus and islands of higher-lying glacial deposits causing local sheltered marine- to brackish sea areas. However, as the sea rose, the entire area was inundated, and by establishment of the Jutland Coastal Current and increasing exposure to the harsh wind and wave conditions from the North Sea, the seabed was exposed to selective erosion and deposition of late Holocene marine sand units, which was intricately related to the circulation and dynamic sediment transport pattern around Horns Rev.

6.1 Bathymetry

The bathymetry of the screening area varies between c. 18 m in the shallowest southern part and about 32 m in the northern and western tip of the area (Figure 6-1). Two more or less parallel shallow sand bank areas in the south are progressively getting deeper towards the north.

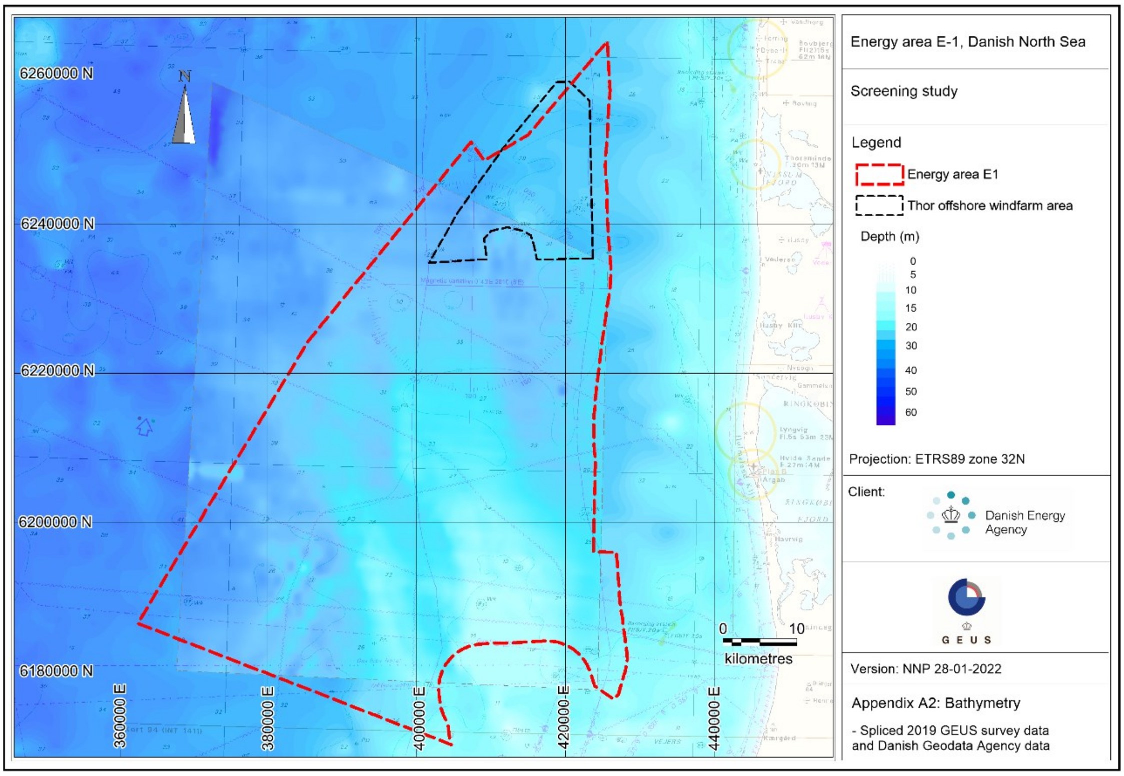

Figure 6-1. Bathymetry of screening area based on 2019 GEUS survey data overlain on background bathymetry data from the Danish Geodata Agency. Appendix A2.

6.2 Seabed surface sediments

The seabed surface sediment map shows that the screening area is dominated by a sandy seabed (Figure 6-2). Gravelly sand is second most common and occur in large irregular long stretched bands in the southwestern part of the area as well as in parts of the Thor windfarm area. Stone covered moraine/till seabed occurs only in relatively small areas (< 5 km^2), typically associated with the gravelly sand areas. Quaternary clay/silt (often semi-consolidated) have been identified in the central to eastern part of the Thor area. Fine-grained silty sand is observed in the southeasternmost part of the area.

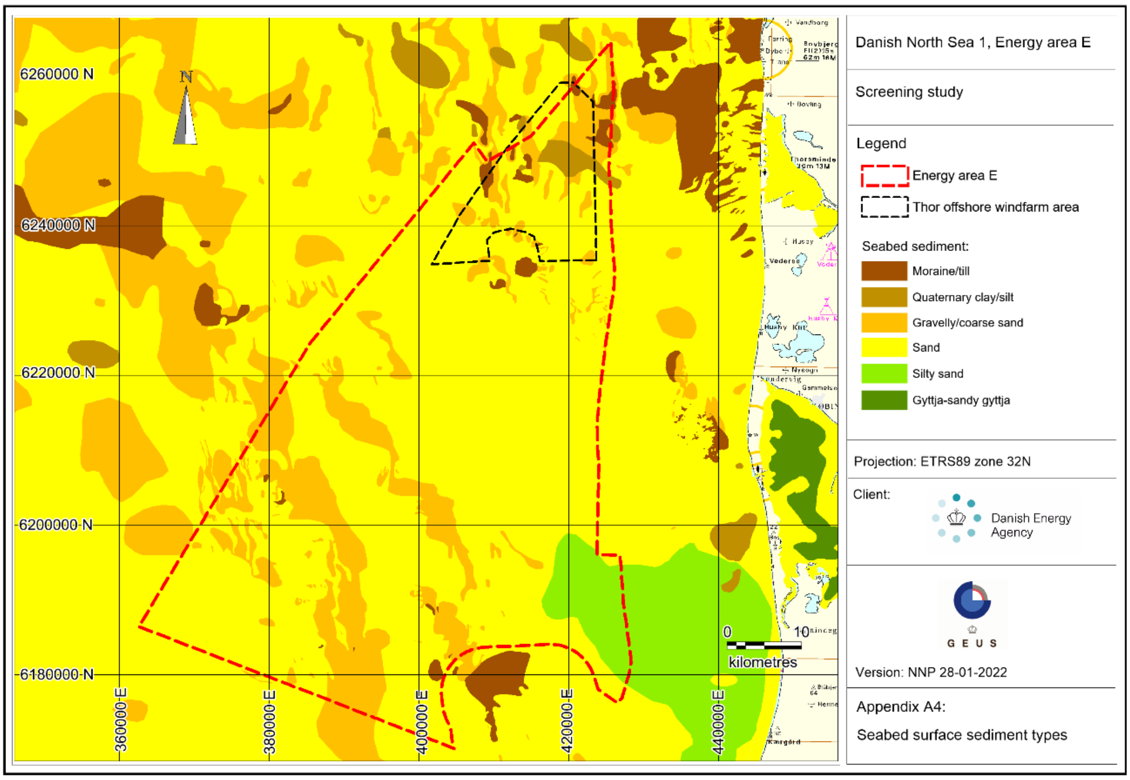

Figure 6-2. Seabed surface sediment map of the screening area (from GEUS' Marta database). Appendix A4.

6.3 Sediment cores

180 sediment cores located in, and adjacent to, the screening area were used for verification of seismic interpretations and general description of the shallow geology (Figure 6-3). Appendix C contains a list of all sediment cores including GEUS Marta database link to a detailed core description for each core. The cores are mostly vibrocores less than 6 m in length. However, longer cores up to c. 50 m in length from the Horns Rev 3 windfarm area also exist.

Figure 6-4 show examples of descriptions of typical vibrocores. Cores 550706.21 and 560722.8 contain glacial and late glacial deposits overlain by early Holocene freshwater peat, marine gyttja and sand. Cores 550701.3 and 550723.5 contains glacial till (Saalian?) overlain by Eemian marine silty clay with numerous shells, Weichselian meltwater sand (termed late glacial in descriptions) and Holocene marine sand and gravel. Core 560730.4 contains meltwater sand and silt (possibly Weichselian) overlain by Holocene marine sand.

Figure 6-5 shows a description of one of the 50 m long sediment cores from the northern part of the Horns Rev 3 windfarm area, immediately to the south of the screening area. The core reveals Miocene sand and clay up to 36 m below sea floor (possibly a glaciotectonically dislocated floe). The Miocene sediments are overlain by a thin stony layer and sand up to 28 m below sea floor. Above this, an 18 m thick dark grey clay layer with shell fragments is found. The clay has been assessed to be of Holocene age, but in light of other scientific geological studies from the Horns Rev area, it appears likely that the marine clay unit is of Eemian age. Above the clay layer, 10 m slightly gravelly Holocene marine sand is found.

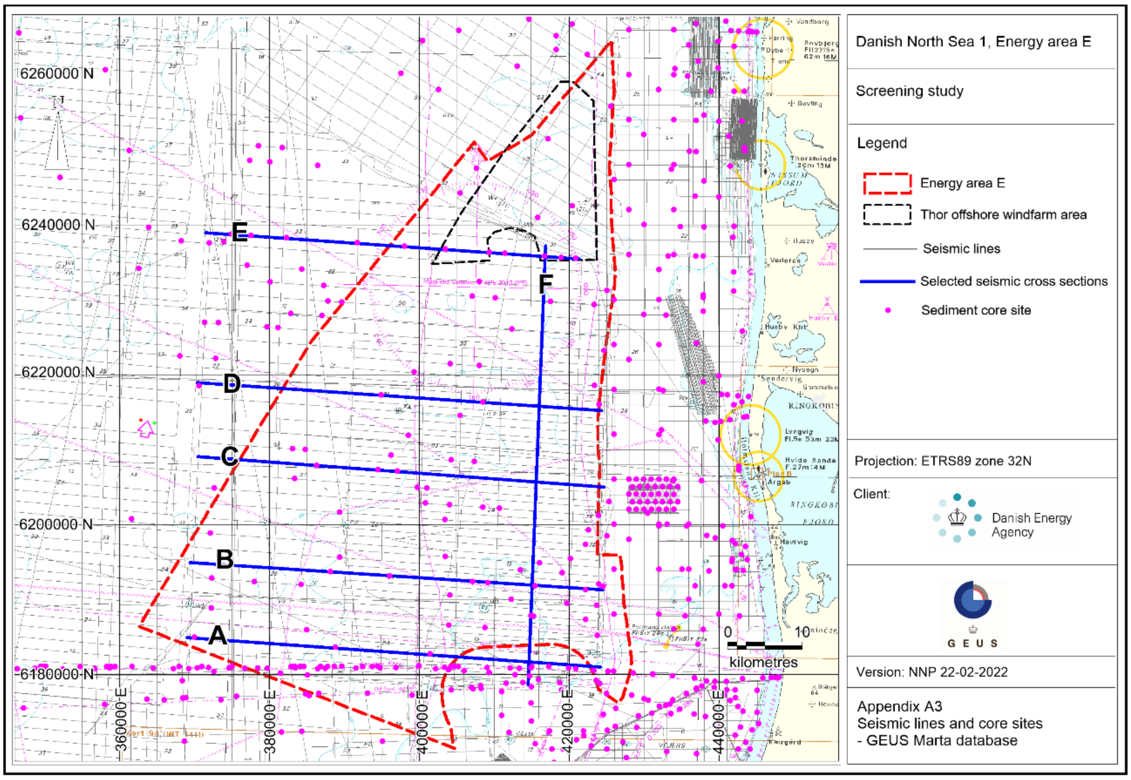

Figure 6-3. Seismic lines and sediment cores in and adjacent to the screening area. Lines A-F are selected lines shown in Appendix B. Appendix A3.

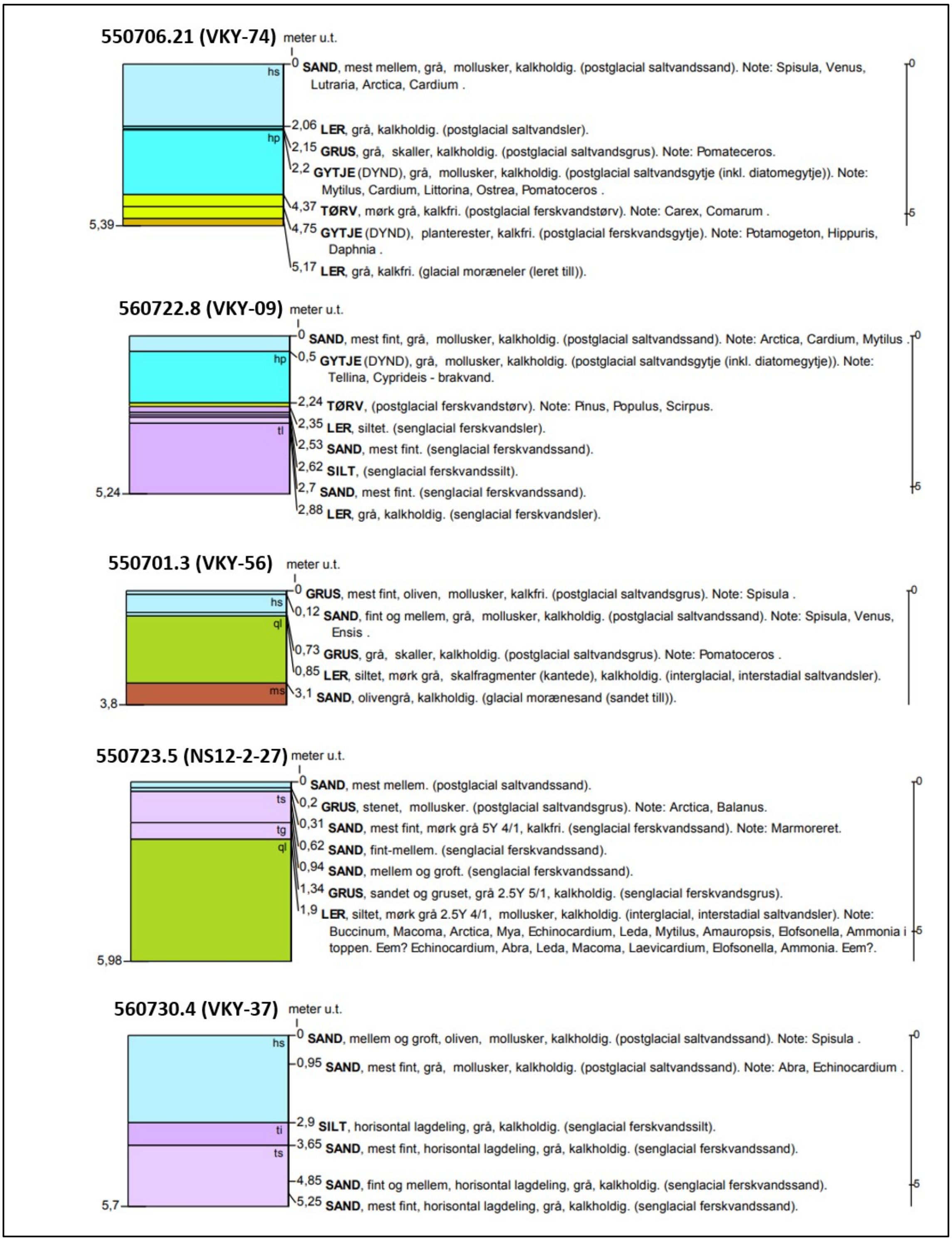

Figure 6-4. Examples of vibrocores up to 6 m long from the screening area (see Appendix C for further descriptions).

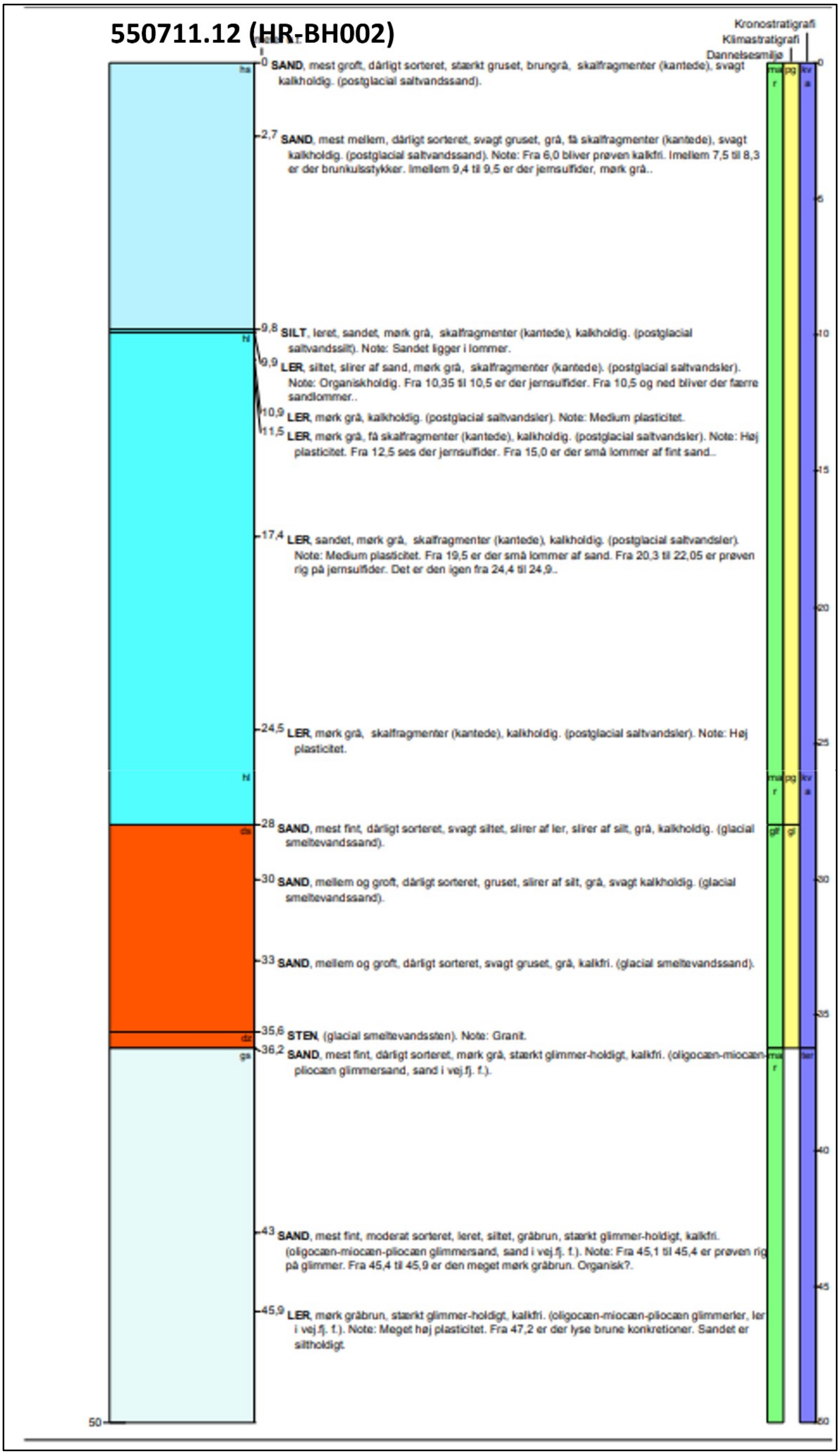

Figure 6-5. Example of 50 m long core from the northern part of the Horns Rev 3 wind farm area.

6.4 Seismic data

Seismic single channel sparker data from two regional raw material surveys for the EPA performed by GEUS in 2012 and 2019 was used for the screening study (Figure 6-3). The seismic data was reprocessed to enhance the signal/noise ratio. The 2012 dataset has a line distance of 2.5 km between east-west orientated lines, with few supplementary north-south orientated lines. The 2019 dataset which covers the central to eastern part of the screening area, has lines placed between the 2012 lines, reducing the line distance in this part of the area to about 1.25 km.

The single channel sparker data in the area generally allows detection of seismic reflectors down to about 50-60 ms TWTT (Two Way Travel Time) below seabed corresponding to about 40-50 m below seabed.

Processed seismic data in SEG-Y format was converted to 2DS-file format and analysed in the GeoGraphix seismic interpretation software. Seismic interpretation was performed with integration of available sediment cores, of which many was retrieved in 2020 as part of the regional raw material mapping for the EPA by GEUS.

6.5 Geological/seismic units

Seven distinct seismic units was identified and boundaries between units was traced on seismic profiles. Table 6-1 gives a general description of the seismic units as well as corresponding lithology (based on sediment core data), proposed depositional environment and stratigraphic age.

Table 6-1. Description of seismic units, corresponding lithology, depositional environment and estimated age.

Unit	Seismic reflection pattern	Lithology	Depositional environment	Age
1	Youngest unit, well defined medium amplitude parallel reflections, occasionally as sigmoidal fill of depressions	Mostly well-sorted sand with shell fragments, lower part more fine-grained at channel/valley fill sites	Shallow marine	Holocene
2	High amplitude reflection pattern, rare units in local depressions	Peat or gyttja sediment	Freshwater bog	Early Holocene
3	High amplitude reflection pattern with discontinuous and undulating reflections, lower boundary distinct undulating (erosive)	Sandy, occasionally gravelly, sediment alternating with fine laminated clay-silt units	Glaciofluviatile/-lacustrine meltwater plain	Weichselian
4	Transparent unit with low amplitude parallel reflections, where preserved, upper part with more distinct medium amplitude reflections	Silty clay with marine (interglacial) shells	Shallow marine	Eemian
5	High amplitude reflection pattern with discontinuous and undulating reflection, lower	Sandy, occasionally gravelly, sediment alternating with fine laminated clay-silt units	Glaciofluviatile/-lacustrine meltwater plain	Late Saalian

	boundary distinct undulating (erosive)			
6	Massive-chaotic reflections, distinct reflector marks upper boundary	Clayey-sandy till, buried valley fills and glaciotectonic units with more varied lithology: sand, silt, clay, gravel	Sub-glacial	Saalian or older glacial period
7	Parallel reflections, deformed and/or inclined layering is common	Well-sorted sandy to clayey sediment, often rich in mica minerals	Shallow marine-fluvio-deltaic	Pre-Quaternary (Miocene)

6.6 Seismic type profiles

Six long seismic sparker profiles A-F (Figure 6-3) were selected and presented with subdivision of main seismic units in order to demonstrate the variability of the seismic architecture in different parts of the screening area (Appendix B). The five west-east orientated profiles A-E are shown in Figure 6-6.

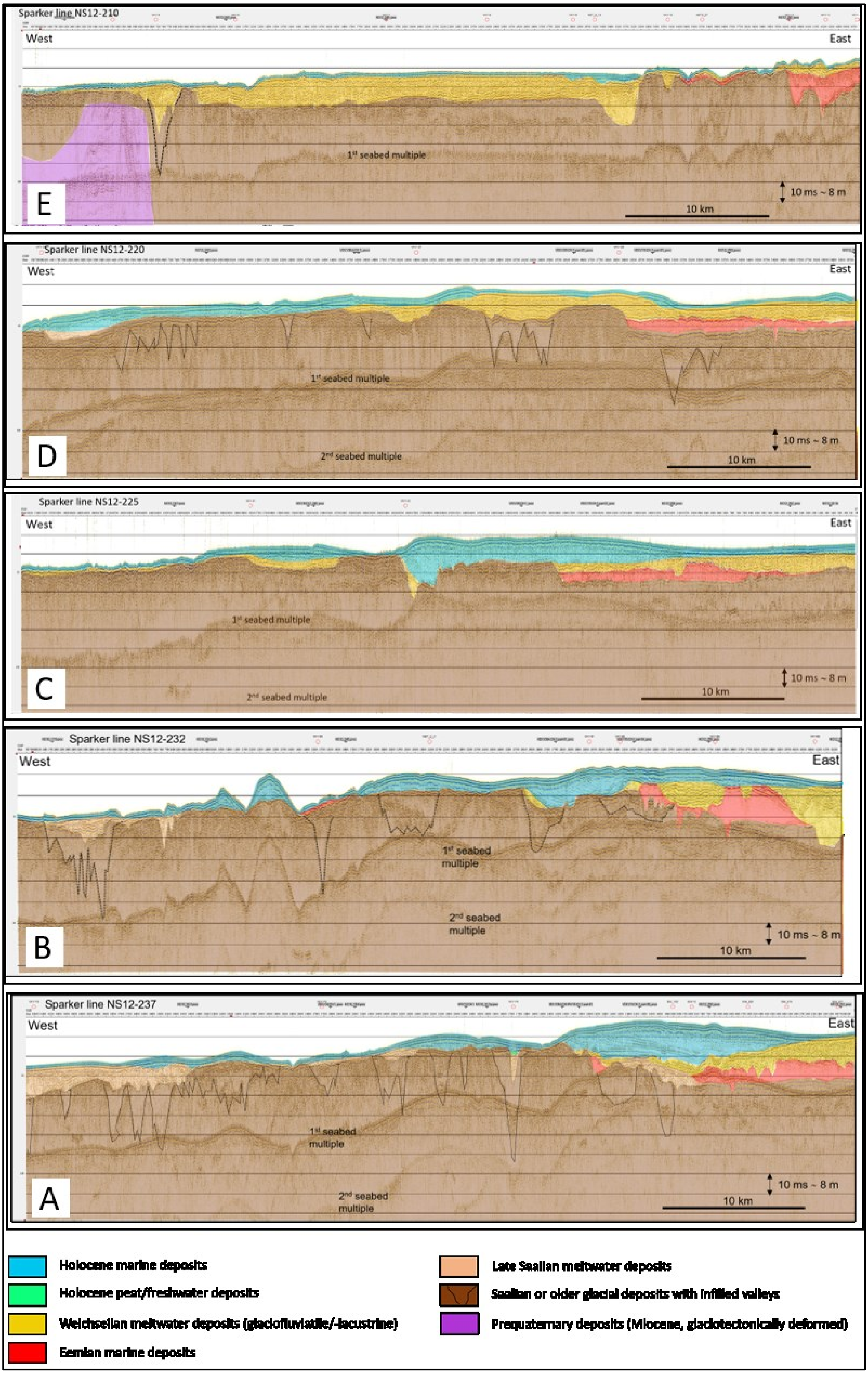

Figure 6-6. Interpreted seismic profiles with colouration of main seismo-stratigraphic units. Appendix B.

6.7 Conceptual geological model

A conceptual model of the upper 50 m of the subsurface geology of the screening area was established based on the interpretation of seismic sparker profiles verified by numerous sediment cores (Figure 6-7). The schematic geological cross section shows a high-lying Saalian glacial surface with in-filled valleys. In the eastern part, where the Saalian surface is lower, Eemian marine clayey deposits and Weichselian sandy meltwater deposits partly fill the accommodation space. On top of these, early Holocene marine, fine-grained deposits fill a channel-like feature. In late Holocene sedimentation continued with build-up of positive morphology sandy bar forms. This model appears in general to be in accordance with the stratigraphic model established for the northern Horns Rev area by Larsen & Andersen (2005) and described in section 5.4. In the western part of the screening area, erosional remnants of possibly both Saalian and Weichselian sandy meltwater deposits are found on top of the slightly lower Saalian glacial surface. The meltwater deposits are overlain by a thin cover of sandy Holocene marine deposits. Early Holocene freshwater deposits in the form of peat and gyttja appears to be very thin and only occurs locally in former landscape depressions.

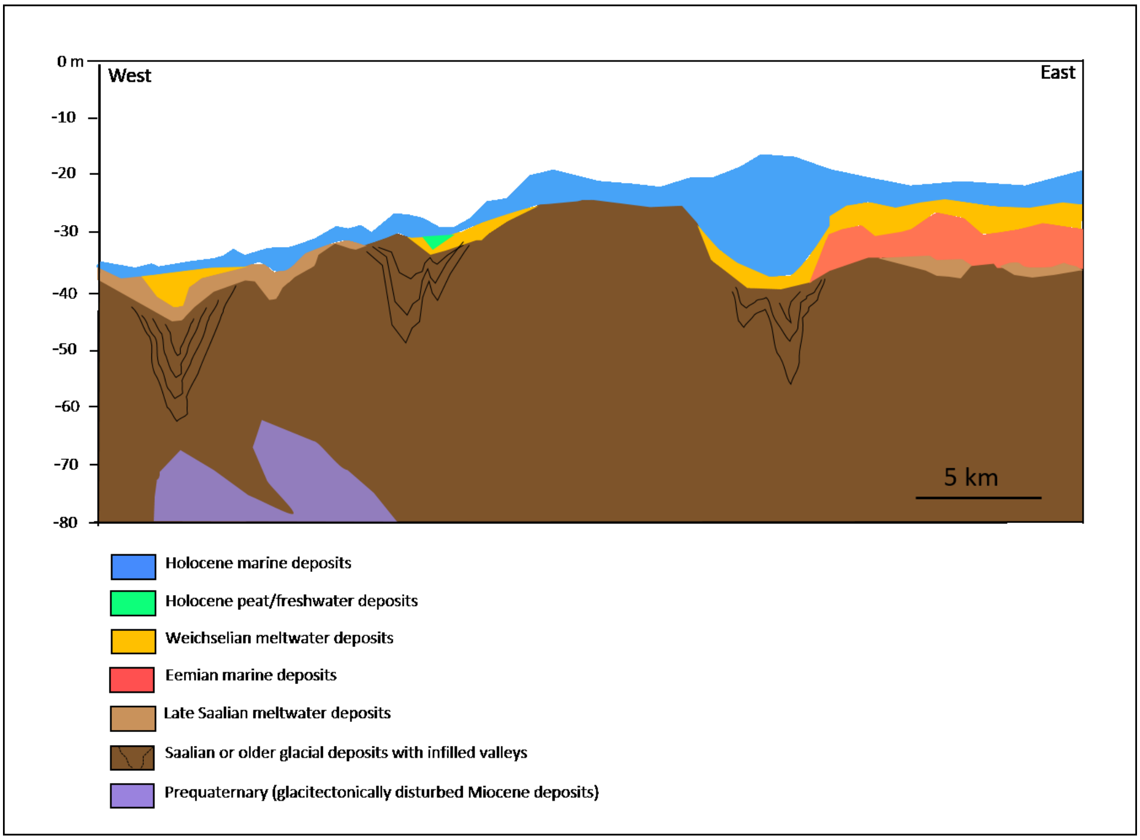

Figure 6-7. Conceptual geological model established for the screening area.

6.8 Buried Quaternary valleys

Large in-filled Quaternary channel systems or buried overdeepened valleys in the upper c. 100-400 m of the Quaternary succession have been observed in many parts of the North

Sea. The buried valleys are primarily interpreted as subglacial tunnel valleys, although some have also been identified as subaerial river systems (Gaffney et al., 2007; Cotteril et al., 2017). Tunnel valleys are assumed to drain towards the ice margin and are therefore used to interpret maximum ice sheet extent during glaciations. Detailed 3D-seismic studies have confirmed that the tunnel valley systems are often of composite nature, with rejuvenation of parts of the systems during subsequent glaciations.

Huuse & Lykke-Andersen (2000) mapped out the extension of buried Quaternary valleys in the eastern part of the Danish North Sea. The valleys can typically be followed over tens of kilometres, are about 1-5 km wide and incised to more than 300 m below present sea level. Figure 6-8 shows the distribution of mapped valleys in the screening area, and from this it appears, that buried valleys occur extensively in the eastern to central part of the area. Figure 6-9 from the central part of the screening area shows a high-resolution multichannel seismic profile of a buried valley truncating glaciotectonic thrust structures in the eastern part of the profile.

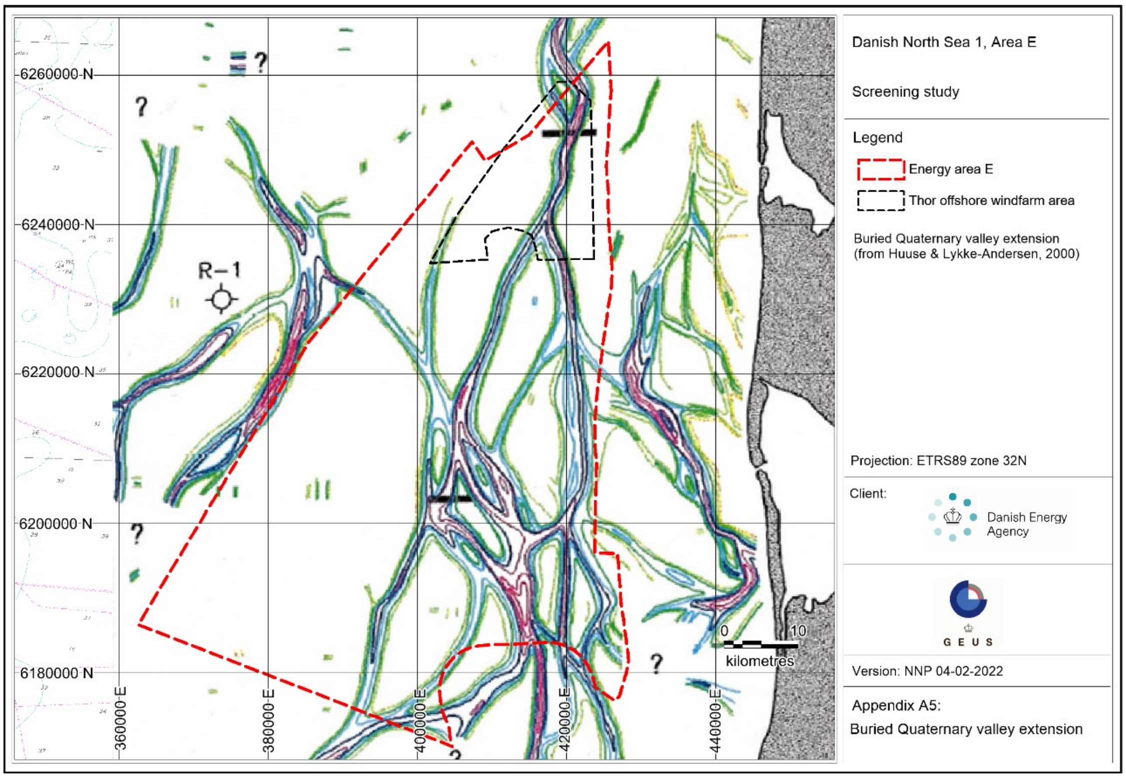

Figure 6-8. Mapped buried valley pattern in the screening area (modified from Huuse & Lykke-Andersen, 2000). Appendix A5.

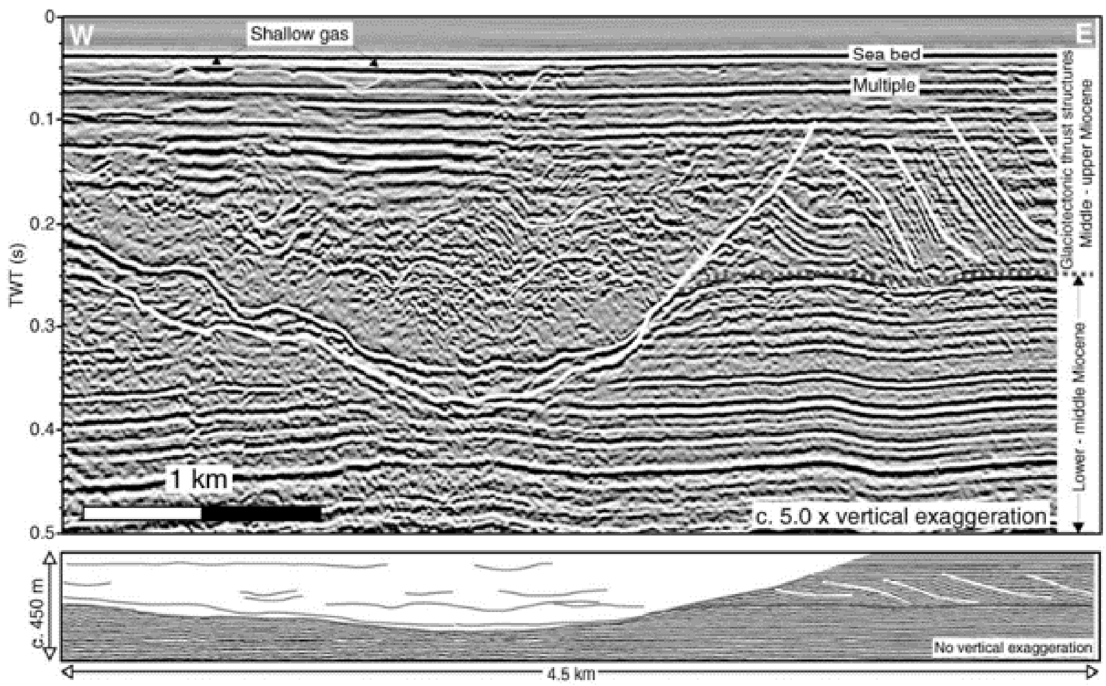

Figure 6-9. Example of multichannel seismic profile of a large buried valley eroding into pre-Quaternary layers in the central part of the screening area. The valley formation is postdating the formation of glaciotectonic thrust structures observed in the eastern part of the section (from Huuse & Lykke-Andersen, 2000).

6.9 Geological surfaces and isopach maps

The seabed and boundaries between main seismic units were interpreted on the available seismic profiles. Gridded data files of the seismic surfaces (xyz grid files) were produced and exported for visualisation in GIS software and subsequent production of isopach maps (thickness) of specific units as well as maps of depth below seafloor and below sea level of the seismic units.

The following maps are presented in Figure 6-10 to Figure 6-17 below, and in larger scale in Appendix A:
A11 - Top of Saalian or older glacial unit (depth below sea level)
A10 - Top of Saalian or older glacial unit (depth below sea floor)
A9 - Eemian unit thickness (isopach map)
A8 - Weichsel Meltwater unit thickness (isopach map)
A7 - Base of Holocene unit (depth below sea level)
A6 - Holocene unit thickness (isopach map)

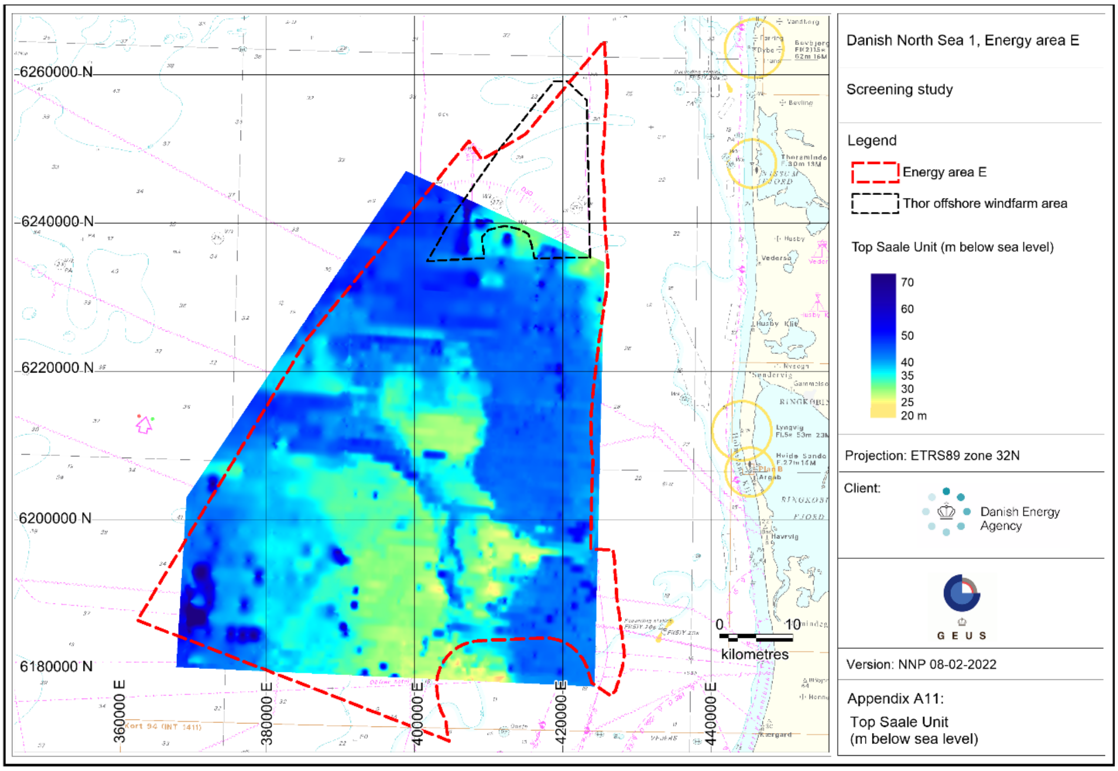

Figure 6-10. Mapped Top Saale Unit (m below sea level). Appendix A11.

The map in Figure 6-10 shows how the top of the Saalian or older unit lies deepest (c. 50 m below sea level) in the eastern, northern and westernmost part of the mapped area and more shallow in the central-southern part (c. 25-30 m below sea level).

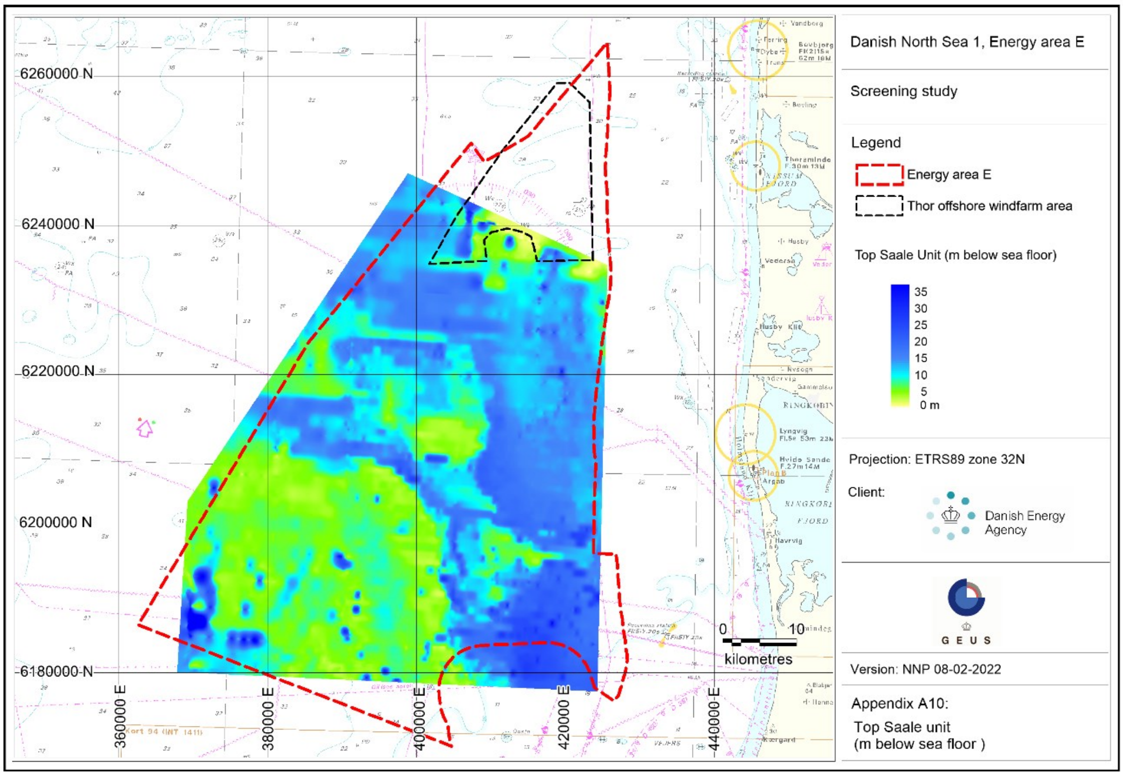

Figure 6-11. Mapped Top Saale Unit (m below sea floor). Corresponds to isopach map of superimposed deposits. Appendix A10.

The map in Figure 6-11 shows that the thickness of the deposits above the Saalian or older unit is up to 15-30 m in the eastern and northern part of the mapped area and around 5 m or less in the southwestern part. In Figure 6-12 the corresponding mapped base of non-glaciated layers in Thor OWF (COWI, 2021) is shown.

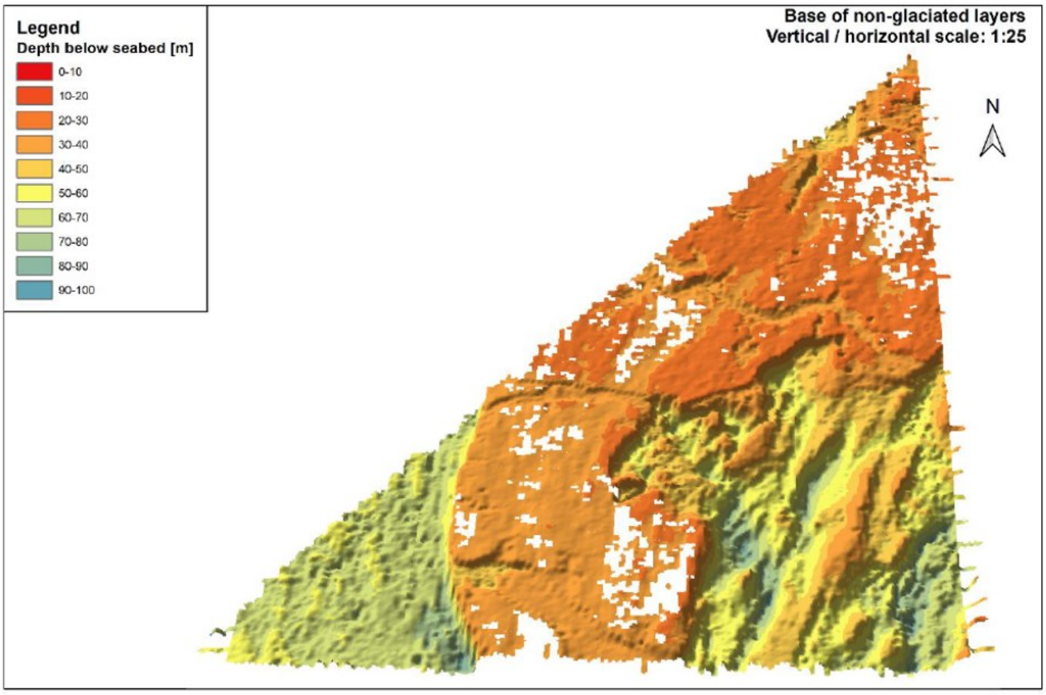

Figure 6-12. Detailed mapped base of non-glaciated layers in Thor OWF (COWI, 2021).

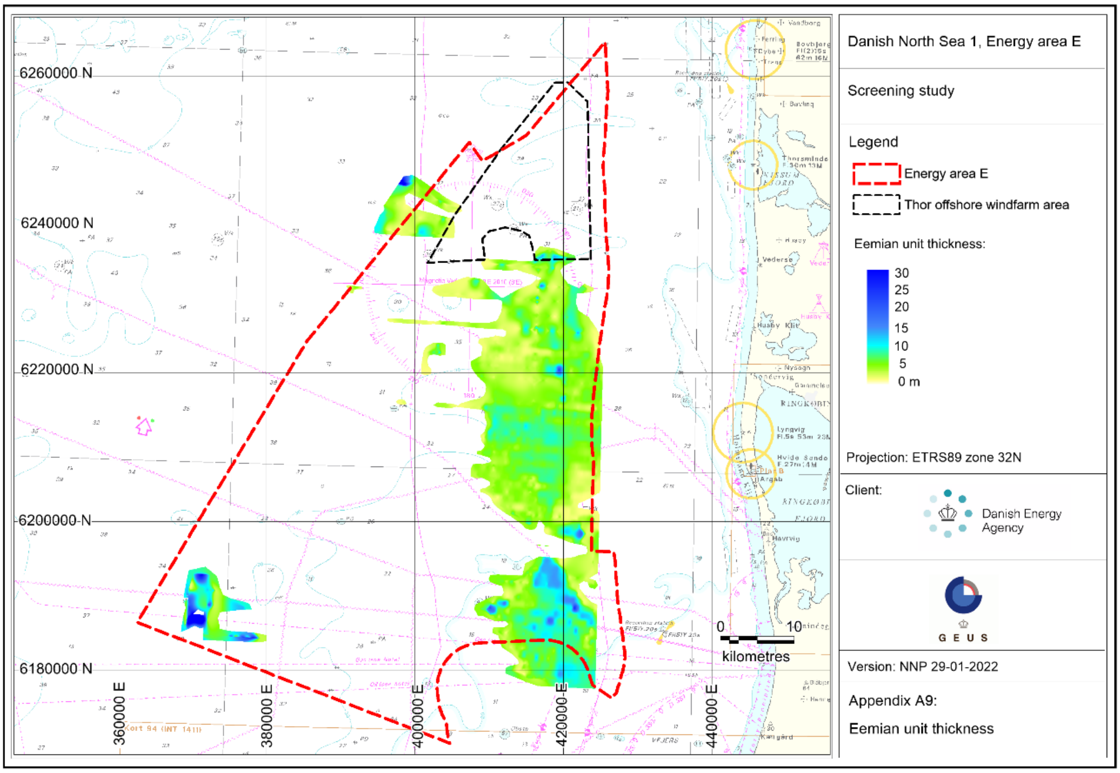

Figure 6-13. Mapped thickness (m) of Eemian Unit. Appendix A9.

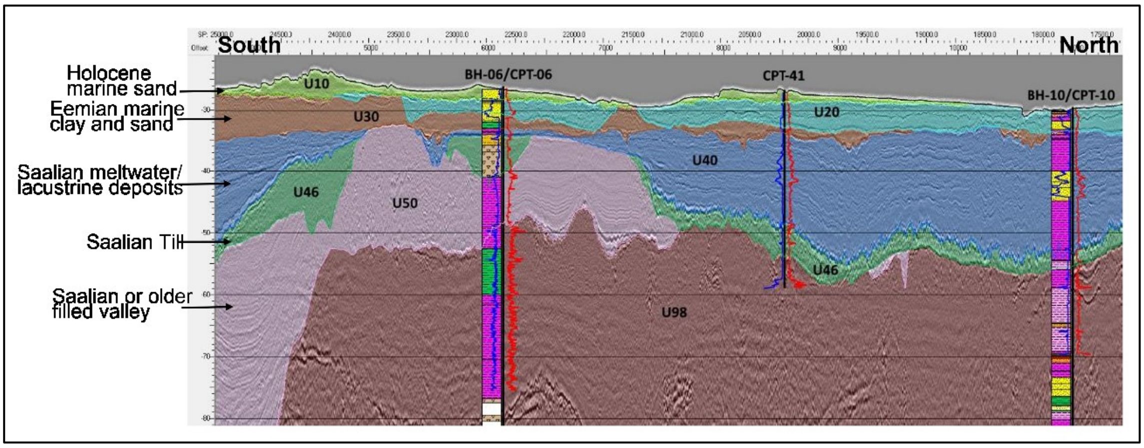

Figure 6-14. Thor OWF seismic profile from eastern part of area. Stratigraphic units have been labelled at left side of figure. Modified from COWI Report (2021.)

The map in Figure 6-13 shows that the Eemian unit is present in the eastern part of the mapped area with a thickness around 5-10 m and in places up to 15-20 m
as well as in the southwestern corner of the area, thus filling in the relief of the Saalian surface. Figure 6-14 shows that the Eemian unit U30 identified in the eastern part of the Thor OWF area is thinning from south to north.

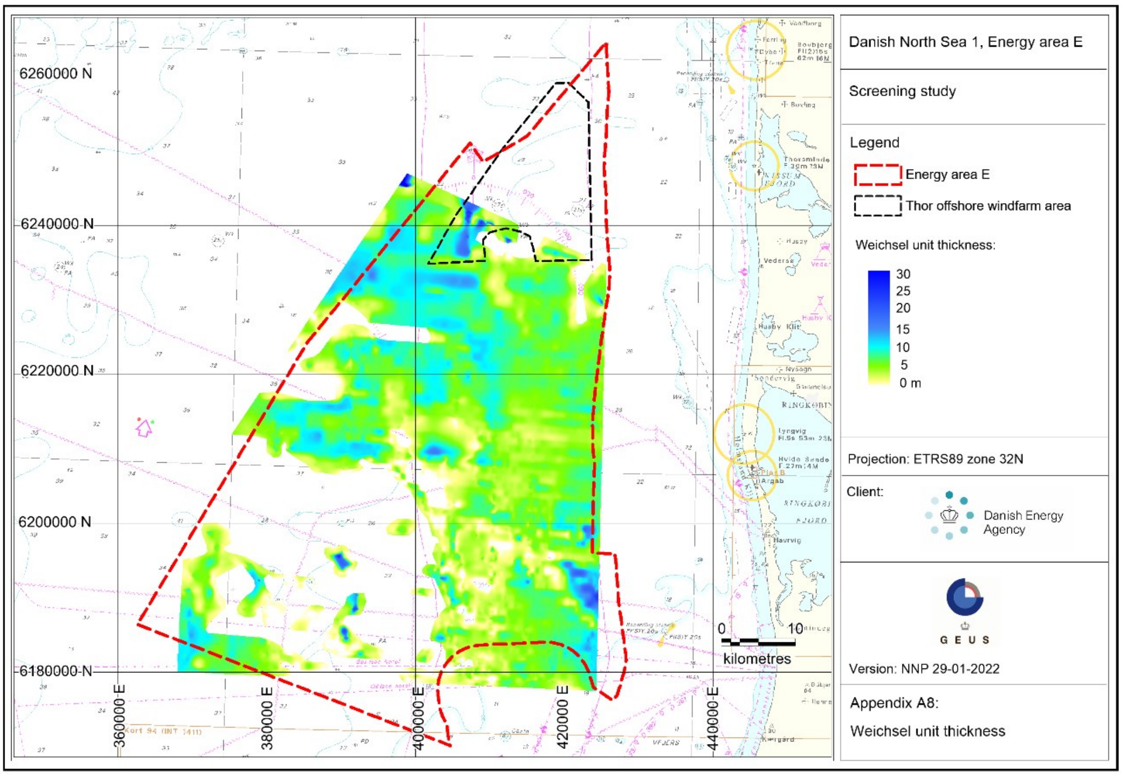

Figure 6-15. Mapped thickness (m) of Weichselian Meltwater Unit. Appendix A8.

The map in Figure 6-15 shows that the Weichselian unit is present in the eastern and northern part of the mapped area with a thickness around 5-10 m and in places up to 20 m or more as well as in the southwestern corner of the area with a thickness up to c. 10 m, thus filling in the relief of the Saalian surface.

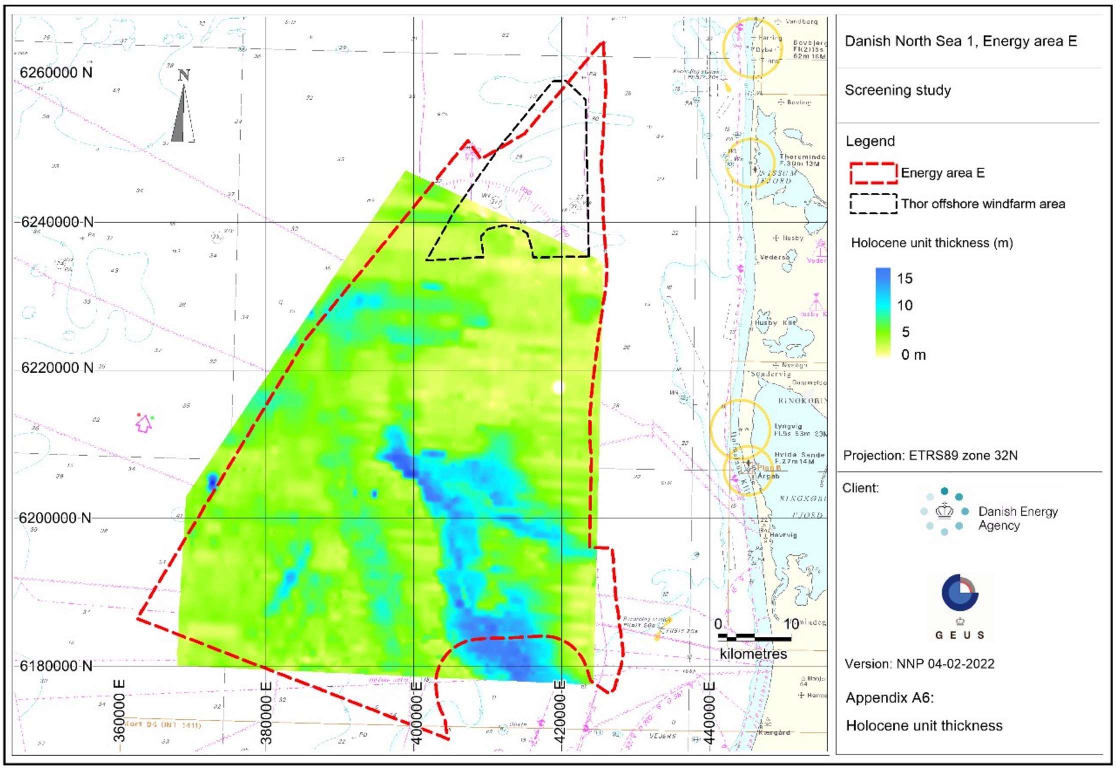

Figure 6-16. Mapped thickness (m) of Holocene Unit. Appendix A6.

The map in Figure 6-16 shows how the thickness of the Holocene unit is relatively uniform and just a few metres in most of the mapped area except in the central and southeastern part, where two longitudinal areas with a thickness of up to 15 m can be seen.

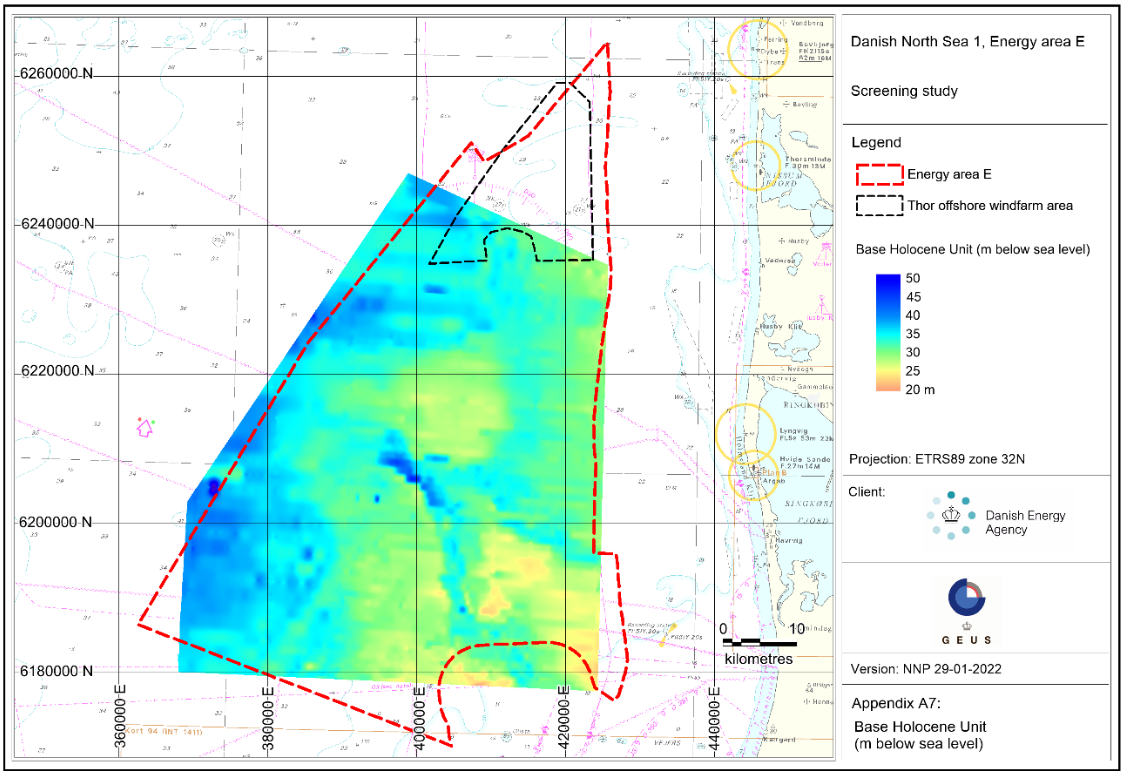

Figure 6-17. Mapped base of Holocene Unit (m below sea level). Corresponds to paleolandscape before Holocene marine transgression. Appendix A7.

The map in Figure 6-17 shows the relief at the base of the Holocene unit with the most shallow position of the base to the southeast around 20-35 m deepening towards northwest to around 30-45 m or more along the northwestern boundary of the mapped area. The relief of the mapped surface corresponds to the paleolandscape before the Holocene marine transgression of the area.

7. Key geological conditions

The screening has revealed geological conditions and sediment characteristics that may have implications for the assessment of wind farm foundation conditions. The following key geological characteristics are shortly discussed here:

- High-lying over-consolidated glacial sediments
- Glaciotectonic deformations
- Buried Quaternary valleys/paleo-channels
- Marine dynamic sand deposits
- Soft silty marine clays and gyttja
- Peat layers

With reference to Velenturf et al. (2021), some of the possible implications of these geological conditions are described below:

Soft sediments can imply a risk for low geotechnical strength and be a challenge for the foundation design. At the seabed, soft sediments can potentially be unable to bear large loads from e.g. a jack-up rig during construction.

Marine dynamic sand deposits may imply migrating erosional and depositional bedforms that can change the seabed topography over the operational lifetime of an OWF site in terms of scouring or burial of e.g. piles or cables.

The old glacial deposits may represent over-consolidated and strong sediments, which generally can provide a difficulty during construction e.g. for driving piles. They may also comprise more specific hard, potentially heterogeneous, coarse lag deposits (gravel to boulders) that can be difficult to penetrate and may lead to refusal of foundation infrastructure or damage of equipment. Near the seabed, a hard, heterogeneous surface can make it more difficult predict scour behavior.

Furthermore, the sediment thickness and lithology may vary abruptly over short distances especially in the glacial deposits, and the Quaternary deposits in general, complicating turbine siting and cable routing as well as foundation design(s). In glaciotectonically deformed areas, steeply dipping and alternating layering may occur with dislocated floes of soft sediments and abrupt changes in geotechnical properties.

The occurrence of paleochannels or buried valleys with steep sides may also imply sharp variations in sediment composition in either side and within the channel fill, potentially complicating foundation design.

No signs of gas or over-pressured pore fluids have been observed in the shallow subsurface, but if present, it may lead to blow outs when drilling for sediment sampling and infrastructure construction. The presence of shallow gas/pressured fluids may be indicated by pockmarks in the seabed and can also be indicated by acoustic blanking of seismic reflection data, preventing interpretation of units below. Pockmark areas can be unstable and should be avoided for turbine locations and cable routing.

In Table 7-1 an overview of sediment types identified in the screening area, related potentially critical geotechnical conditions and general foundation suitability is given.

Table 7-1. Sediment types identified in the screening area, related potentially critical geotechnical conditions and general foundation suitability.

Sediment type	**Critical geotechnical conditions/challenges**	**Foundation suitability**
Marine sand	n.a.	Well suited
Marine clay/soft mud	Low geotechnical strength	Not well suited if thick
Peat	High compressibility, low geotechnical strength	Not well suited
Meltwater sand	n.a.	Well suited
Meltwater clay	Low geotechnical strength if not overconsolidated	Not well suited if thick
Moraine clay/till	Overconsolidated and potentially heterogeneous, can contain coarse lag deposits, boulder stones and dislo-cated slabs of older sediments	Potentially problematic
Buried valley sedi-ments	Potentially heterogeneous with variable glacial/non gla-cial deposits, sharp variations in sediment composition across flanks	Potentially problematic
Miocene sand	n.a.	Well suited
Miocene clay	Low geotechnical strength if not overconsolidated	Not well suited if thick

An overview map has been compiled of the areal extent of key geological units that might have considerable influence on the variability of sediment characteristics and planning of turbine locations and foundation design. The extension of the following units was delineated: High-lying Saalian glacial surface, buried valleys, Eemian silty clays, Holocene marine silty clays and gyttja (Figure 7-1, Appendix A12). Moreover, the pointwise identification of peat layers in cores are shown.

The screening area is generally characterised by high-lying glacial sediments from Saalian or older glacial periods. The glacial sediments are especially close to seabed in the south-western part of the screening area. The glacial sediments can be expected to be of hetero-geneous composition and over-consolidated, due to prior ice-loading, subaerial exposure and desiccation. The sediments consist of clayey or sandy tills with variable stone content, deformed meltwater sediment layers (sand, gravel and clay) and locally glaciotectonically disturbed slabs of Miocene sediments (sands and clays). From deeper seismic sections the area is also well-known for intensive glaciotectonic thrust structure complexes (Huuse & Lykke-Andersen, 2000; Nielsen et al., 2008). Thrust structure complexes can locally bring slabs of pre-Quaternary sediments (clay or sand) close to the surface and in general create a complicated stratigraphy with low lateral predictability.

The area is dissected by a dense network of buried Quaternary valleys, several hundred metres in depth and cutting into the pre-Quaternary unit. Buried valleys are especially com-mon in the eastern to central part of the screening area. As described above, the buried valleys can show sharp variations in sediment composition across the flanks and within the channel fill. Little is known about the lithology of the complex sediment in-fill of the valleys, but a few drilled sections through similar structures in other parts of the North Sea, suggest a variable composition with both sandy, clayey and gravelly sediment fill (Cotterill et al., 2017).

Thicker units of soft clayey sediments are related to interglacial deposits from the Eemian period as well as early Holocene deposits. Moreover, older interglacial or late glacial lacustrine clays may also occur as interbedded subunits in Saalian and Weichselian meltwater units, respectively. Eemian silty clays is present in the eastern part of the screening area, as well as in two minor areas in the western part. The thickness of the unit is mostly in the range of 5-10 m, but locally it may reach 15 m. Early Holocene marine clays and gyttja appear to be located in paleo-landscape depressions in the central and southeastern part of the screening area, where the thickness of the Holocene unit may reach about 15 m. However, only the lower 5-10 m of the Holocene unit appears to be fine-grained material.

Peat layers observed in sediment cores appear to be very thin (few decimetres) and likewise located in Holocene paleo-landscape depressions, that later was drowned during the Littorina transgression in early Holocene. The peat findings appear to be quite randomly localized outside the main Holocene paleo-channel system. This may rather reflect the limited length of the vibrocores retrieved (typically <6 m), i.e. peat has only been verified in the more shallow landscape depressions, where the corer was able to penetrate down to the peat-covered lower part of the depression.

Based on the overview map of key geological units in Figure 7-1, it may be concluded that most parts of the screening area are characterised by specific geological conditions that will have to be considered in the planning of the most optimal location of wind farm sites.

It shall be noted that the Horns Rev 2 and Horns Rev 3 wind farm parks are located in areas with similar geological settings as the southwestern and the southeastern part of the screening area, respectively. In this sense, specific considerations and lessons learned from these projects may be highly relevant for further site evaluation of area E.

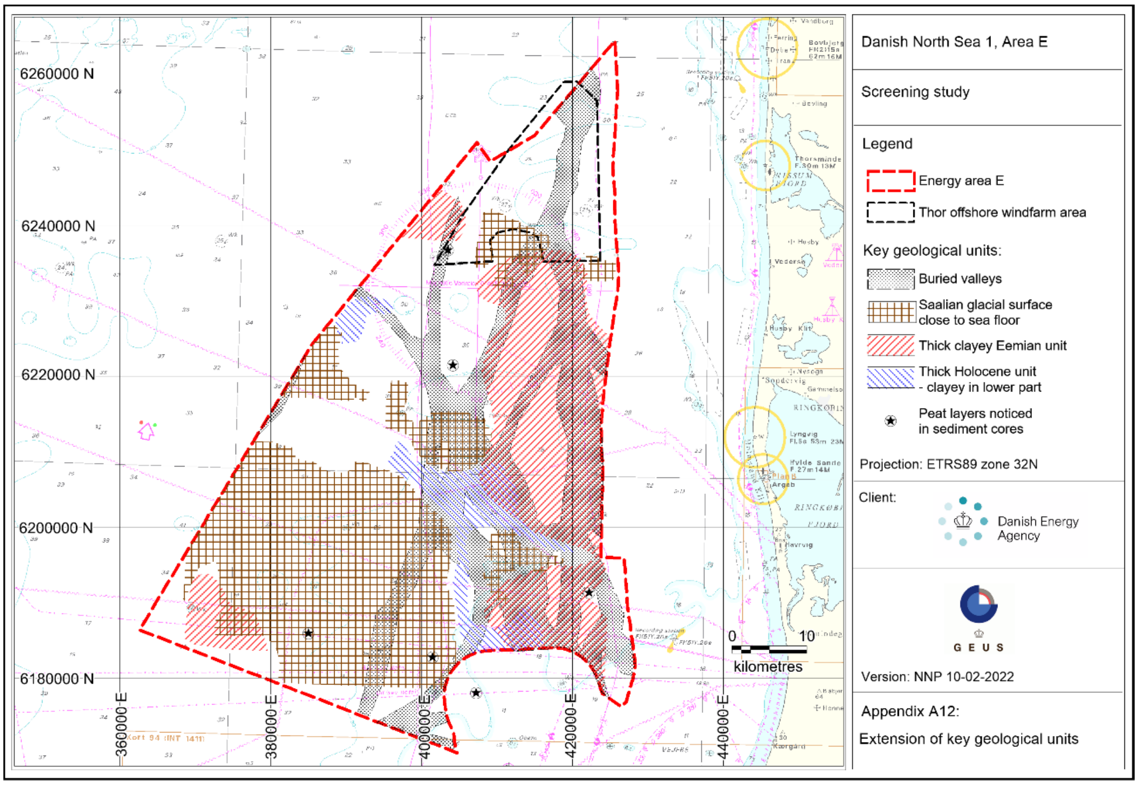

Figure 7-1. Key geological unit distribution in the screening area. Appendix A12.

8. Archaeological interests

Apart from known positions of newer historical shipwrecks, the probability of making archaeological finds in the screening area is expected to be low.

According to existing coastal displacement curves, the screening area may have been transgressed and inundated by the North Sea in the period from c. 9.000 to 7.000 years BP (Figure 8-1), and hence it can be expected that only early Mesolithic Maglemose culture remains can be found in the area. The paleo-landscape are expected to have been quite similar to the mapped topographic features of the base Holocene (Appendix A7), with hilly areas dissected by lower lying bogs and possible river tributaries. As the sea rose, the coastline was progressively shifted to the east and, in the last part, leaving only small islands above the sea surface and the chance of making finds of older stone age cultures appear to be very limited.

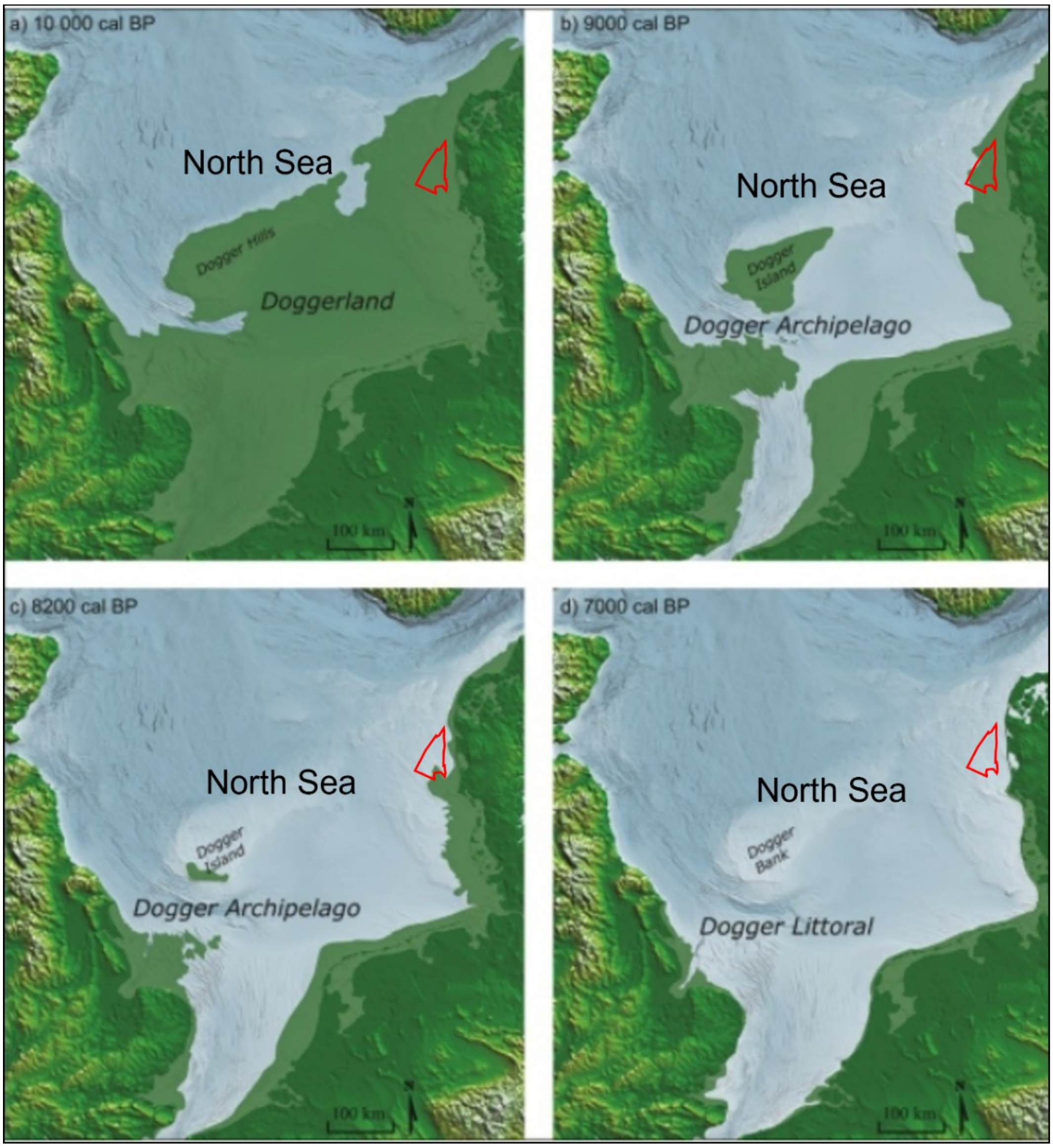

Figure 8-1. Reconstructed coastline and paleolandscapes of the North Sea for the Holocene time slices: 10.000 yrs BP, 9000 yrs BP, 8200 Years BP and 7000 yrs BP. Modified from Walker et al. (2020).

Archaeological analyses of Horns Rev 2, Horns Rev 3 and Thor OWF areas have similarly shown a theoretical possibility for settlements of the older Maglemose culture. However, no archaeological objects appear to have been found during specific dedicated studies.

9. Other potential points of attention

The screening area is not characterised by designated nature protection areas or aggregate dredging or reservation areas (Figure 9-1). Based on GEUS' seabed sediment map, stone reefs are expected to be quite rare in the sand-dominated screening area. Bubble reefs have also not been identified in the area and are in Danish waters mostly found in the Skagerrak to northern Kattegat area. Moreover, no clear signs of gas in sediments were found in the area.

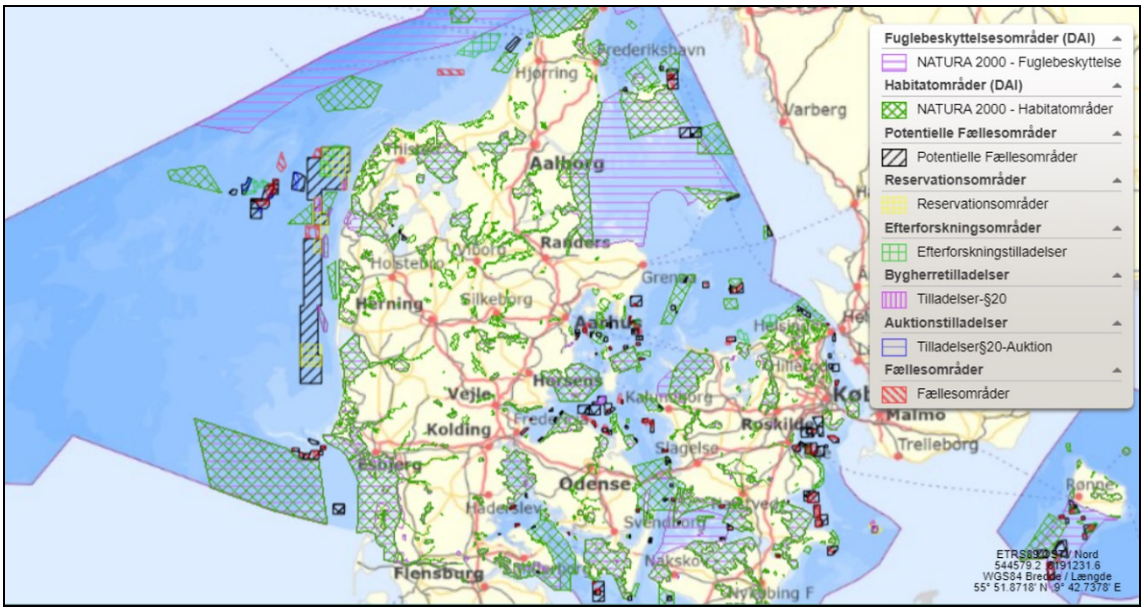

Figure 9-1. Overview of Natura-2000 protection areas and marine aggregate dredging and reservation areas in Denmark. From Miljøstyrelsen/miljøgis.

10. Conclusions

Screening of existing shallow seismic data, sediment cores and published literature of North Sea 1, Area E has given an overview of the geological development and composition of Quaternary units in the area. Thickness and levels of main stratigraphic/genetic units have been compiled by mapping of key seismic surfaces and verification with sediment core data.

The following observations are emphasized:

- Most parts of the screening area are characterised by specific geological conditions that will have to be considered in the planning of the most optimal location of wind farm sites.
- The screening area is dominated by a high lying glacial surface of Saalian or older glacial age and the glacial unit is cut by major buried valley systems. It can be anticipated that parts of the glacial unit have been glaciotectonically deformed, causing laterally heterogenous soil conditions including both very hard and soft beds.
- Meltwater sediments from both the late Saalian glacial period as well as the Weichselian glacial period occur as channel elements and as major sheets which have partly levelled the older glacial landscape. The unconsolidated sediments are mostly less than 15 m thick and are varying between sandy and more soft silty-clayey subunits.
- Eemian (last interglacial) soft marine clayey sediments are mainly confined to the eastern part of the area where the unit reaches a thickness of about 5-10 m. The unit is typically overlain by c. 5- 15 m of Weichselian meltwater sand and Holocene marine sediments.
- The uppermost marine Holocene unit is mostly composed of fine-medium grained sand but soft silty and clayey or even gyttja like sediments, possibly early Holocene, appear in confined/channelized areas where the Holocene unit reaches up to 15 m in thickness.
- Peat layers have only been observed in a limited number of sediment cores, and typically only few decimetres in thickness. However, as the landscape was subaerially exposed in early Holocene, many depressions in the area may have had a bog character giving rise to peat formation.

Based on the mapping results of the screening and settings of nearby OWF's, it is concluded that most parts of area E appear to be suitable for foundation of wind turbines. However, the area exhibits different character with respect to the level of the glacial surface, the occurrence of several hundred meter deep buried valleys and composition and thickness of surficial sediment units composed mostly of sandy or clayey deposits. The occurrence of soft marine clays with up to 10-20 m in total thickness in the eastern part of the area, as well as minor areas in the western part, is a point of attention. The same clay unit was identified by Thor and Horns Rev 3 OWF integrated geological model studies and geotechnical parameters from these projects may thus serve as a guide for potential challenges and foundation solutions. Apart from known positions of newer historical shipwrecks, the probability of making archaeological finds in the screening area is expected to be low.

11. References

Cohen, K.M., Westley, K., Erkens, G., Hijma, M.P. & Weerts, H.J.T. 2017. Chatter 7, The North Sea. In: Submerged landscapes of the European continental shelf: Quaternary Paleoenvironments, First Edition. Ed. By N.C. Flemming, J. Harff, D. Moura, A. Burgess and G.N. Baily. J.

Cotterill, Carol J.; Phillips, Emrys; James, Leo; Forsberg, Carl Fredrik; Tjelta, Tor Inge; Carter, Gareth; Dove, Dayton. 2017 The evolution of the Dogger Bank, North Sea: a complex history of terrestrial, glacial and marine environmental change. *Quaternary Science Reviews*, 171. 136-153. https://doi.org/10.1016/j.quascirev.2017.07.006

Gaffney, V., Gaffney, V., Thomson, K., Fitch, S., Briggs, K., Bunch, M., & Holford, S. (2007). An Atlas of the Palaeolandscapes of the Southern North Sea. In *Mapping Doggerland: the Mesolithic Landscapes of the Southern North Sea*

Huuse, M. & Lykke-Andersen, H. 2000a. Overdeepened Quaternary valleys in the eastern Danish North Sea: morphology and origin. Quat. Sci. Rew. 19, 1233-1253.

Konradi, P.B., Larsen, B. & Sørensen, Aa.B. 2005. Marine Eemian in the Danish eastern North Sea. Quaternary International 133, 21–31.

Larsen, B. & Andersen, L.T. 2005. Late Quaternary stratigraphy and morphogenesis in the Danish eastern North Sea and its relation to onshore geology. Netherlands Journal of Geosciences, Geologie en Mijnbouw, 84, 2.

Larsen, N.K., Knudsen, K.L., Krohn C.F., Kronborg, C., Murray, A.S. & Nielsen, O.B. 2009. Late Quaternary ice sheet, lake and sea history of southwest Scandinavia – a synthesis. Boreas, Vol. 38, pp. 732–761.

Nielsen, T., Mathiesen, A. & Bryde-Auken, M. 2008. Base Quaternary in the Danish parts of the North Sea and Skagerak. Geological Survey of Denmark and Greenland Bulletin, 15, 37-40.

Velenturf, A.P.M., Emery, A.R., Hodgson, D.M., Barlow, N.L.M., Mohtaj Khorasani, A.M., Van Alstine, J., Peterson, E.L., Piazolo, S. & Thorp, M. 2021. Geoscience Solutions for Sustainable Offshore Wind Development. Earth Science, Systems and Society. The Geological Society of London. 2 November 2021. Volume 1. Article 10042.

Walker, J., Gaffney, V., Fitch, S., Muru, M., Fraser, A., Bates, M., & Bates, R. (2020). A great wave: The Storegga tsunami and the end of Doggerland? *Antiquity, 94*(378), 1409-1425. doi:10.15184/aqy.2020.49

11.1 Background reports

COWI for Energinet.DK. 2014. OWF Horns Rev 3 – Integrated Geological Model (Final Report).

COWI for Energinet Eltransmission A/S, 2021. Thor offshore windfarm - integrated geological model. Report.

De kulturhistoriske Museer, Holstebro Kommune, 2020. M. Johnson & P.M. Astrup. Thor Offshore wind farm – Geoarchaeological analysis. 55 pp.

GEO for Kystdirektoratet, 2011. Nordsøen – Efterforskning og kortlægning af sandressourcer, Fase 1A, GEO projekt nr. 33776.

Jensen, J.B., Gravesen, P. & Lomholt, S. 2008. Geology of outer Horns Rev, Danish North Sea. Geological Survey of Denmark and Greenland Bulletin, 15, 41-44.

Larsen, B. & Leth, J.O., 2001. Geologisk kortlægning af Vestkysten. Regionalgeologisk tolkning og en samlet vurdering af aflejringsforholdene i området mellem Nymindegab og Horns Rev. Udført for Kystdirektoratet 2000 og 2001. Vol. 1 og 2.

GEUS, 2006. Jensen, J.B. & Lomholt, S. 2006: Råstoffer ved HR2 Vindmølleparken. Vurdering af mulige sand- og grusforekomster på Horns Rev. Udarbejdet for ENERGI E2. GEUS Rapport 2006/4, 15 pp.

GEUS, 2009. Gravesen, P., Leth, J.O. & Jensen, J.B., 2009. Nordsøen - Havbundsdata og kortlægning. Status for data, kortlægning, ressourcer, Kvartær stratigrafi og fremtidsperspektiver. GEUS Rapport 2009/48, 48 pp.

GEUS, 2013. Lomholt, S., Leth, J.O., Skar, S. Marin råstofkortlægning i Nordsøen 2012. Detaljeret undersøgelse af 3 delområder. Udført for Naturstyrelsen. GEUS Rapport 2013/5.

11.2 Supplementary papers

Andersen, L.T. 2004. The Fanø Bugt Glaciotectonic Thrust Fault Complex, Southeastern Danish North Sea. Ph.D.Thesis. 2004. Danmarks og Grønlands Geologiske Undersøgelse Rapport 2004/30, 35-68.

Anthony, D. & Leth, J.O. 2002. Large-scale bedforms, sediment distribution and sand mobility in the eastern North Sea off the Danish west coast. Marine Geology 182, 247-263.

Bockelmann, F.-D., Puls, W., Kleeberg, U., Müller, D. & Emeis, K.-C. 2018. Mapping mud content and median grain-size of North Sea sediments – A geostatistical approach. Marine Geology 397, 60-71.

Coughlan, M., Fleischer, M., Wheeler, A.J., Hepp, D.A., Hebbeln, D. & Mörz, T., 2018. A revised stratigraphical framework for the Quaternary deposits of the German North Sea sector: a geological-geotechnical approach. Boreas 47, 80-105.

Gibling, M.R. 2006. Width and Thickness of Fluvial Channel Bodies and Valley Fills in the Geological Record: A Literature Compilation and Classification. Journal of Sedimentary Research 76, 731-770.

Gravesen, P., Pedersen, S.A.S. & Midtgaard, H.H. 2021. Studies of geological properties and conditions for deep disposal of radioactive waste, Denmark. Phase 1, report no. 2. Geological setting and structural framework of Danish onshore areas.

Hepp, D.A., Warnke, U., Hebbeln, D. & Mörz, T. 2017. Tributaries of the Elbe Palaeovalley: Features of a Hidden Palaeolandscape in the German Bight, North Sea, Under the Sea: Archaeology and Palaeolandscapes of the Continental Shelf, pp. 211-222.

Houmark-Nielsen, M. 2003. The Pleistocene of Denmark: a review of stratigraphy and glaciation history. In: Ehlers, J. & Gibbard, P. (eds): Quaternary Glaciation-extend and chronology. Vol. 1 Europe. Elsevier (Amsterdam): 321-336.

Huuse, M. & Lykke-Andersen, H. 2000. Large-scale glaciotectonic thrust structures in the eastern Danish North Sea. In: Maltman, A., Hambrey, M. & Hubbard, B. (eds): Deformation of Glacial Materials. Geological Society, London, Special Publications 176, 293-305.

Huuse, M., Lykke Andersen, H. & Michelson, O. 2001. Cenozoic evolution of the eastern Danish North Sea. Marine Geology 177, 243-269.

Jensen, J.B. & Lomholt, S. 2006: Råstoffer ved HR2 Vindmølleparken. Vurdering af mulige sand- og grusforekomster på Horns Rev. Udarbejdet for ENERGI E2. GEUS Rapport 2006/4, 15 pp.

Knudsen, K.L. 1985. Foraminiferal stratigraphy of Quaternary deposits in the Roar, Skjord and Dan fields, central North Sea. Boreas 14, 311–324.

Larsen, B. & Leth, J.O. 2001. Geologisk kortlægning af Vestkysten. Regionalgeologisk tolkning og en samlet vurdering af aflejringsforholdene i området mellem Nymindegab og Horns Rev. Udført for Kystdirektoratet 2000 og 2001. Vol. 1 og 2.

O Cofaigh, C. 1996. Tunnel valley genesis. Progress in Physical Geography 20, 1-19.

Ottesen, D., Batchelor, C.L., Dowdeswell, J.A. & Løseth, H. 2018. Morphology and pattern of Quaternary sedimentation in the North Sea Basin (52–62°N). Marine and Petroleum Geology 98, 836-859.

Overeem, I., Weltje, G.J., Bishop-Kay, C. & Kroonenberg, S.B. 2001. The Late Cenozoic Eridanos delta system in the Southern North Sea Basin: a climate signal in sediment supply? BasinResearch 13, 293-312.

Peryt, T.M., Geluk, M.C., Mathiesen, A., Paul, J. & Smith, K. 2010. Zechstein. In: Doornenbal, J.C., Stevenson, A.G., (Eds.), Petroleum Geological Atlas of the Southern Permian Basin Area, EAGE Publications, pp. 123-147.

Prins, L.T., Andresen, K.J., Clausen, O.R. & Piotrowski, J.A. 2020. Formation and widening of a North Sea tunnel valley - The impact of slope processes on valley morphology. Geomorphology 368.

Rasmussen, E.S., Vejbæk, O.V., Bidstrup, T., Piasecki, S. & Dybkjær, K. 2005. Late Cenozoic petroleum systems. In: Doré, A.G. & Vinning, B.A. (Eds). Petroleum Geology: North-West Europe and Global Perspectives. Proceedings of the 6th Petroleum Geology Conference, 1347–1358. Geological Society, London.

Rasmussen, E.S., Dybkjær, K. & Piasecki, S. 2010. Lithostratigraphy of the Upper Oligocene – Miocene succession of Denmark. Geological Survey of Denmark and Greenland Bulletin 22, 1–92.

Appendixes

A. Maps:

A1: Screening area map

A2: Bathymetry map

A3: Seismic profiles and sediment core site map

A4: Seafloor sediment map

A5: Buried valley map

A6: Holocene unit (isopach map)

A7: Base Holocene unit (m below sea level)

A8: Weichsel Meltwater Unit (isopach map)

A9: Eemian unit (isopach map)

A10: Top Saale unit (m below sea floor)

A11: Top Saale unit (m below sea level)

A12: Extension of key geological units

B. Selected long sparker seismic sections (w. unit interpretation):

B1: Profile A

B2: Profile B

B3: Profile C

B4: Profile D

B5: Profile E

B6: Profile F

C. Table with available sediment cores (w. link to description)

A1

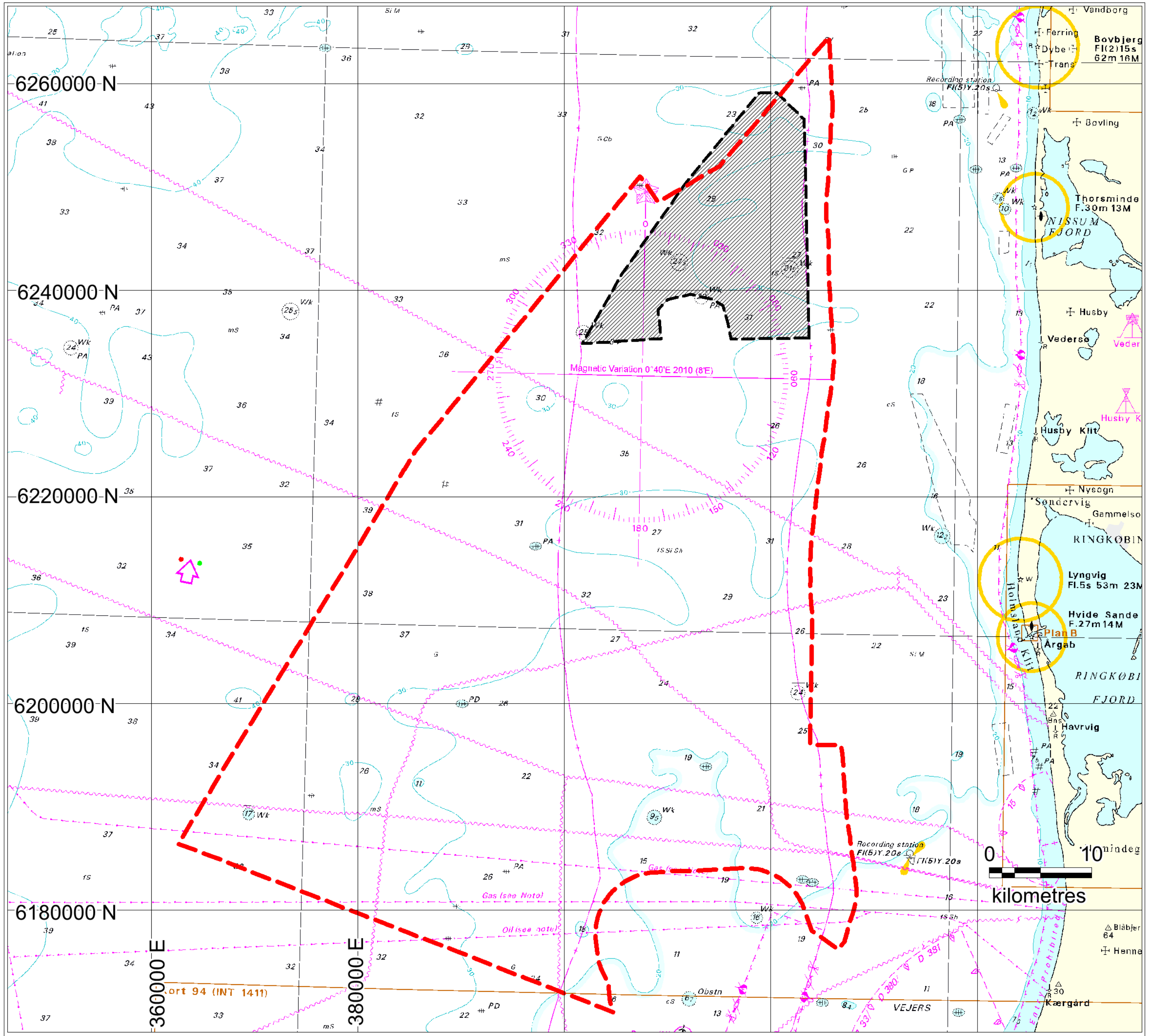

Danish North Sea 1, Energy area E

Screening study

Legend

Energy area E

Thor offshore windfarm area

Projection: ETRS89 zone 32N

Client:

Danish Energy Agency

GEUS

Version: NNP 28-01-2022

Appendix A1:

Screening area

A2

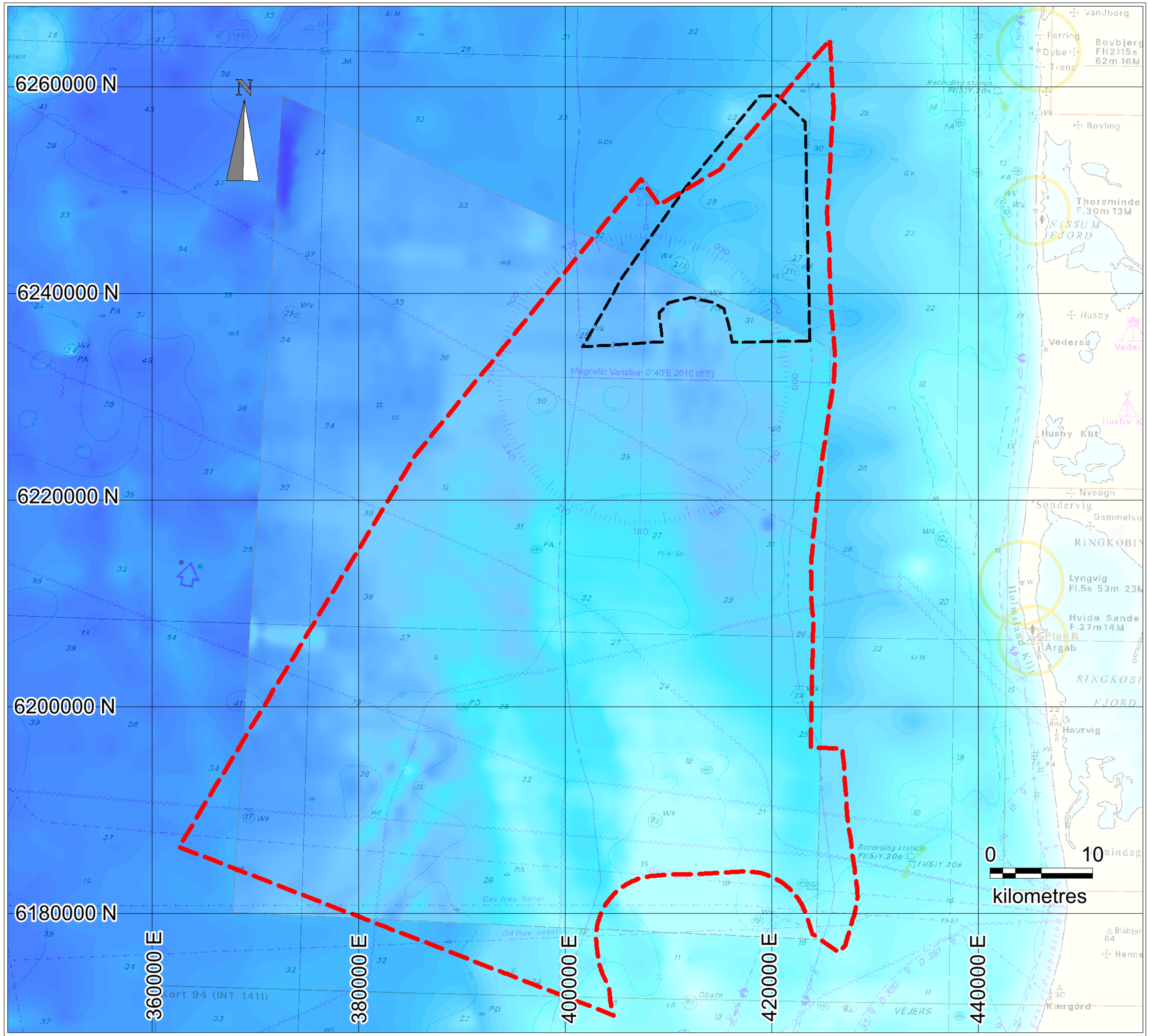

Energy area E-1, Danish North Sea

Screening study

Legend

Energy area E1

Thor offshore windfarm area

Depth (m)

0
5
10
15
20
30
40
50
60

Projection: ETRS89 zone 32N

Client: Danish Energy Agency

GEUS

Version: NNP 28-01-2022

Appendix A1: Bathymetry

- Spliced 2019 GEUS survey data and Danish Geodata Agency data

A3

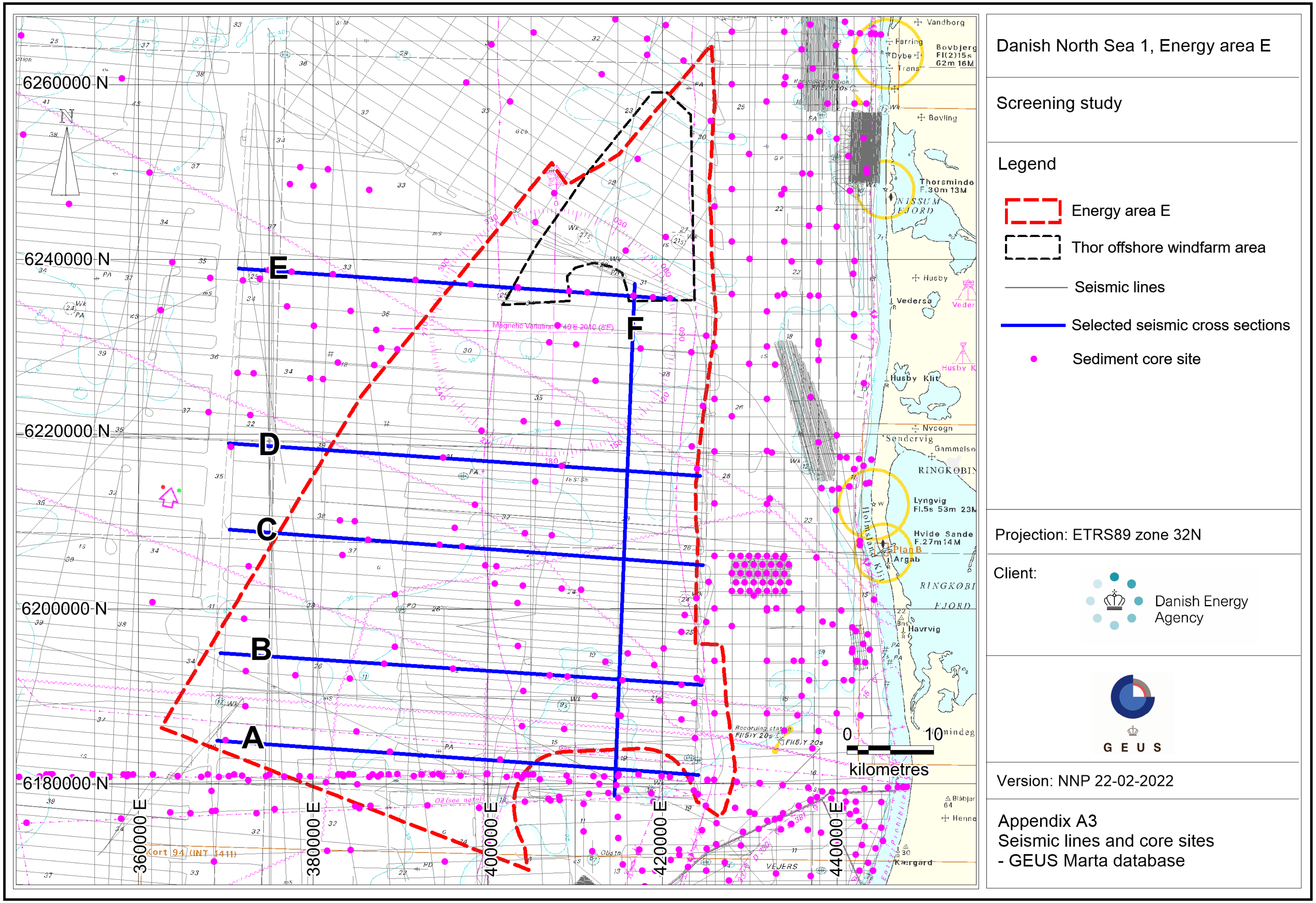
Danish North Sea 1, Energy area E
Screening study
Legend
Energy area E
Thor offshore windfarm area
Seismic lines
Selected seismic cross sections
Sediment core site
Projection: ETRS89 zone 32N
Client:
Danish Energy Agency
G E U S
Version: NNP 22-02-2022
Appendix A3
Seismic lines and core sites
- GEUS Marta database
6260000 N
6240000 N
6220000 N
6200000 N
6180000 N
360000 E
380000 E
400000 E
420000 E
440000 E
A
B
C
D
E
F
0
10
kilometres

A4

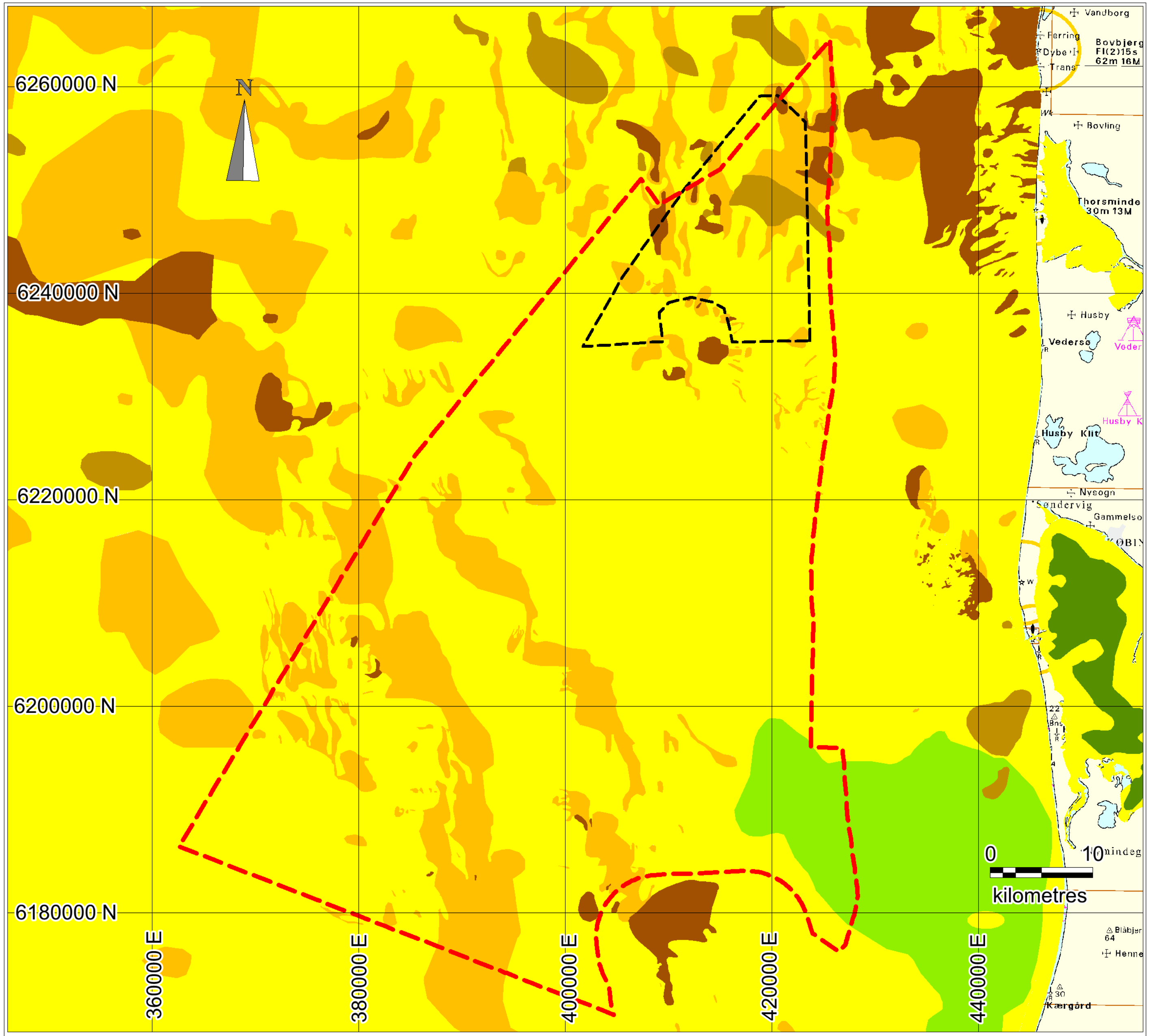

Danish North Sea 1, Energy area E

Screening study

Legend

- Energy area E
- Thor offshore windfarm area

Seabed sediment:

- Moraine/till
- Quaternary clay/silt
- Gravelly/coarse sand
- Sand
- Silty sand
- Gyttja-sandy gyttja

Projection: ETRS89 zone 32N

Client: Danish Energy Agency

GEUS

Version: NNP 28-01-2022

Appendix A4:

Seabed surface sediment types

A5

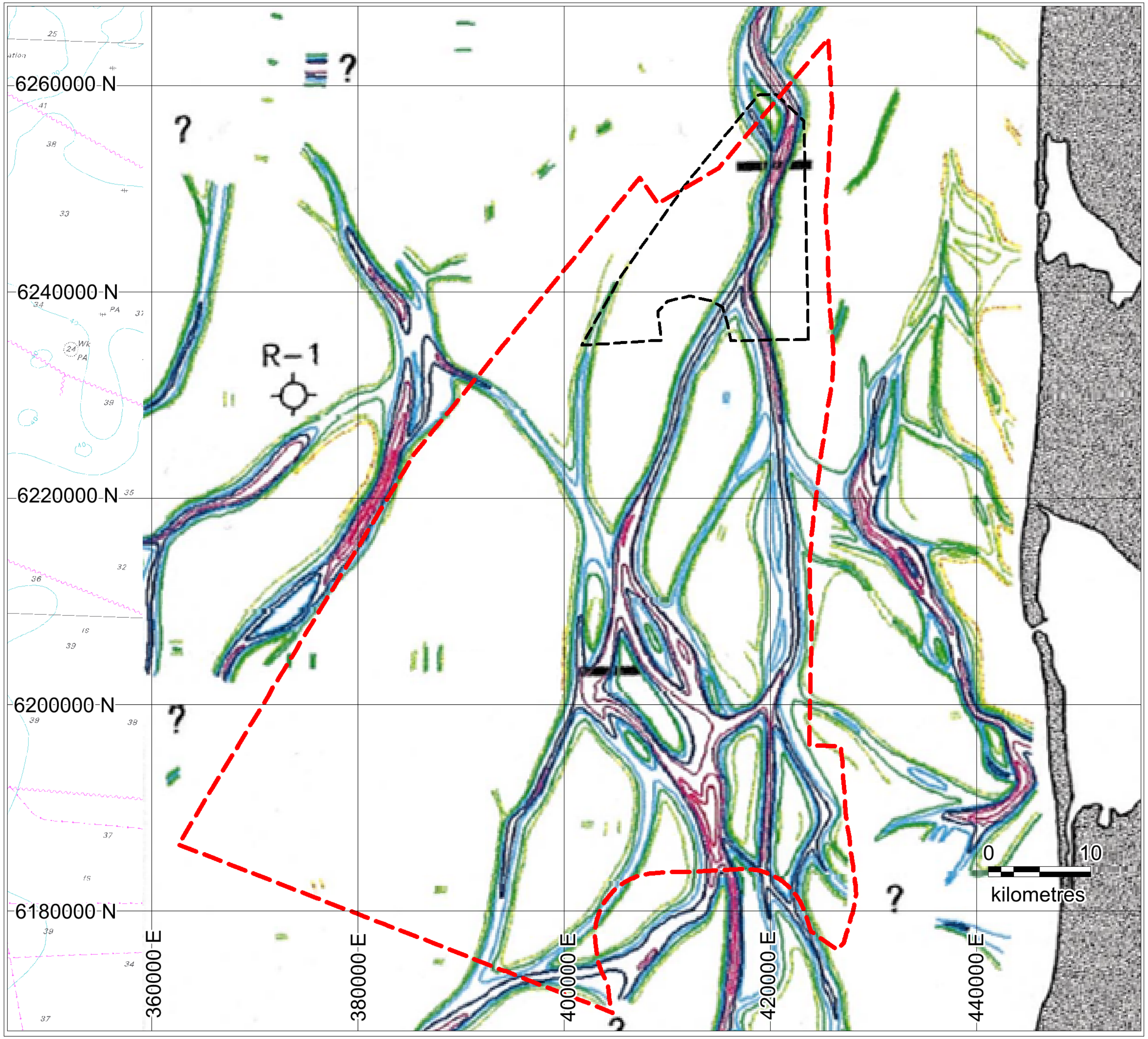

Danish North Sea 1, Area E

Screening study

Legend

Energy area E

Thor offshore windfarm area

Buried Quaternary valley extension
(from Huuse & Lykke-Andersen, 2000)

Projection: ETRS89 zone 32N

Client: Danish Energy Agency

GEUS

Version: NNP 04-02-2022

Appendix A5:
Buried Quaternary valley extension

A6

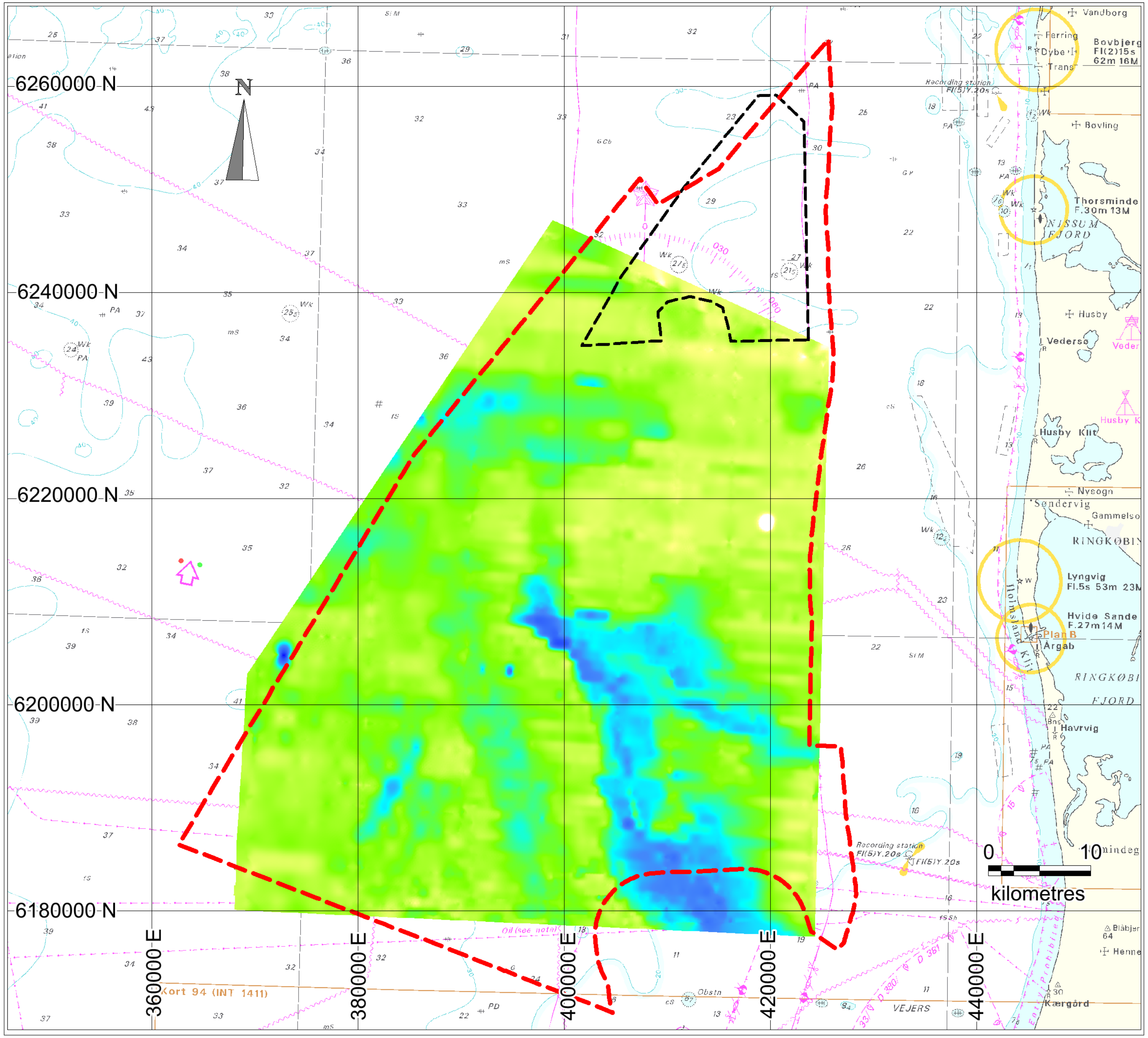

Danish North Sea 1, Energy area E

Screening study

Legend

Energy area E

Thor offshore windfarm area

Holocene unit thickness (m)

15
10
5
0 m

Projection: ETRS89 zone 32N

Client:

Danish Energy Agency

G E U S

Version: NNP 04-02-2022

Appendix A6:

Holocene unit thickness

A7

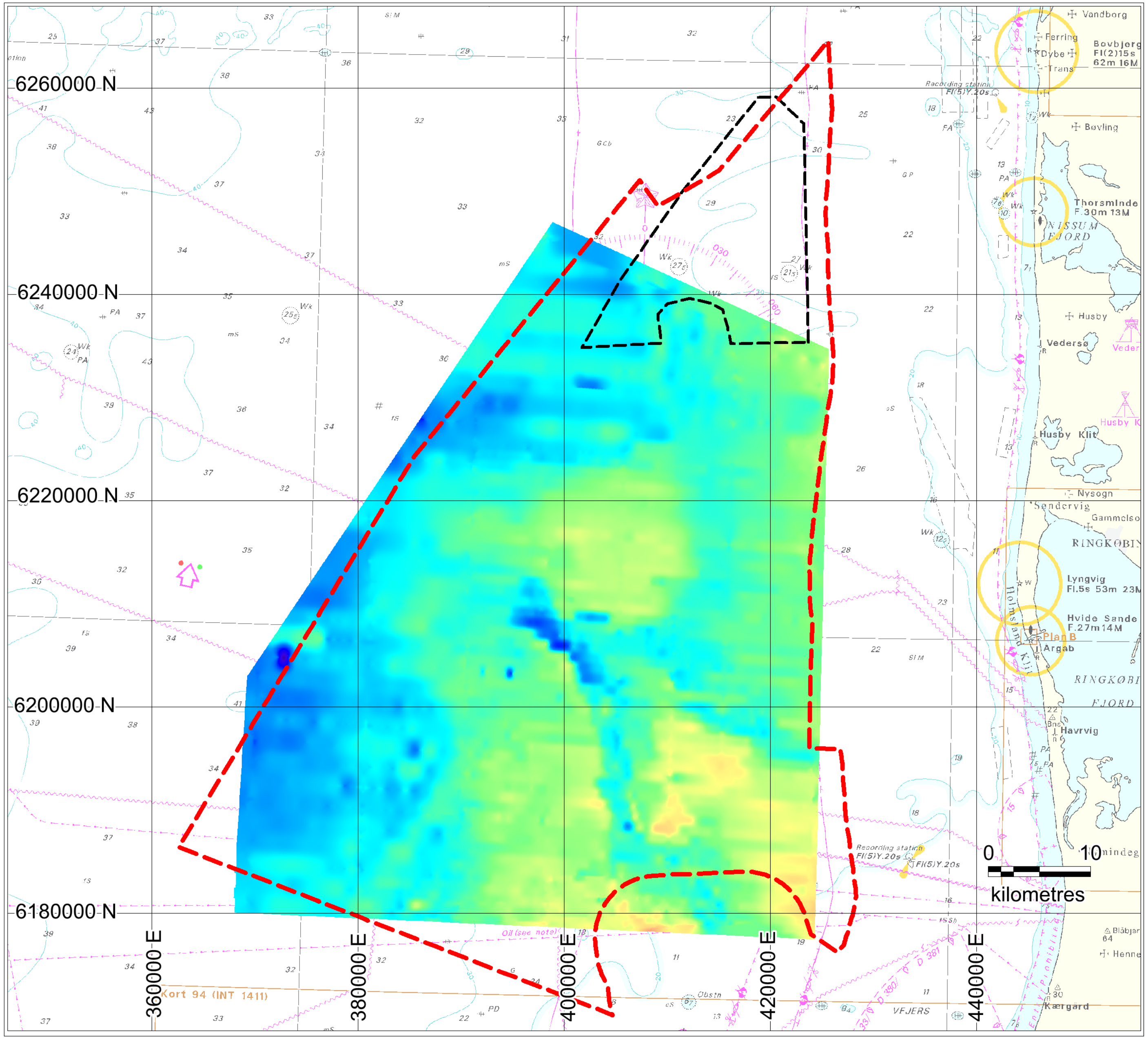

Danish North Sea 1, Energy area E

Screening study

Legend

Energy area E

Thor offshore windfarm area

Base Holocene Unit (m below sea level)

50
45
40
35
30
25
20 m

Projection: ETRS89 zone 32N

Client: Danish Energy Agency

GEUS

Version: NNP 29-01-2022

Appendix A7:

Base Holocene Unit (m below sea level)

A8

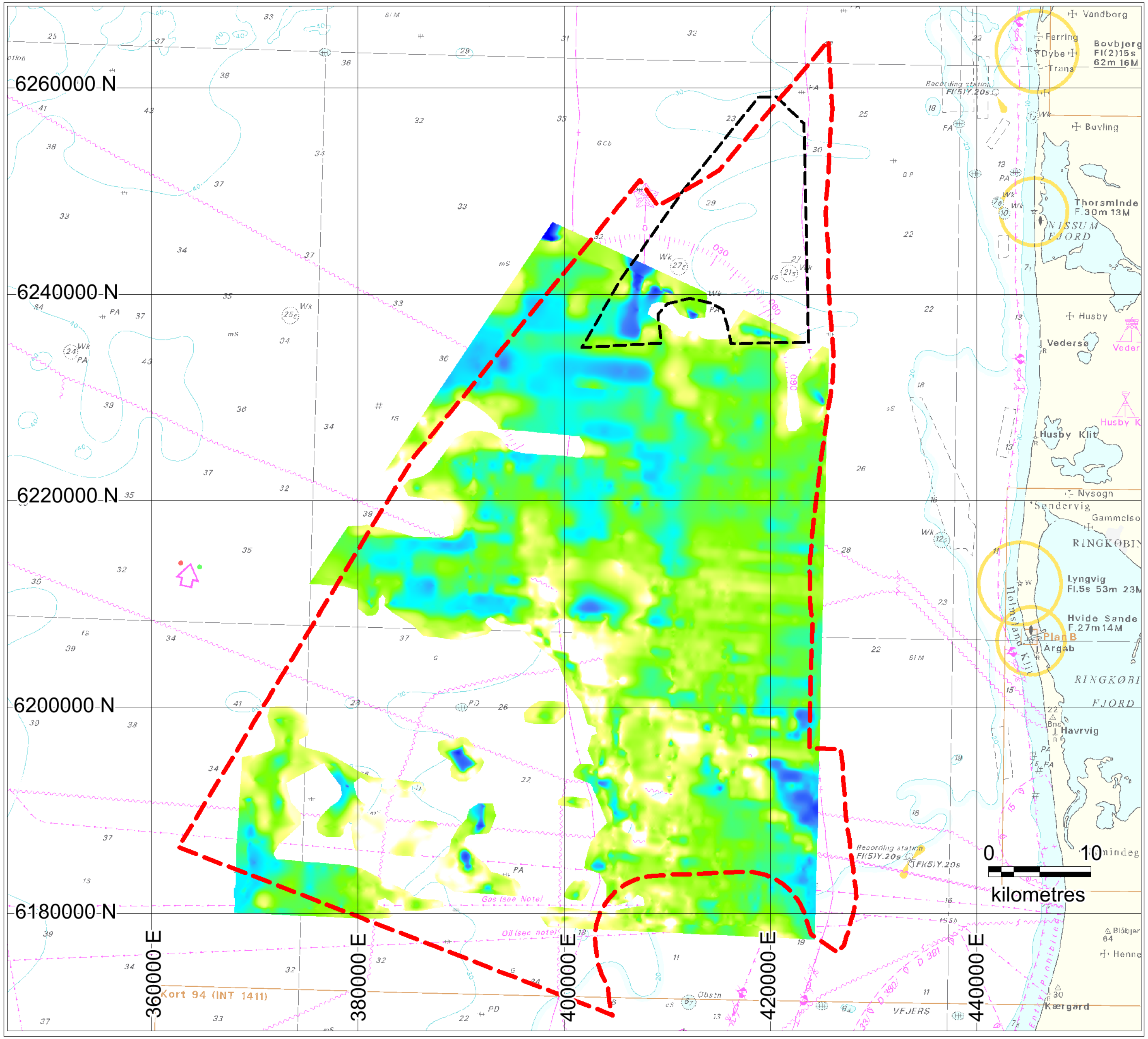

Danish North Sea 1, Energy area E

Screening study

Legend

Energy area E

Thor offshore windfarm area

Weichsel unit thickness:

30
25
20
15
10
5
0 m

Projection: ETRS89 zone 32N

Client: Danish Energy Agency

GEUS

Version: NNP 29-01-2022

Appendix A8:

Weichsel unit thickness

A9

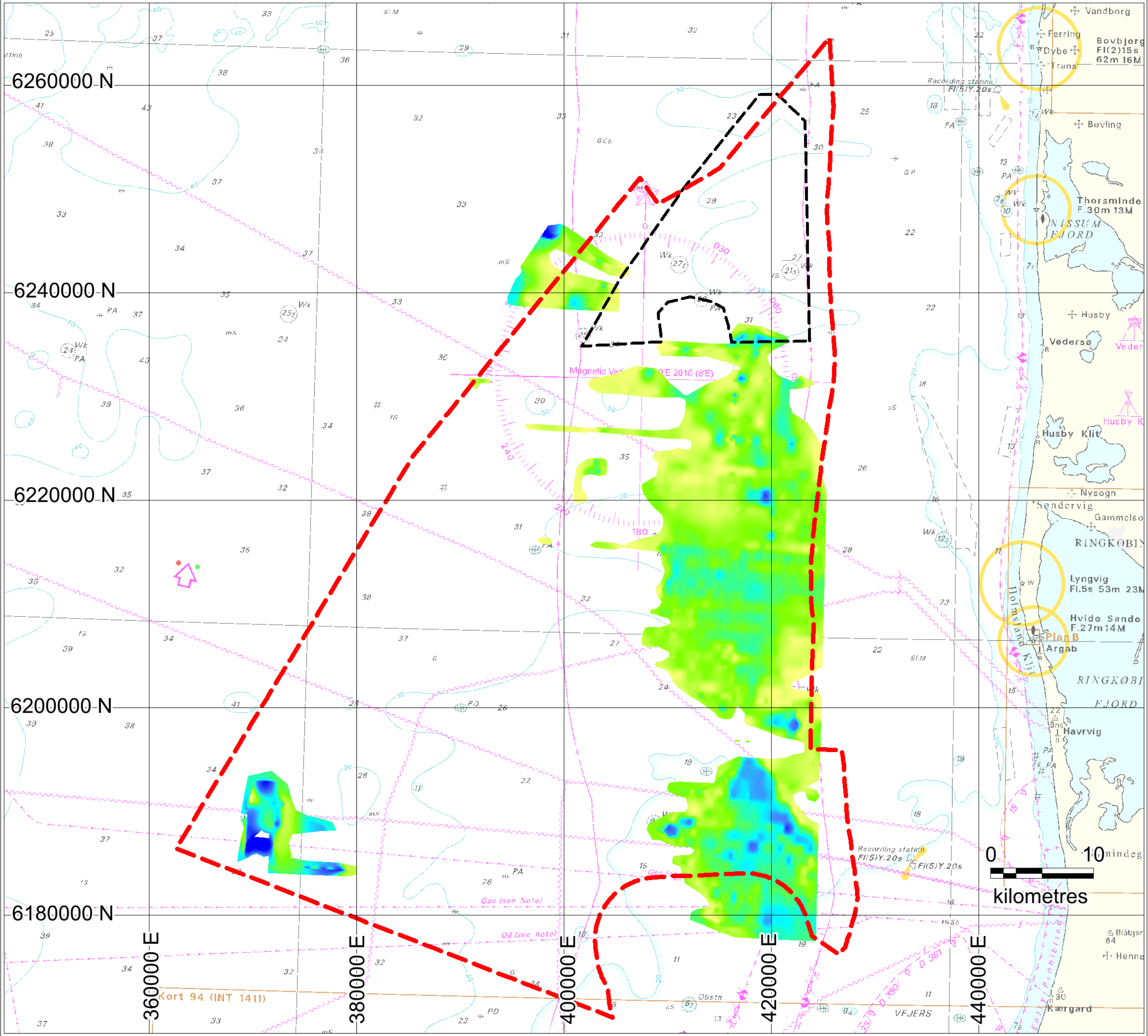

Danish North Sea 1, Energy area E

Screening study

Legend

Energy area E

Thor offshore windfarm area

Eemian unit thickness:

30
25
20
15
10
5
0 m

Projection: ETRS89 zone 32N

Client: Danish Energy Agency

GEUS

Version: NNP 29-01-2022

Appendix A9:

Eemian unit thickness

A10

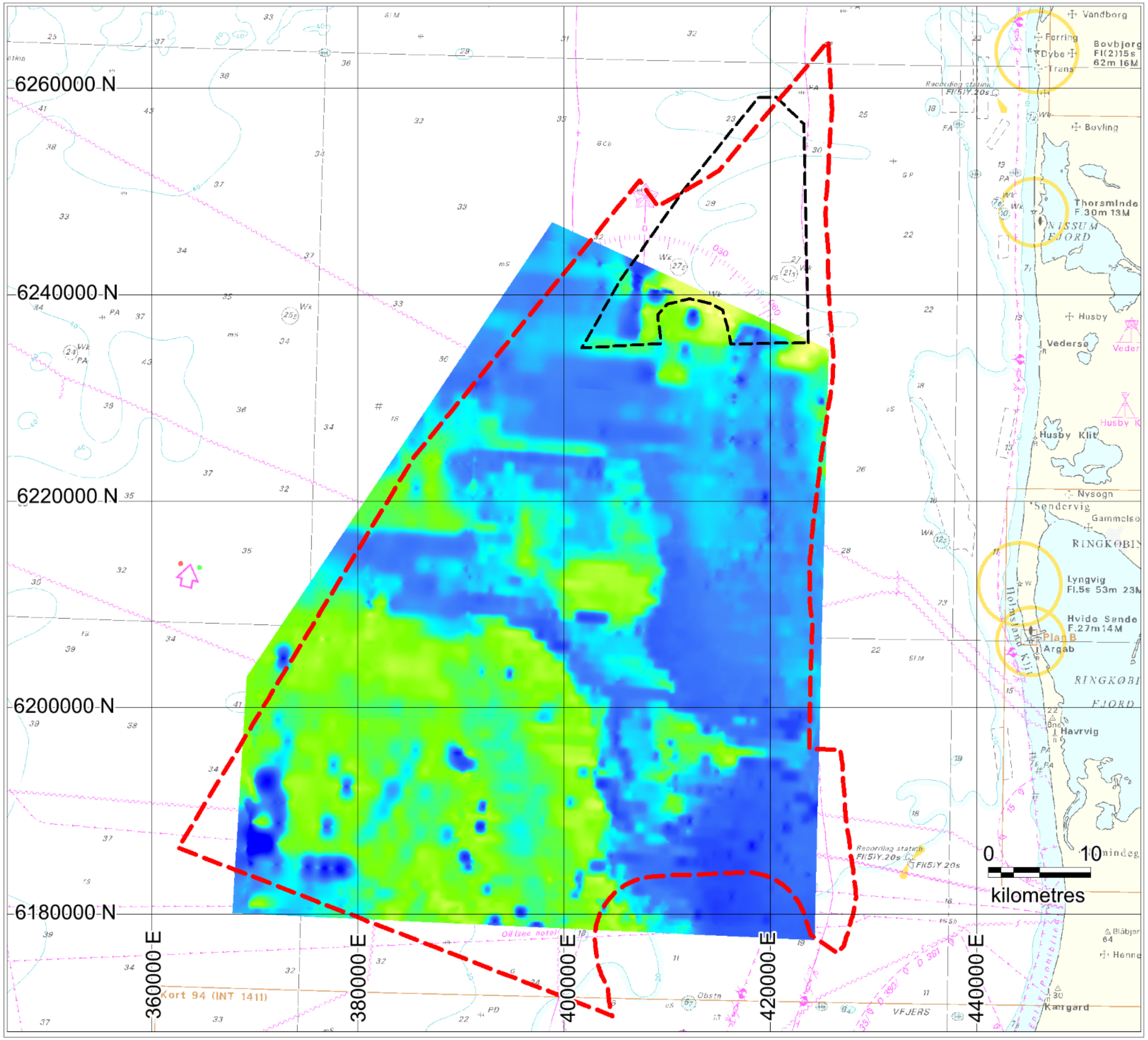

Danish North Sea 1, Energy area E

Screening study

Legend

Energy area E

Thor offshore windfarm area

Top Saale Unit (m below sea floor)

35
30
25
20
15
10
5
0 m

Projection: ETRS89 zone 32N

Client: Danish Energy Agency

GEUS

Version: NNP 08-02-2022

Appendix A10:

Top Saale unit
(m below sea floor)

A11

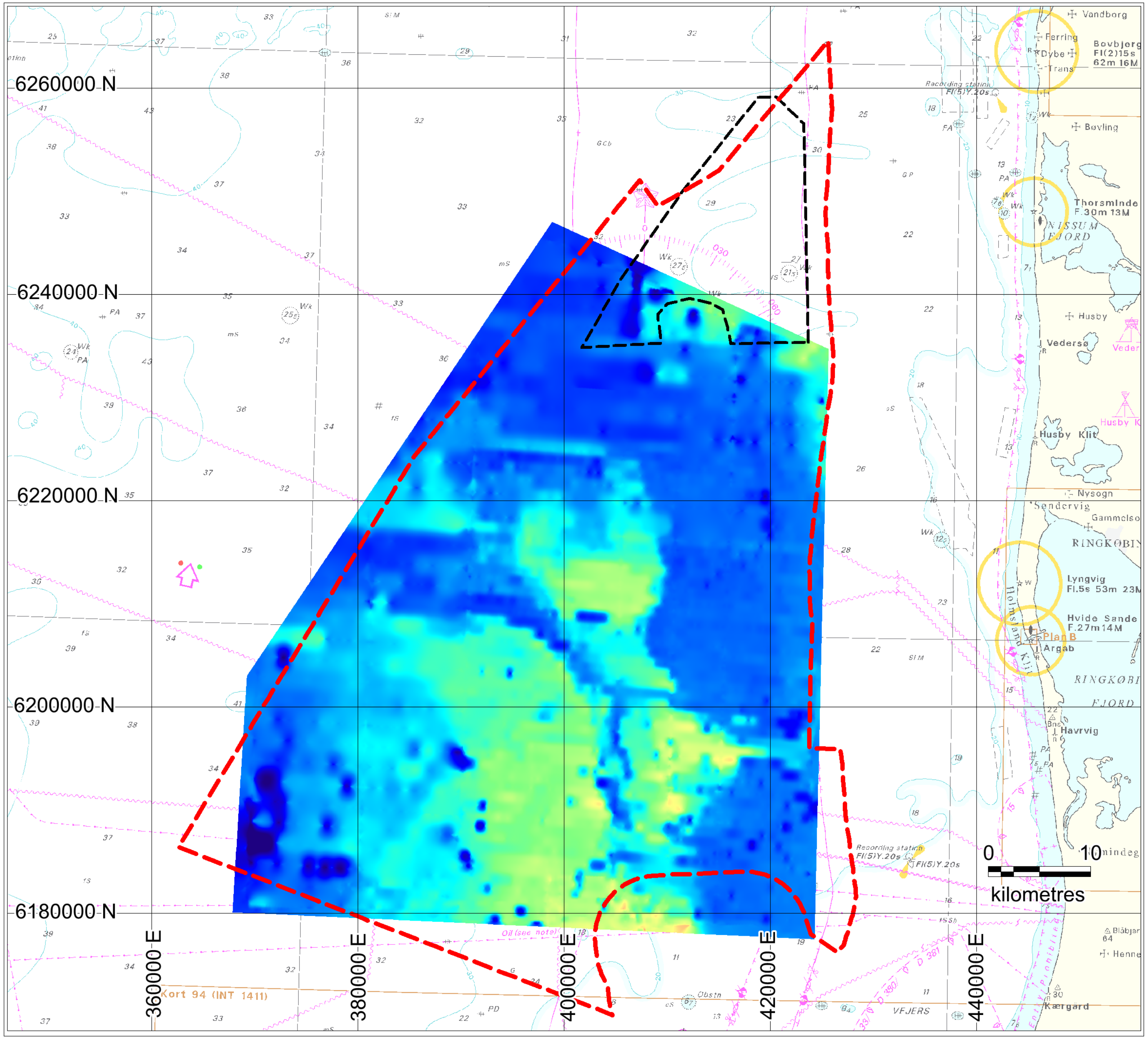

Danish North Sea 1, Energy area E

Screening study

Legend

Energy area E

Thor offshore windfarm area

Top Saale Unit (m below sea level)

70
60
50
40
35
30
25
20 m

Projection: ETRS89 zone 32N

Client:

Danish Energy Agency

G E U S

Version: NNP 08-02-2022

Appendix A11:

Top Saale Unit (m below sea level)

A12

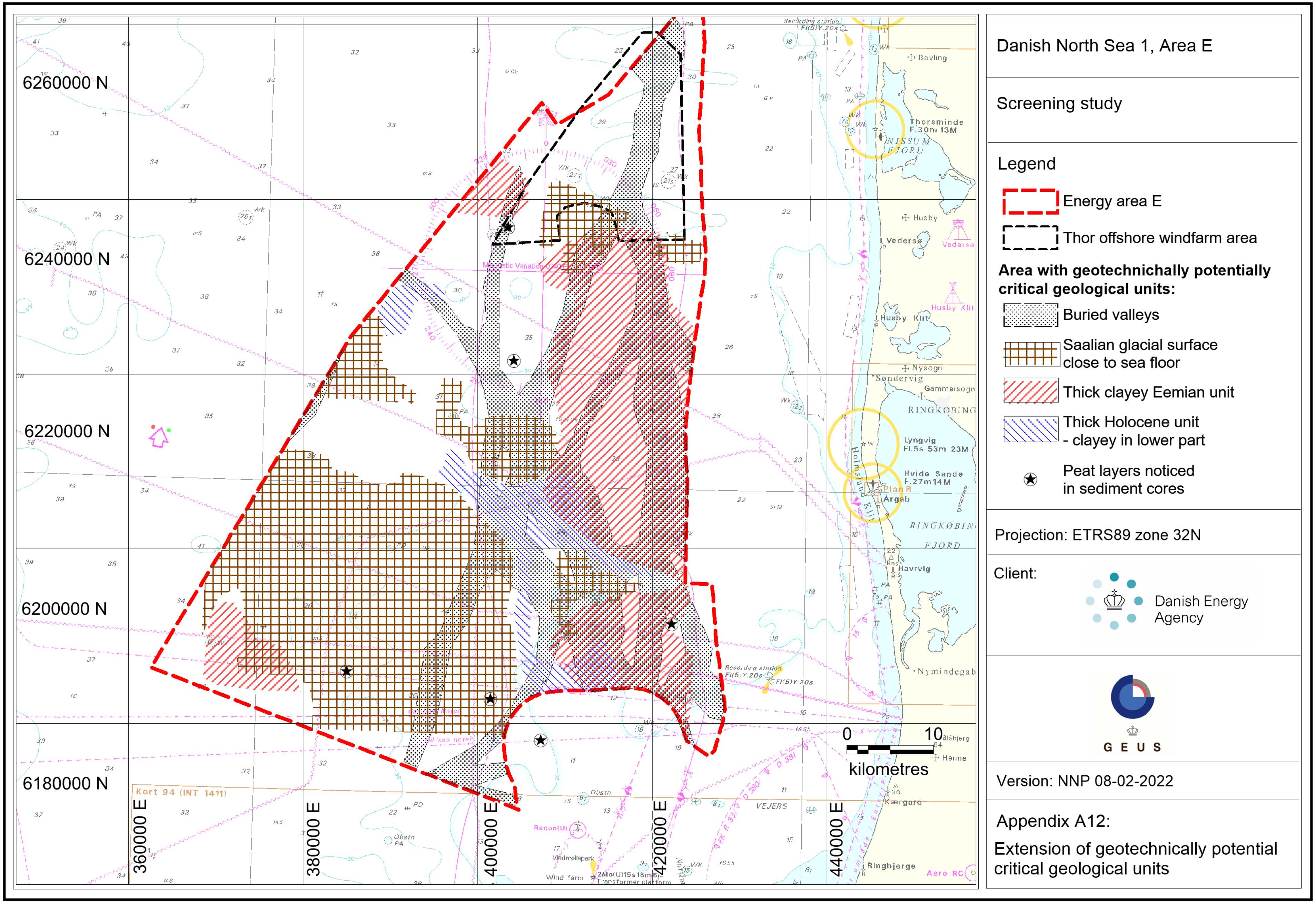

6260000 N
6240000 N
6220000 N
6200000 N
6180000 N
360000 E
380000 E
400000 E
420000 E
440000 E
0
10
kilometres
Danish North Sea 1, Area E
Screening study
Legend
Energy area E
Thor offshore windfarm area
Area with geotechnichally potentially critical geological units:
Buried valleys
Saalian glacial surface close to sea floor
Thick clayey Eemian unit
Thick Holocene unit - clayey in lower part
Peat layers noticed in sediment cores
Projection: ETRS89 zone 32N
Client:
Danish Energy Agency
G E U S
Version: NNP 08-02-2022
Appendix A12:
Extension of geotechnically potential critical geological units

B1

GEUS

Profile A

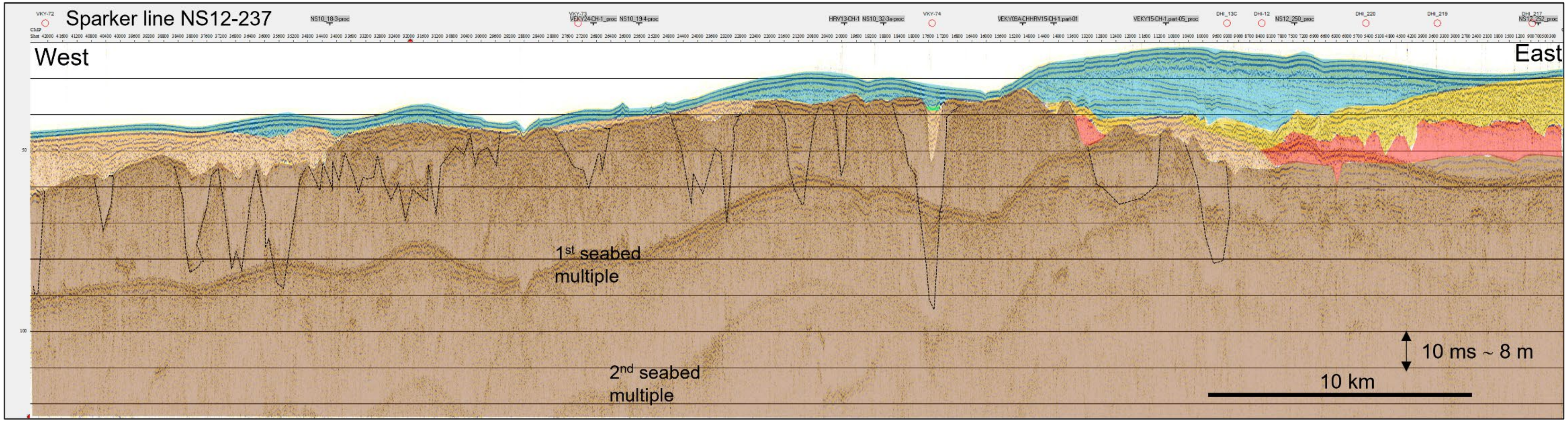

- Holocene marine deposits
- Holocene peat/freshwater deposits
- Weichselian meltwater deposits (glaciofluviatile/-lacustrine)
- Eemian marine deposits
- Late Saalian meltwater deposits
- Saalian or older glacial deposits with infilled valleys

B2

Profile B

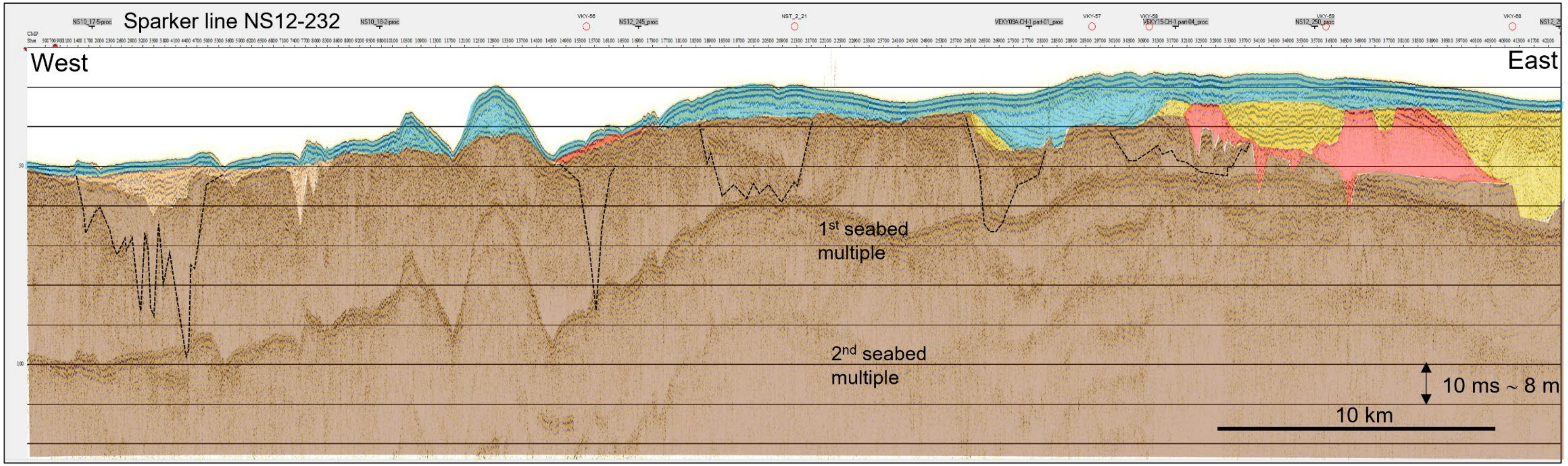

- Holocene marine deposits
- Holocene peat/freshwater deposits
- Weichselian meltwater deposits (glaciofluviatile/-lacustrine)
- Eemian marine deposits
- Late Saalian meltwater deposits
- Saalian or older glacial deposits with infilled valleys

B3

Profile C

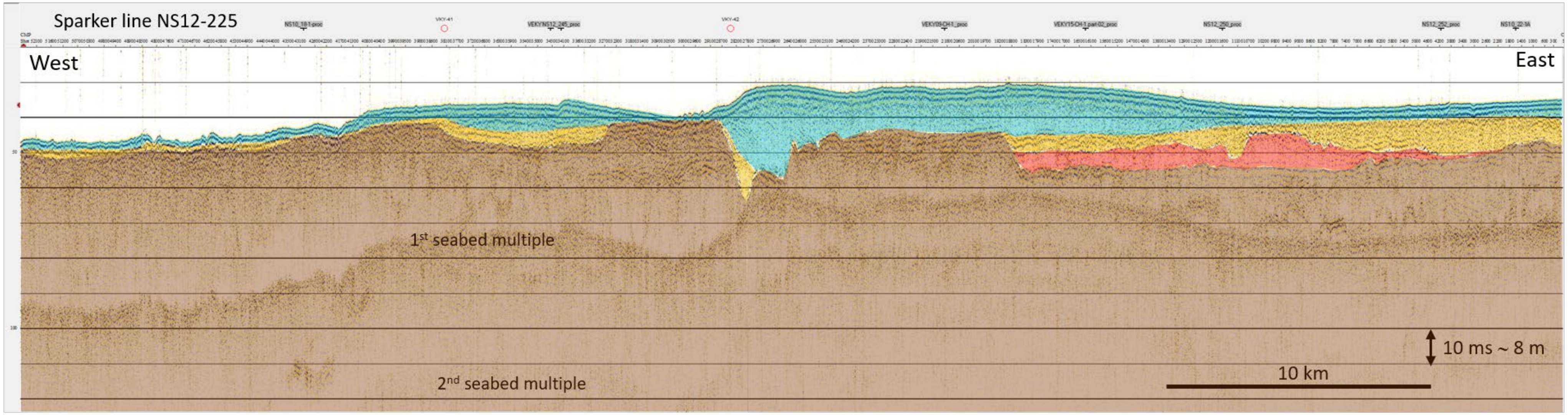

- Holocene marine deposits
- Holocene peat/freshwater deposits
- Weichselian meltwater deposits (glaciofluvial/-lacustrine)
- Eemian marine deposits
- Late Saalian meltwater deposits
- Saalian or older glacial deposits with infilled valleys

B4

Profile D

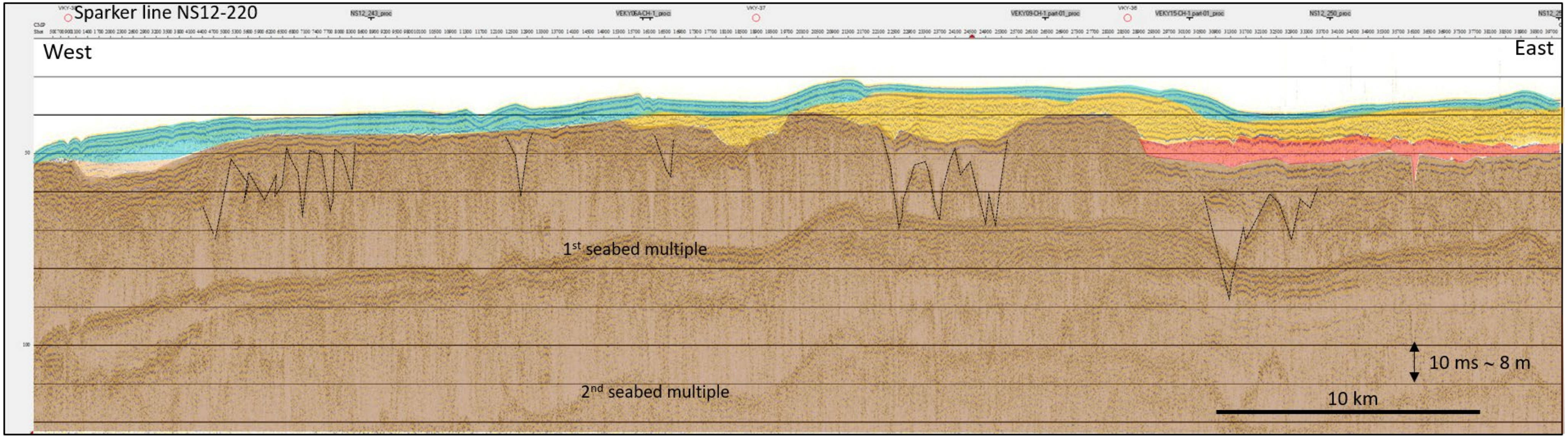

- Holocene marine deposits
- Holocene peat/freshwater deposits
- Weichselian meltwater deposits (glaciofluviatile/-lacustrine)
- Eemian marine deposits
- Late Saalian meltwater deposits
- Saalian or older glacial deposits with infilled valleys

B5

Profile E

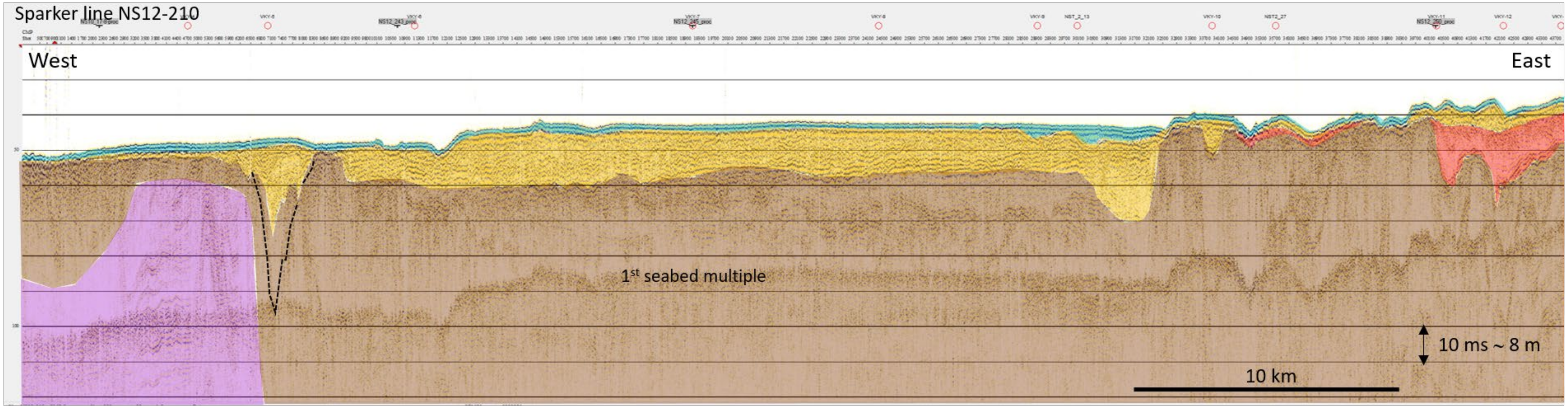

- Holocene marine deposits
- Holocene peat/freshwater deposits
- Weichselian meltwater deposits (glaciofluviatile/-lacustrine)
- Eemian marine deposits
- Late Saalian meltwater deposits
- Saalian or older glacial deposits with infilled valleys
- Prequaternary deposits (Miocene, glaciotectonically deformed)

B6

Profile F

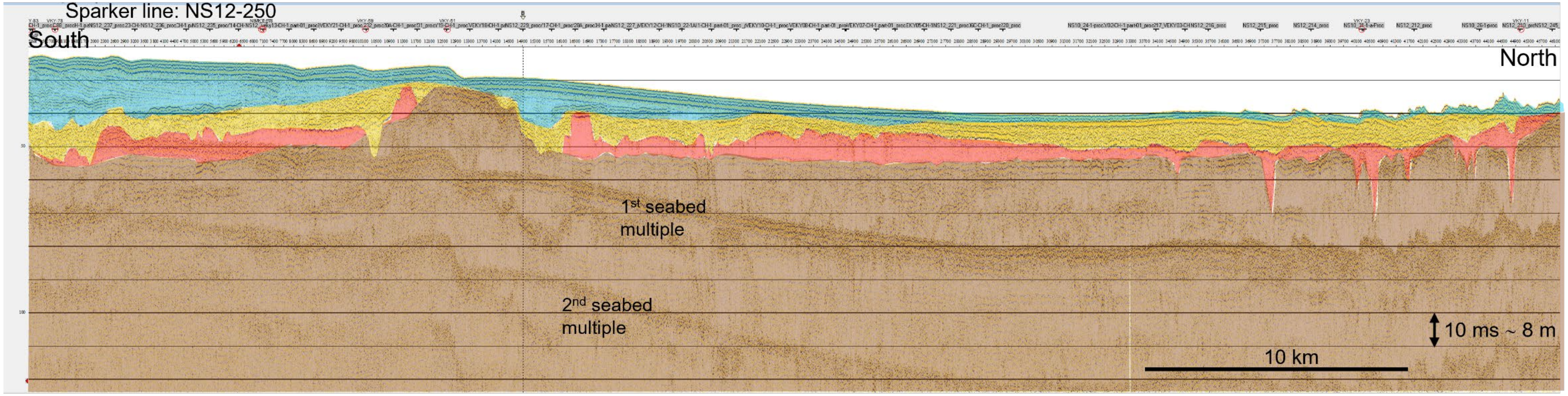

- Holocene marine deposits
- Holocene peat/freshwater deposits
- Weichselian meltwater deposits (glaciofluviatile/-lacustrine)
- Eemian marine deposits
- Late Saalian meltwater deposits
- Saalian or older glacial deposits with infilled valleys

C.

GEUS Core No.	Coring device	Year	X UTM32 EUREF89	Y UTM32 EUREF89	Core top level (m rel. to sea level)	LITHOLOGY (if information available)	Orig. Core no.	Core description
550707.6	Gravity sampler		420919	6180712		[0.00m:s]		Link
550708.11	Vibrocore		425214	6180351		[0.00m:s],[1.00m:s],[1.10m:s]		Link
550712.17	Vibrocore	2009	422998	6170438	-12	[0.00m:hs],[0.56m:hs],[1.56m:hs],[2.56m:hs],[3.56m:hs],[4.56m:hs]		Link
550712.4	Vibrocore	1977	430595	6176517	-17.7	[0.00m:s],[0.40m:l],[0.41m:s],[0.48m:l],[1.60m:s]	8	Link
550712.5	Vibrocore	1977	430021	6176700	-17.8	[0.00m:s],[0.16m:s],[0.47m:l],[0.48m:s],[0.84m:s],[2.68m:s],[4.10m:s]	9	Link
550712.6	Vibrocore	1977	428359	6177162	-4.88	[0.00m:s],[0.60m:s],[0.75m:s],[1.07m:s],[3.35m:s],[3.76m:s],[4.00m:s]	10	Link
550707.1	Vibrocore	1977	414933	6180837	-17	[0.00m:s],[1.00m:s],[1.10m:s],[2.00m:s]	11	Link
550707.2	Vibrocore	1977	413408	6180778	-16.4	[0.00m:s],[0.90m:s],[2.53m:s],[4.00m:s]	12	Link
550707.4	Vibrocore	1977	409070	6180843	-15.8	[0.00m:s],[1.70m:s],[2.00m:s],[2.40m:s],[2.80m:s],[4.00m:i]	14	Link
550706.1	Vibrocore	1977	403423	6180889	-23.7	[0.00m:s],[0.05m:s],[0.58m:i],[2.00m:l]	16	Link
550706.2	Vibrocore	1977	402218	6180724	-22.7	[0.00m:s],[4.00m:l]	17	Link
550706.3	Vibrocore	1977	396930	6180856	-21.2	[0.00m:s],[2.10m:s],[2.40m:s]	18	Link
550706.4	Vibrocore	1977	394785	6180825	-23.4	[0.00m:s],[0.30m:s],[0.80m:s],[1.00m:s]	20	Link
550706.5	Vibrocore	1977	391576	6180831	-26.3	[0.00m:s]	22	Link
550705.3	Vibrocore	1977	386477	6180739	-27.8		26	Link
550705.4	Vibrocore	1977	383500	6180796	-31.4		28	Link
550705.5	Vibrocore	1977	379768	6180763	-28.3		31	Link
550705.6	Vibrocore	1977	378507	6180836	-32.1		32	Link
550705.7	Vibrocore	1977	376728	6180755	-30.2		33	Link
550705.8	Vibrocore	1977	374648	6180814	-29.1		35	Link
550608.1	Vibrocore	1977	371911	6180843	-30.9		37	Link
550608.2	Vibrocore	1977	370426	6180824	-31.9		38	Link
550608.3	Vibrocore	1977	369253	6180729	-33.3		39	Link
550608.4	Vibrocore	1977	367230	6180739	-32.6		41	Link
550608.5	Vibrocore	1977	364566	6180800	-33.2		43	Link
550707.3	Vibrocore	1977	412175	6180818	-15.4	[0.00m:s],[1.15m:s],[1.33m:g],[1.53m:s],[2.02m:s]	13C	Link
550708.8	Vibrocore		428586	6180156		[0.00m:s],[0.20m:s],[1.50m:s],[3.80m:s],[4.15m:s],[4.35m:l],[4.36m:s]	214	Link
550708.9	Vibrocore		425948	6180392		[0.00m:s],[0.35m:s],[1.00m:s],[2.00m:s]	215	Link
550708.10	Vibrocore		425205	6180407		[0.00m:s],[0.55m:s]	216	Link
550708.12	Vibrocore		423335	6180493		[0.00m:s],[1.46m:s],[2.35m:s],[5.40m:s]	217	Link
550707.7	Vibrocore		419945	6180799		[0.00m:s],[0.05m:s],[3.85m:s]	219	Link
550707.8	Vibrocore		417320	6181013		[0.00m:s],[5.40m:s]	220	Link
550707.9	Vibrocore		415042	6181013		[0.00m:s],[0.15m:s]	221	Link

550706.6	Vibrocore	1980	405253	6181003	-20	[0.00m:s],[0.45m:s],[0.65m:s]	222	Link
550706.7	Vibrocore		404390	6181000	-22.5	[0.00m:s],[0.30m:s],[0.75m:g]	223	Link
550706.9	Vibrocore	1980	404513	6181030	-23.8	[0.00m:s],[0.05m:g],[0.35m:s],[0.70m:g]	224	Link
550706.10	Vibrocore	1980	404279	6181026	-24.8	[0.00m:s],[0.37m:l]	225	Link
550706.11	Vibrocore	1980	399977	6181089	-21.8	[0.00m:s]	226	Link
550706.15	Vibrocore	1980	394491	6181047	-24.1	[0.00m:s],[0.32m:s],[1.00m:s]	227	Link
550706.16	Vibrocore	1980	393775	6181019	-25.4	[0.00m:s],[0.66m:s]	228	Link
550706.17	Vibrocore	1980	392473	6181027	-26.8	[0.00m:s],[1.95m:s]	229	Link
550705.9	Vibrocore	1980	389685	6181039	-29.3	[0.00m:s],[1.80m:s]	230	Link
550705.10	Vibrocore	1980	388695	6181007	-30.7	[0.00m:s],[0.17m:s],[0.47m:s]	231	Link
550705.11	Vibrocore	1980	387801	6180993	-31.9	[0.00m:s],[1.20m:s]	232	Link
550705.12	Vibrocore		386847	6181007	-29.5	[0.00m:s],[1.75m:s]	233	Link
550705.13	Vibrocore		384633	6181021	-32.4	[0.00m:s],[0.40m:s],[0.80m:s],[1.05m:s]	234	Link
550705.14	Vibrocore		384170	6181068	-34.3	[0.00m:s],[0.05m:s]	235	Link
550705.15	Vibrocore	1980	383259	6181000	-32	[0.00m:s],[0.35m:i],[0.80m:l],[1.20m:i]	236	Link
550705.17	Vibrocore	1980	382951	6180982	-30.1	[0.00m:s],[1.00m:s]	237	Link
550705.18	Vibrocore	1980	375058	6180999	-30.6	[0.00m:s]	238	Link
550608.7	Vibrocore	1980	371015	6181005	-31.5	[0.00m:s],[0.55m:s],[1.00m:i],[1.25m:l]	239	Link
550608.8	Vibrocore	1980	368013	6180985	-32.7	[0.00m:s],[0.67m:g],[0.71m:i]	240	Link
550705.1	Vibrocore	1977	387489	6180764	-30.8		25A	Link
550705.2	Vibrocore	1977	387489	6180764	-30.8		25B	Link
550712.15	Vibrocore	1981	424114	6178747		[0.00m:hs],[0.82m:hs],[1.50m:hs]	301	Link
550710.1	Vibrocore	1981	404317	6177878	-21.8	[0.00m:hs],[1.28m:hs],[1.45m:hs],[1.65m:s]	305	Link
550612.2	Vibrocore	1981	366013	6176576	-34.1	[0.00m:hs],[0.68m:hs],[0.95m:hs]	309	Link
550711.7	Vibrocore	1981	414987	6178315	-15.5	[0.00m:hs],[0.60m:hs],[0.85m:hs]	302 A	Link
550711.8	Vibrocore	1981	408264	6178051	-17.1	[0.00m:hs],[0.15m:hs],[0.35m:hg]	303 A	Link
550711.9	Vibrocore	1981	407258	6178012	-21.5	[0.00m:hs],[0.98m:ft]	304 A	Link
550710.2	Vibrocore	1981	393144	6177451	-26.4	[0.00m:hs],[0.90m:hs],[1.50m:hs]	306 A	Link
550709.1	Vibrocore	1981	385356	6177107	-33.5	[0.00m:hs],[1.70m:hs],[2.35m:hs],[2.80m:hs],[3.05m:hs],[3.60m:ds]	307 A	Link
550612.1	Vibrocore	1981	373558	6176576	-33.4	[0.00m:hs],[0.55m:hs],[0.65m:hs],[1.18m:hs]	308 A	Link
560716.8	Vibrocore	2010	428011	6266004	-27.1	[0.00m:ms],[0.80m:gs]	VC-31	Link
560720.9	Vibrocore	2010	428001	6259996	-28.6	[0.00m:hs],[1.00m:dg],[1.30m:ds],[5.20m:ds]	VC-34	Link
560720.12	Vibrocore	2010	427991	6253996	-25.7	[0.00m:dg],[0.60m:ds],[1.20m:dg],[1.50m:ds],[2.70m:ds],[3.70m:ds],[4.60m:ds],[4.90 m:dg],[5.20m:ds]	VC-37	Link
560720.14	Vibrocore	2010	429994	6251995	-27.5	[0.00m:hg],[0.20m:gs],[2.60m:gs],[2.80m:gl],[2.90m:gs],[4.70m:gl],[4.80m:gs]	VC-39	Link
560724.9	Vibrocore	2010	427998	6247999	-27	[0.00m:hg],[0.30m:hs],[0.70m:gs],[1.80m:gs]	VC-40	Link
560724.11	Vibrocore	2010	426008	6245992	-28.6	[0.00m:dl],[1.40m:ds],[3.50m:ms],[3.90m:ql]	VC-42	Link
560724.12	Vibrocore	2010	428001	6241990	-24.5	[0.00m:hs],[0.40m:hs],[0.50m:hs],[2.10m:hi],[2.20m:hs],[3.90m:hs],[4.30m:ds],[4.80 m:ds],[5.20m:ds],[5.40m:dg],[5.41m:ds]	VC-43	Link
560724.14	Vibrocore	2010	430006	6239993	-23.1	[0.00m:hs],[0.70m:hs],[2.10m:ml]	VC-45	Link

560724.15	Vibrocore	2010	428009	6236004	-24.6	[0.00m:hs],[0.30m:hs],[1.90m:hs],[2.50m:hs],[2.70m:hs],[3.30m:hs],[3.70m:ml],[4.10m:dl]	VC-46	Link
560728.4	Vibrocore	2010	426003	6229999	-26	[0.00m:hg],[0.10m:hs],[2.40m:hs],[4.30m:ds],[4.60m:ds],[5.00m:ds]	VC-49	Link
560728.6	Vibrocore	2010	429997	6227997	-23.5	[0.00m:hs],[0.50m:hp],[0.90m:ds]	VC-51	Link
560728.7	Vibrocore	2010	425991	6224003	-26.1	[0.00m:hs],[1.40m:ds]	VC-52	Link
560728.9	Vibrocore	2010	428005	6221993	-24.2	[0.00m:hs],[0.40m:hs],[0.80m:hs],[1.00m:hp],[1.10m:hs],[1.30m:hp],[1.40m:hs],[1.60m:hg],[1.90m:ds],[4.60m:ds]	VC-54	Link
560732.3	Vibrocore	2010	425993	6217998	-27.3	[0.00m:hs],[1.20m:hs],[4.10m:qi]	VC-55	Link
560732.5	Vibrocore	2010	424001	6215999	-28.2	[0.00m:hs],[0.40m:qs],[0.70m:qs],[4.60m:qs],[4.61m:qi]	VC-57	Link
560732.6	Vibrocore	2010	426003	6211997	-27.5	[0.00m:hs],[0.40m:hs],[0.80m:qs],[2.20m:qs],[3.80m:ql],[4.20m:qi]	VC-58	Link
550704.5	Vibrocore	2010	425994	6205999	-26.9	[0.00m:hs],[0.50m:gs]	VC-61	Link
550704.7	Vibrocore	2010	430004	6204001	-24	[0.00m:hs],[0.50m:gs]	VC-63	Link
550704.8	Vibrocore	2010	426006	6200008	-24.7	[0.00m:hs],[0.40m:hs],[3.60m:ds],[4.20m:ds],[5.50m:qs]	VC-64	Link
550704.11	Vibrocore	2010	427996	6197995	-23.5	[0.00m:hs],[2.60m:hs],[3.50m:ds]	VC-67	Link
550704.12	Vibrocore	2010	425991	6194000	-24.4	[0.00m:hs],[0.40m:hs],[4.90m:hs],[5.00m:ds]	VC-68	Link
550708.13	Vibrocore	2010	423998	6192004	-24.6	[0.00m:hs],[0.10m:hs],[0.30m:ds],[3.50m:dl],[3.51m:ds],[5.30m:ds]	VC-71	Link
550708.14	Vibrocore	2010	426006	6188006	-23.1	[0.00m:qs]	VC-72	Link
550706.8	Vibrocore	1980	404742	6181002	-22.5	[0.00m:s],[0.10m:s],[0.57m:l],[0.68m:s],[1.30m:s]	223 II	Link
550706.12	Vibrocore	1980	400010	6181079	-21.8	[0.00m:s],[0.50m:s]	226 II	Link
550706.14	Vibrocore	1980	399952	6181047	-21.8	[0.00m:s],[0.60m:s]	226 IV	Link
550705.16	Vibrocore	1980	383459	6181024	-32	[0.00m:s],[0.20m:l],[1.10m:l]	236 II	Link
550705.19	Vibrocore	1980	375057	6181010	-30.6	[0.00m:s],[0.10m:s],[2.00m:s],[2.17m:s],[3.70m:s],[6.10m:s]	238 II	Link
550709.2	Vibrocore	2020	386625	6177411	-29	[0.00m:hs],[1.40m:hg],[1.65m:hs],[1.85m:hg],[1.90m:hs]	HRV-01	Link
550709.3	Vibrocore	2020	384881	6177357	-30	[0.00m:hs],[2.82m:tl]	HRV-02	Link
550709.4	Vibrocore	2020	375675	6177054	-31	[0.00m:hs],[2.00m:hg],[2.20m:hs],[2.55m:hg],[2.80m:ts]	HRV-03	Link
550612.3	Vibrocore	2020	368496	6176807	-34	[0.00m:hs],[2.43m:hg],[3.45m:hg]	HRV-04	Link
550612.4	Vibrocore	2020	368420	6179096	-31	[0.00m:hs],[2.50m:ts]	HRV-05	Link
550612.5	Vibrocore	2020	363719	6176640	-35	[0.00m:hs],[1.27m:hg],[1.33m:hi],[1.81m:hs],[1.94m:hg],[1.98m:hs]	HRV-06	Link
550709.5	Vibrocore	2020	384362	6172335	-31	[0.00m:hv],[1.75m:hs],[4.30m:hg]	HRV-07	Link
550710.8	Vibrocore	2020	400186	6172860	-19	[0.00m:hs],[3.33m:hs],[4.38m:hg],[4.48m:ms]	HRV-08	Link
550710.9	Vibrocore	2020	395143	6171023	-22	[0.00m:hs],[2.50m:hg],[3.00m:hs]	HRV-09	Link
550612.6	Vibrocore	2020	368891	6176825	-33	[0.00m:hs],[2.14m:ts]	HRV-10	Link
550612.8	Vibrocore	2020	368697	6171051	-33	[0.00m:hs],[0.72m:tv]	HRV-20	Link
550709.6	Vibrocore	2020	381668	6172249	-31	[0.00m:hs],[4.60m:hs],[5.20m:hs]	HRV-41	Link
550608.12	Vibrocore	2020	372631	6180356	-30	[0.00m:hs],[3.73m:hs],[3.83m:ti],[3.95m:ts]	HRV-43	Link
550705.22	Vibrocore	2020	385102	6179867	-26	[0.00m:hs],[3.30m:hg],[3.60m:hs]	HRV-45	Link
560624.3	Vibrocore	2020	373976	6237732	-36	[0.00m:hs],[1.10m:ts]	VKY-01	Link
560624.4	Vibrocore	2020	372021	6237540	-36	[0.00m:hs],[0.20m:ks]	VKY-02	Link
560624.5	Vibrocore	2020	368298	6237815	-36	[0.00m:hs]	VKY-03	Link
560624.6	Vibrocore	2020	374976	6238724	-37	[0.00m:hs],[1.40m:hg],[1.65m:ts]	VKY-04	Link

560721.3	Vibrocore	2020	377580	6238544	-36	[0.00m:hs],[0.73m:ts],[1.18m:ti],[4.40m:tl]	VKY-05	Link
560721.4	Vibrocore	2020	382304	6238248	-36	[0.00m:hs],[0.57m:ts],[4.63m:ti],[5.48m:tl]	VKY-06	Link
560722.6	Vibrocore	2020	391763	6237574	-32	[0.00m:hs],[0.90m:ts]	VKY-07	Link
560722.7	Vibrocore	2020	398051	6237102	-32	[0.00m:hs],[0.78m:ts]	VKY-08	Link
560722.8	Vibrocore	2020	403487	6236723	-32	[0.00m:hs],[0.50m:hp],[2.24m:ft],[2.35m:tl],[2.53m:ts],[2.62m:ti],[2.70m:ts],[2.88m:tl]	VKY-09	Link
560723.8	Vibrocore	2020	409378	6236331	-30	[0.00m:hs],[0.77m:hg],[0.96m:ts],[1.52m:tv]	VKY-10	Link
560723.9	Vibrocore	2020	416744	6235806	-29	[0.00m:hs],[0.97m:hs],[1.15m:hs],[1.85m:hg],[2.40m:hi]	VKY-11	Link
560723.10	Vibrocore	2020	418977	6235631	-29	[0.00m:hs],[0.70m:ts],[3.20m:qs]	VKY-12	Link
560723.11	Vibrocore	2020	420887	6235504	-26	[0.00m:hs],[1.34m:ts]	VKY-13	Link
560721.5	Vibrocore	2020	380103	6248371	-34	[0.00m:hs],[0.20m:hg],[0.75m:hs]	VKY-14	Link
560721.6	Vibrocore	2020	386501	6247921	-34	[0.00m:hs],[0.15m:ml],[0.95m:dl]	VKY-15	Link
560717.3	Vibrocore	2020	381737	6250267	-34	[0.00m:hs],[0.91m:tl]	VKY-16	Link
560717.4	Vibrocore	2020	378591	6250519	-34	[0.00m:hs],[0.78m:ts],[2.24m:tl],[3.56m:ts]	VKY-17	Link
560725.2	Vibrocore	2020	377061	6234571	-36	[0.00m:hs],[2.90m:gv]	VKY-18	Link
560725.3	Vibrocore	2020	384376	6234051	-35	[0.00m:hs],[0.76m:ts],[2.67m:ts]	VKY-19	Link
560727.2	Vibrocore	2020	408066	6232393	-31	[0.00m:hs],[1.37m:hp],[1.66m:ti],[1.76m:ts]	VKY-20	Link
560728.32	Vibrocore	2020	425051	6231206	-27	[0.00m:hs],[1.25m:ts]	VKY-21	Link
560728.33	Vibrocore	2020	423340	6229320	-27	[0.00m:hs],[0.96m:hs]	VKY-22	Link
560727.3	Vibrocore	2020	417525	6229734	-30	[0.00m:hs],[0.86m:ts]	VKY-23	Link
560727.4	Vibrocore	2020	410184	6230244	-30	[0.00m:hs],[1.64m:ts]	VKY-24	Link
560727.5	Vibrocore	2020	407095	6230461	-30	[0.00m:hs],[1.85m:hl],[2.45m:hv],[2.61m:hl],[3.01m:hv],[3.41m:hs]	VKY-25	Link
560725.4	Vibrocore	2020	387266	6231862	-35	[0.00m:hs],[0.32m:ts]	VKY-26	Link
560725.5	Vibrocore	2020	380132	6232365	-35	[0.00m:hs],[0.92m:hs],[1.02m:tv],[1.84m:tg],[1.86m:ts]	VKY-27	Link
560725.6	Vibrocore	2020	387853	6229805	-35	[0.00m:hs],[0.11m:hs],[3.61m:hv]	VKY-28	Link
560725.7	Vibrocore	2020	389719	6229661	-30	[0.00m:hs],[0.78m:hs]	VKY-29	Link
560725.8	Vibrocore	2020	387045	6227869	-34	[0.00m:hs],[0.59m:hs],[2.59m:hi],[3.59m:hl],[5.10m:ts]	VKY-30	Link
560725.9	Vibrocore	2020	382891	6228163	-35	[0.00m:hs],[1.66m:tl]	VKY-31	Link
560728.34	Vibrocore	2020	424707	6223200	-26	[0.00m:hs],[1.80m:ts]	VKY-32	Link
560725.10	Vibrocore	2020	381214	6226253	-34	[0.00m:hs],[1.79m:ms],[2.86m:ds],[5.10m:ml]	VKY-33	Link
560726.1	Vibrocore	2020	404169	6221448		[0.00m:hs],[1.00m:hs],[1.10m:hs],[2.50m:hp],[3.38m:ft],[4.16m:ts],[4.82m:tv]	VKY-34	Link
560727.6	Vibrocore	2020	408025	6221187	-27	[0.00m:hs],[0.40m:ti],[1.00m:tv],[1.70m:tl]	VKY-35	Link
560731.2	Vibrocore	2020	408537	6216331	-26	[0.00m:hs],[1.00m:hs],[1.19m:ts]	VKY-36	Link
560730.4	Vibrocore	2020	394962	6217270	-28	[0.00m:hs],[0.95m:hs],[2.90m:ti],[3.65m:ts],[4.85m:ts],[5.25m:ts]	VKY-37	Link
560632.1	Vibrocore	2020	370653	6218514	-36	[0.00m:hs],[0.62m:hs],[4.25m:hs]	VKY-38	Link
560730.5	Vibrocore	2020	405501	6214514	-25	[0.00m:hs],[1.33m:hs],[1.43m:hs],[1.58m:hs],[1.72m:hs],[2.66m:ts]	VKY-39	Link
560730.6	Vibrocore	2020	404310	6208594	-24	[0.00m:hs],[0.30m:hs],[4.70m:hv]	VKY-40	Link
560729.3	Vibrocore	2020	386322	6207847	-28	[0.00m:hs],[3.32m:hg],[3.62m:hs]	VKY-41	Link
550702.2	Vibrocore	2020	397114	6207091	-27	[0.00m:hs],[0.28m:hs]	VKY-42	Link

550702.3	Vibrocore	2020	401062	6204838	-24	[0.00m:hg],[0.20m:hs]	VKY-43	Link
550702.4	Vibrocore	2020	399776	6204932	-25	[0.00m:hg],[0.29m:hs]	VKY-44	Link
550604.2	Vibrocore	2020	372671	6204816	-35	[0.00m:hg],[0.08m:ts],[2.48m:ts],[4.78m:tg],[5.23m:ts]	VKY-45	Link
550702.5	Vibrocore	2020	400877	6202843	-25	[0.00m:hg],[1.00m:hs]	VKY-46	Link
550702.6	Vibrocore	2020	404083	6202603	-23	[0.00m:hs],[0.90m:hg],[1.40m:hs]	VKY-47	Link
550704.183	Vibrocore	2020	425053	6198440	-25	[0.00m:hs],[2.60m:ts]	VKY-48	Link
550704.184	Vibrocore	2020	422234	6197332	-26	[0.00m:hs],[1.65m:hs],[5.53m:hs]	VKY-49	Link
550702.7	Vibrocore	2020	403505	6195707	-25	[0.00m:hs],[0.70m:hg],[0.97m:hi],[3.47m:hg]	VKY-50	Link
550703.2	Vibrocore	2020	416092	6194857	-21	[0.00m:hs],[2.44m:hg],[2.58m:hs],[2.75m:hg],[2.92m:ts]	VKY-51	Link
550701.2	Vibrocore	2020	389420	6195599	-31	[0.00m:hg],[0.17m:ms]	VKY-52	Link
550703.3	Vibrocore	2020	413514	6193914	-21	[0.00m:hs],[0.28m:hs]	VKY-53	Link
550703.4	Vibrocore	2020	419111	6193516	-23	[0.00m:hs],[3.65m:hg],[3.72m:hs],[3.77m:hg],[3.83m:hs]	VKY-54	Link
550708.32	Vibrocore	2020	424553	6191708	-25	[0.00m:hs],[0.86m:ts]	VKY-55	Link
550701.3	Vibrocore	2020	388188	6193680	-33	[0.00m:hg],[0.12m:hs],[0.73m:hg],[0.85m:ql],[3.10m:ms]	VKY-56	Link
550707.13	Vibrocore	2020	407134	6192368	-20	[0.00m:hs],[0.23m:hg],[0.33m:hs],[1.30m:hg]	VKY-57	Link
550707.14	Vibrocore	2020	409166	6192217	-20	[0.00m:hs],[1.30m:hg]	VKY-58	Link
550707.15	Vibrocore	2020	415482	6191776	-21	[0.00m:hs],[0.44m:hg],[0.64m:hs],[2.06m:hg],[2.37m:hs],[4.60m:hs]	VKY-59	Link
550708.33	Vibrocore	2020	422247	6191282	-26	[0.00m:hs],[0.93m:hp],[1.00m:ft],[1.44m:ts]	VKY-60	Link
550608.13	Vibrocore	2020	372329	6192805	-36	[0.00m:hs],[1.26m:hg],[1.32m:hs],[1.82m:hg],[1.97m:ts]	VKY-61	Link
550705.23	Vibrocore	2020	378011	6192335	-36	[0.00m:hs],[0.58m:ml],[3.63m:ds],[4.69m:ds]	VKY-62	Link
550705.24	Vibrocore	2020	384262	6191953	-28	[0.00m:hs],[0.50m:hs],[0.60m:hs]	VKY-63	Link
550706.20	Vibrocore	2020	404104	6190551	-23	[0.00m:hs],[0.21m:hs],[0.67m:hg],[0.94m:hs],[4.40m:hp]	VKY-64	Link
550707.16	Vibrocore	2020	412300	6189990	-19	[0.00m:hs]	VKY-65	Link
550708.34	Vibrocore	2020	423716	6189180	-25	[0.00m:hs],[0.50m:ts]	VKY-66	Link
550707.17	Vibrocore	2020	414954	6187807	-20	[0.00m:hs],[3.20m:hg],[3.95m:hs],[4.38m:hg],[4.56m:hs]	VKY-67	Link
550708.35	Vibrocore	2020	422243	6187295	-25	[0.00m:hs]	VKY-68	Link
550608.14	Vibrocore	2020	372325	6188796	-35	[0.00m:hs],[1.70m:hv],[2.13m:ts]	VKY-69	Link
550707.18	Vibrocore	2020	408811	6186217	-18	[0.00m:hg],[0.86m:hs]	VKY-70	Link
550708.36	Vibrocore	2020	423792	6185153	-24	[0.00m:hs],[0.15m:ts]	VKY-71	Link
550608.15	Vibrocore	2020	370056	6184945	-34	[0.00m:hs],[1.35m:ts]	VKY-72	Link
550705.25	Vibrocore	2020	388849	6183621	-29	[0.00m:hs],[2.30m:hg],[3.25m:ts]	VKY-73	Link
550706.21	Vibrocore	2020	401464	6182721	-25	[0.00m:hs],[2.06m:hl],[2.15m:hg],[2.20m:hp],[4.37m:ft],[4.75m:fp],[5.17m:ml]	VKY-74	Link
550706.22	Vibrocore	2020	403955	6180559	-25	[0.00m:hs],[0.70m:hg],[0.80m:hp],[2.68m:ti],[3.00m:ts],[3.76m:ms]	VKY-75	Link
550707.19	Vibrocore	2020	406007	6180415	-20	[0.00m:hg],[1.00m:hg],[1.10m:hs],[3.10m:ms],[5.75m:ds]	VKY-76	Link
550707.20	Vibrocore	2020	409390	6180181	-17	[0.00m:hs],[2.25m:hg]	VKY-77	Link
550707.21	Vibrocore	2020	414755	6179794	-18	[0.00m:hs]	VKY-78	Link
550708.37	Vibrocore	2020	423636	6179181	-21	[0.00m:hs],[1.46m:hs],[1.70m:hl],[1.77m:hs],[2.09m:hs]	VKY-79	Link
550711.69	Vibrocore	2020	407010	6178195	-22	[0.00m:hs],[1.84m:hg],[2.04m:ql]	VKY-80	Link
550711.70	Vibrocore	2020	408211	6178465	-17	[0.00m:hg],[0.40m:hs],[1.47m:hg],[1.95m:hs],[3.20m:hs]	VKY-81	Link

550711.71	Vibrocore	2020	411624	6178780	-15	[0.00m:hs],[2.30m:hg],[3.10m:hs]	VKY-82	Link
550711.72	Vibrocore	2020	413843	6178890	-17	[0.00m:hs],[0.81m:hi],[0.88m:hs]	VKY-83	Link
550711.73	Vibrocore	2020	418788	6178817	-20	[0.00m:hs]	VKY-84	Link
550712.61	Vibrocore	2020	426232	6175405	-17	[0.00m:hs],[1.05m:hv],[1.73m:hs]	VKY-85	Link
550604.3	Vibrocore	2020	372176	6198815	-35	[0.00m:hs],[1.45m:hg],[1.90m:ts]	VKY-90	Link
550702.8	Vibrocore	2020	403470	6200625	-23	[0.00m:hg],[0.37m:hs],[0.48m:hg],[0.58m:hs]	VKY-91	Link
550704.185	Vibrocore	2020	422611	6199274	-26	[0.00m:hs],[4.03m:hs]	VKY-94	Link
550701.4	Vibrocore	2020	389409	6201620	-26	[0.00m:hs]	VKY-95	Link
550704.186	Vibrocore	2020	423912	6201212	-26	[0.00m:hs],[2.96m:ts]	VKY-96	Link
550703.5	Vibrocore	2020	410736	6202130	-23	[0.00m:hs],[0.30m:hs]	VKY-98	Link
550703.6	Vibrocore	2020	408512	6202293	-22	[0.00m:hs]	VKY-99	Link
550706.13	Vibrocore	1980	399960	6181043	-21.8	[0.00m:s],[0.50m:s]	226 III	Link
550712.13	Vibrocore	2001	427177	6170921	-10.7	[0.00m:hs],[1.12m:hs],[3.62m:hs]	578.159	Link
550712.14	Vibrocore	2001	426185	6172992	-14.5	[0.00m:hs],[4.81m:hs]	578.160	Link
550711.5	Vibrocore	2001	417718	6169997	-16.7	[0.00m:hg],[0.15m:hs],[4.78m:hs]	578.162	Link
550711.6	Vibrocore	2001	414940	6176123	-17.9	[0.00m:hs],[0.62m:hs]	578.163	Link
550707.5	Vibrocore	2001	415956	6179266	-17.9	[0.00m:hs],[2.23m:hs],[5.76m:hs]	578.164	Link
550712.55	Vibrocore	2020	429044	6172865	-14	[0.00m:hs]	HRNE-17	Link
550712.58	Vibrocore	2020	427651	6168849	-13	[0.00m:hs],[1.87m:hs],[2.05m:hs],[3.23m:hs],[4.87m:hg]	HRNE-34	Link
550701.1	Vibrocore	2020	383404	6206132	-32	[0.00m:hg],[0.20m:hs],[0.32m:hg],[0.51m:hs],[0.60m:ts]	VKY-101	Link
550704.182	Vibrocore	2020	425343	6203055	-26	[0.00m:hs],[0.97m:ts],[1.42m:tg],[1.56m:ts]	VKY-105	Link
550702.1	Vibrocore	2020	394528	6207280	-29	[0.00m:hs],[0.27m:hg],[0.62m:hs],[1.99m:hg],[2.11m:ts]	VKY-106	Link
560729.1	Vibrocore	2020	383131	6210087	-30	[0.00m:hs],[2.63m:hg],[3.15m:ts]	VKY-110	Link
560729.2	Vibrocore	2020	384841	6209967	-30	[0.00m:hs],[0.78m:hs],[2.70m:hg],[2.98m:hs]	VKY-111	Link
560730.2	Vibrocore	2020	396251	6209212	-30	[0.00m:hs],[0.59m:hs],[0.74m:ts]	VKY-112	Link
560731.1	Vibrocore	2020	407393	6208383	-24	[0.00m:hs],[0.73m:hs],[4.98m:ts]	VKY-114	Link
560730.3	Vibrocore	2020	398583	6211894	-24	[0.00m:hs]	VKY-117	Link
560628.2	Vibrocore	2020	368086	6222489	-38	[0.00m:hs],[0.37m:hs],[3.70m:hs],[5.60m:ts]	VKY-120	Link
560628.3	Vibrocore	2020	372878	6222147	-36	[0.00m:hs],[0.64m:hs],[4.15m:hi]	VKY-121	Link
560732.44	Vibrocore	2020	423402	6218550	-26	[0.00m:hs],[0.25m:ts]	VKY-124	Link
560628.4	Vibrocore	2020	373234	6226891	-36	[0.00m:hg],[0.42m:ms]	VKY-127	Link
560628.5	Vibrocore	2020	371384	6226940	-36	[0.00m:hs],[0.26m:ml]	VKY-128	Link
550711.11	Kerneboring	2013	411002	6174501		[0.00m:hs],[0.90m:hs],[2.60m:hs],[6.50m:dl],[8.30m:ms],[9.00m:ml],[9.10m:dl],[10.10m:dl],[11.50m:ds],[12.30m:dg],[12.40m:ds],[13.20m:ds],[13.50m:ml],[14.40m:dl],[14.70m:ds],[15.10m:ds],[22.30m:ds],[25.50m:ds],[32.80m:dl],[35.80m:dl],[38.80m:dl],[41.80m:ds],[44.80m:ml],[46.50m:ds]	HR-BH001	Link
550711.12	Kerneboring	2013	411010	6177671		[0.00m:hs],[2.70m:hs],[9.80m:hi],[9.90m:hl],[10.90m:hl],[11.50m:hl],[17.40m:hl],[24.50m:hl],[28.00m:ds],[30.00m:ds],[33.00m:ds],[35.60m:dz],[36.20m:gs],[43.00m:gs],[45.90m:gl]	HR-BH002	Link

550711.13	Kerneboring	2013	412004	6172202		[0.00m:hs],[1.40m:hs],[5.90m:hs],[7.10m:hs],[8.90m:hs],[10.40m:hs],[11.90m:ms],[13.40m:ds],[16.10m:ds],[19.10m:ds],[22.10m:ds],[31.10m:ds],[37.10m:ds],[40.10m:ds],[41.60m:dl],[41.80m:ds],[46.30m:di],[46.50m:ds],[49.10m:di],[49.30m:ds]	HR-BH003	Link
550711.14	Kerneboring	2013	415003	6173702		[0.00m:hs],[1.20m:hs],[2.50m:hs],[4.20m:hs],[5.70m:hi],[9.70m:hs],[10.40m:hs],[14.80m:hl],[19.90m:hl],[20.20m:hs],[21.70m:hs],[21.90m:hl],[22.30m:hl],[26.70m:ds],[27.70m:ds],[29.70m:ds],[32.20m:ds],[33.70m:ds],[37.60m:ds],[40.70m:ds],[43.00m:ds],[47.40m:ds],[48.50m:ds],[53.00m:ds]	HR-BH004	Link
550711.15	Kerneboring	2013	415501	6170704		[0.00m:hs],[5.90m:hs],[7.80m:hs],[8.10m:hi],[17.50m:hl],[18.40m:hs],[19.10m:ht],[19.15m:ds],[19.40m:ds],[19.60m:ds],[23.10m:dl],[26.10m:ds],[30.60m:ds],[48.60m:ds],[55.60m:dl],[63.60m:ds]	HR-BH005	Link
550711.16	Kerneboring	2013	417403	6172399		[0.00m:hs],[0.30m:hs],[6.20m:hi],[8.00m:hi],[11.10m:hs],[11.60m:hs],[14.50m:hs],[17.60m:hs],[21.10m:hl],[24.10m:hl],[27.10m:ds],[33.30m:ds],[36.10m:ds],[45.10m:ds],[60.20m:ml],[63.60m:ms],[66.10m:dl],[66.30m:ds],[66.50m:ds]	HR-BH006	Link
550711.17	Kerneboring	2013	417997	6168201		[0.00m:hs],[0.50m:hs],[1.50m:hs],[8.10m:hi],[9.30m:hs],[10.20m:hs],[15.00m:hl],[18.00m:hl],[20.50m:hl],[23.50m:hl],[27.30m:hl],[29.00m:hs],[34.80m:ds],[42.30m:ds],[48.30m:ds],[51.30m:dl],[57.20m:ds],[60.30m:ds]	HR-BH007	Link
550711.18	Kerneboring	2013	419001	6177902		[0.00m:hs],[1.50m:hs],[9.20m:ht],[9.50m:hs],[10.20m:hs],[15.50m:hl],[17.40m:hl],[20.00m:hl],[21.20m:hs],[22.70m:ds],[25.20m:ds],[30.60m:dg],[32.20m:ds],[35.70m:ds],[37.20m:ds],[45.50m:di],[45.90m:ds],[50.70m:dg],[51.50m:gs],[55.20m:c],[55.70m:gl],[56.80m:gl],[59.20m:gs],[59.50m:gl],[68.70m:gl]	HR-BH008	Link
550711.19	Kerneboring	2013	421004	6171201		[0.00m:hs],[0.10m:hs],[0.50m:hs],[2.80m:hs],[7.30m:hs],[10.30m:hs],[11.30m:hi],[12.30m:hs],[13.30m:hp],[15.40m:hs],[16.70m:hs],[17.70m:hl],[23.80m:hl],[26.10m:hs],[28.50m:hl],[30.80m:ds],[32.00m:ds],[33.50m:ds],[35.70m:ds],[38.10m:ds],[41.10m:ds],[43.00m:ds],[56.10m:ds],[62.10m:ds]	HR-BH009	Link
550712.19	Kerneboring	2013	421999	6171803		[0.00m:hs],[3.40m:hs],[5.20m:hs],[7.90m:hs],[9.70m:hs],[11.00m:hi],[16.50m:hl],[20.80m:hl],[25.10m:hs],[26.00m:hl],[26.20m:hs],[27.50m:hs],[29.00m:ds],[31.00m:ds],[35.30m:ds],[41.00m:ds]	HR-BH010	Link
550712.20	Kerneboring	2013	425000	6177400		[0.00m:hs],[1.20m:hs],[4.00m:hs],[8.60m:hs],[11.70m:hs],[14.50m:hl],[15.70m:hl],[20.80m:hs],[21.10m:hs],[22.00m:ds],[25.00m:ds],[32.50m:ds],[40.50m:l],[60.00m:ml]	HR-BH011	Link
550712.21	Kerneboring	2013	424599	6174600		[0.00m:hs],[1.50m:hs],[5.50m:hs],[11.70m:hs],[13.90m:hi],[14.50m:hl],[16.50m:hl],[23.00m:hs],[25.70m:ds],[28.80m:ds],[36.80m:ds],[57.80m:ds]	HR-BH036	Link
550712.11	Vibrocore	2001	425042	6169992			578.158.1	Link
550712.12	Vibrocore	2001	425042	6169992	-11.1	[0.00m:x],[0.05m:hs],[1.08m:hs]	578.158.2	Link
550711.3	Vibrocore	2001	419237	6170005			578.161.1	Link
550711.4	Vibrocore	2001	419231	6170018	-16.7	[0.00m:hs],[3.01m:hs],[3.29m:hs],[4.49m:hs],[4.64m:hs]	578.161.2	Link
550706.18	Vibrocore	2012	403997	6186552	-23	[0.00m:hs],[0.80m:hg],[1.00m:hs]	NS12-2-01	Link
560725.1	Vibrocore	2012	379714	6226348	-34.8	[0.00m:hs],[1.20m:hg],[1.28m:hs]	NS12-2-04	Link
550707.10	Vibrocore	2012	419721	6189470	-23.5	[0.00m:hs]	NS12-2-07	Link
560721.1	Vibrocore	2012	377392	6248580	-34	[0.00m:hs],[0.30m:ts],[1.15m:ts],[2.15m:ts],[2.30m:ts],[2.90m:ts],[4.00m:ts]	NS12-2-08	Link
560730.1	Vibrocore	2012	399349	6220356	-32	[0.00m:hs],[1.90m:hs],[3.10m:ts]	NS12-2-14	Link
560727.1	Vibrocore	2012	412386	6226078	-31.5	[0.00m:hs],[0.35m:hs],[0.95m:hs],[1.03m:fs],[1.28m:fs],[1.55m:ts],[2.66m:ti],[3.12m:ts],[3.27m:ti],[3.62m:ts],[3.80m:ts],[4.05m:ts],[4.63m:ts],[4.80m:ts],[4.94m:ts]	NS12-2-15	Link
550707.11	Vibrocore	2012	415281	6187697	-21.8	[0.00m:hs],[2.40m:hs],[3.00m:hs],[3.71m:hg]	NS12-2-18	Link
550705.21	Vibrocore	2012	385010	6185913	-26	[0.00m:hs],[1.66m:hg],[2.23m:hs],[4.50m:hg],[4.59m:hs],[5.85m:ft]	NS12-2-19	Link
550706.19	Vibrocore	2012	396090	6193108	-21.5	[0.00m:hs]	NS12-2-21	Link

550707.12	Vibrocore	2012	412806	6179900	-16.8	[0.00m:s],[1.76m:s],[3.70m:s],[3.87m:s]	NS12-2-22	Link
550705.20	Vibrocore	2012	381506	6180115	-30	[0.00m:s],[0.50m:s],[2.20m:s],[4.00m:s]	NS12-2-23	Link
550710.3	Vibrocore	2012	399054	6177198	-22	[0.00m:hs]	NS12-2-24	Link
550703.1	Vibrocore	2012	420205	6195432	-26.4	[0.00m:hs],[4.85m:hi]	NS12-2-25	Link
560723.5	Vibrocore	2012	411454	6236162	-31	[0.00m:hs],[0.20m:hg],[0.31m:ts],[0.62m:ts],[0.94m:ts],[1.34m:tg],[1.90m:ql]	NS12-2-27	Link
560616.1	Vibrocore	2012	362422	6268134	-41	[0.00m:hs],[1.03m:ts],[1.09m:tl],[5.17m:ts]	NS12-3-05	Link
560624.1	Vibrocore	2012	363924	6239643	-36.8	[0.00m:hs],[0.57m:hs],[0.96m:hg],[1.28m:hs],[2.00m:hi],[2.10m:hs],[2.13m:hs]	NS12-3-16	Link
560628.1	Vibrocore	2012	362601	6234155	-38.7	[0.00m:hs],[2.57m:hg],[2.86m:ts]	NS12-3-17	Link
550704.15	Vibrocore	2011	427979	6205992	-25.8	[0.00m:hs],[1.10m:hs],[3.60m:hs],[4.20m:hs],[4.60m:hs]	VC-1-1-01	Link
550704.16	Vibrocore	2011	429006	6206005	-24.9	[0.00m:hs],[0.30m:gs],[1.60m:gs],[2.60m:gs]	VC-1-1-02	Link
550704.17	Vibrocore	2011	429987	6206002	-23.8	[0.00m:hs],[0.20m:gs]	VC-1-1-03	Link
550704.18	Vibrocore	2011	430980	6206007	-23.3	[0.00m:hs],[0.40m:hs],[2.80m:hs],[3.00m:hs]	VC-1-1-04	Link
550704.21	Vibrocore	2011	428484	6204990	-25.4	[0.00m:hs],[0.70m:hs]	VC-1-1-07	Link
550704.22	Vibrocore	2011	429478	6205006	-25.4	[0.00m:gs]	VC-1-1-08	Link
550704.23	Vibrocore	2011	430503	6205015	-23.7	[0.00m:hs],[0.30m:gs]	VC-1-1-09	Link
550704.28	Vibrocore	2011	428001	6204008	-25.3	[0.00m:hs],[0.30m:hs],[0.50m:hs],[2.50m:hs],[2.60m:hs],[3.30m:hl],[3.40m:hs]	VC-1-1-14	Link
550704.29	Vibrocore	2011	429000	6204009	-24.7	[0.00m:hs],[0.50m:gs],[3.90m:gs]	VC-1-1-15	Link
550704.34	Vibrocore	2011	428486	6203003	-24.7	[0.00m:hs],[0.50m:hs],[1.80m:hs],[4.10m:hg],[4.40m:hs],[5.10m:hs],[5.30m:hs]	VC-1-1-20	Link
550704.35	Vibrocore	2011	429485	6203004	-24.1	[0.00m:gs]	VC-1-1-21	Link
550704.36	Vibrocore	2011	430501	6203013	-23.5	[0.00m:hs],[0.20m:gs]	VC-1-1-22	Link
550704.41	Vibrocore	2011	427990	6201999	-24.8	[0.00m:hs],[0.30m:hs],[2.40m:gs],[2.70m:gs]	VC-1-1-27	Link
550704.42	Vibrocore	2011	429001	6201993	-24	[0.00m:hs],[1.30m:hs],[1.80m:gs]	VC-1-1-28	Link
550704.43	Vibrocore	2011	430007	6201991	-23.8	[0.00m:hs],[0.30m:hs],[0.50m:gs]	VC-1-1-29	Link
550704.44	Vibrocore	2011	431009	6202003	-23.1	[0.00m:hs],[0.20m:hs]	VC-1-1-30	Link
550704.48	Vibrocore	2011	430494	6201485	-23.2	[0.00m:hs],[0.40m:gs]	VC-1-1-34	Link
560722.1	Vibrocore	2010	405507	6244230	-40	[0.00m:hs],[1.30m:hs],[2.00m:hv],[2.30m:dl],[3.22m:dv],[3.45m:dl]	F1P1-VC-36	Link
560715.2	Vibrocore	2010	422441	6262687	-36	[0.00m:hs],[0.10m:ml]	F1P2-VB-27	Link
560715.3	Vibrocore	2010	418307	6265200	-37	[0.00m:hl]	F1P2-VB-28	Link
560715.4	Vibrocore	2010	414683	6267429	-37	[0.00m:hs],[1.20m:dl]	F1P2-VB-29	Link
560723.1	Vibrocore	2010	415847	6240969	-32	[0.00m:hs],[0.80m:hs],[1.46m:hs],[1.85m:hs],[2.78m:hi],[2.88m:hs],[3.20m:hl],[4.14m:hs],[4.25m:hi]	F1P2-VB-31	Link
560720.8	Vibrocore	2010	425579	6255809	-33	[0.00m:hg],[0.22m:hi]	F1P2-VC-33	Link
560723.2	Vibrocore	2010	420423	6242506	-33	[0.00m:hs],[0.30m:hs],[1.40m:tl],[3.80m:ts],[4.23m:ti]	F1P2-VC-34	Link
560718.1	Vibrocore	2010	397582	6260215	-42	[0.00m:hs],[0.65m:hl],[1.09m:dl]	F1P2-VC-35	Link

560714.1	Vibrocore	2010	405298	6265902	-34	[0.00m:hs],[0.60m:hs]	F1P2-VC-37	Link
560723.3	Vibrocore	2010	407674	6247546	-41	[0.00m:hs],[1.50m:hg],[1.80m:ts]	F1P2-VC-38	Link
560718.2	Vibrocore	2010	402598	6258033	-37	[0.00m:hs],[0.90m:hs],[2.80m:hs],[3.76m:hv],[3.90m:dl]	F1P2-VC-40	Link
560715.5	Vibrocore	2010	418282	6263380	-32	[0.00m:hs],[1.88m:hs],[2.82m:hg],[2.92m:hs],[4.07m:hs],[4.10m:hs],[4.66m:hs],[4.70m:hs],[4.80m:hs],[4.82m:hi]	F1P2-VC-42	Link
560715.6	Vibrocore	2010	420443	6266748	-34	[0.00m:hs]	F1P2-VC-43	Link
560715.7	Vibrocore	2010	421385	6268180	-34	[0.00m:hs],[1.10m:hl],[1.14m:hs],[1.18m:hi],[1.90m:hl]	F1P2-VC-44	Link
560719.2	Vibrocore	2010	417210	6251442	-32	[0.00m:hs],[0.90m:hs],[1.90m:hs],[2.05m:hs],[2.90m:hs],[3.20m:hs]	F1P2-VC-45	Link
560714.2	Vibrocore	2010	400459	6264545	-41	[0.00m:hs],[1.30m:hs],[1.34m:hs],[2.38m:hs],[2.44m:hs],[2.65m:hs],[2.74m:hs]	F1P2-VC-46	Link
550704.30	Vibrocore	2011	430980	6204006	-23.4	[0.00m:hs],[1.80m:gs]	VC-1-1-16B	Link
560719.1	Vibrocore	2010	413119	6261129	-34	[0.00m:hs],[0.40m:hs],[0.57m:hs],[1.90m:hs],[2.20m:hs],[5.53m:dl]	F1P2 -VC-41	Link
550712.26	Vibrocore	2014	429293	6174434	-16.32	[0.00m:hs],[0.40m:hs],[0.50m:hs],[0.70m:hs],[1.50m:hs],[2.40m:hs]	HR3_CR2_VC020	Link
550712.27	Vibrocore	2014	429293	6174434	-14.89	[0.00m:hs],[0.80m:hs],[1.60m:hs]	HR3_CR2_VC022	Link
550712.28	Vibrocore	2014	425101	6172472	-14.92	[0.00m:hs],[0.60m:hs],[1.00m:hs],[3.00m:hs],[3.40m:hs]	HR3_CR2_VC024	Link
550712.29	Vibrocore	2014	421959	6172400	-17.11	[0.00m:hs],[0.40m:hs],[1.10m:hs],[3.00m:hs]	HR3_CR2_VC026	Link